•Eukaryotic cells are about 1000 times larger than bacteria cells and also have a membrane enclosed nucleus containing their DNA, and several other internal structures known as organelles.

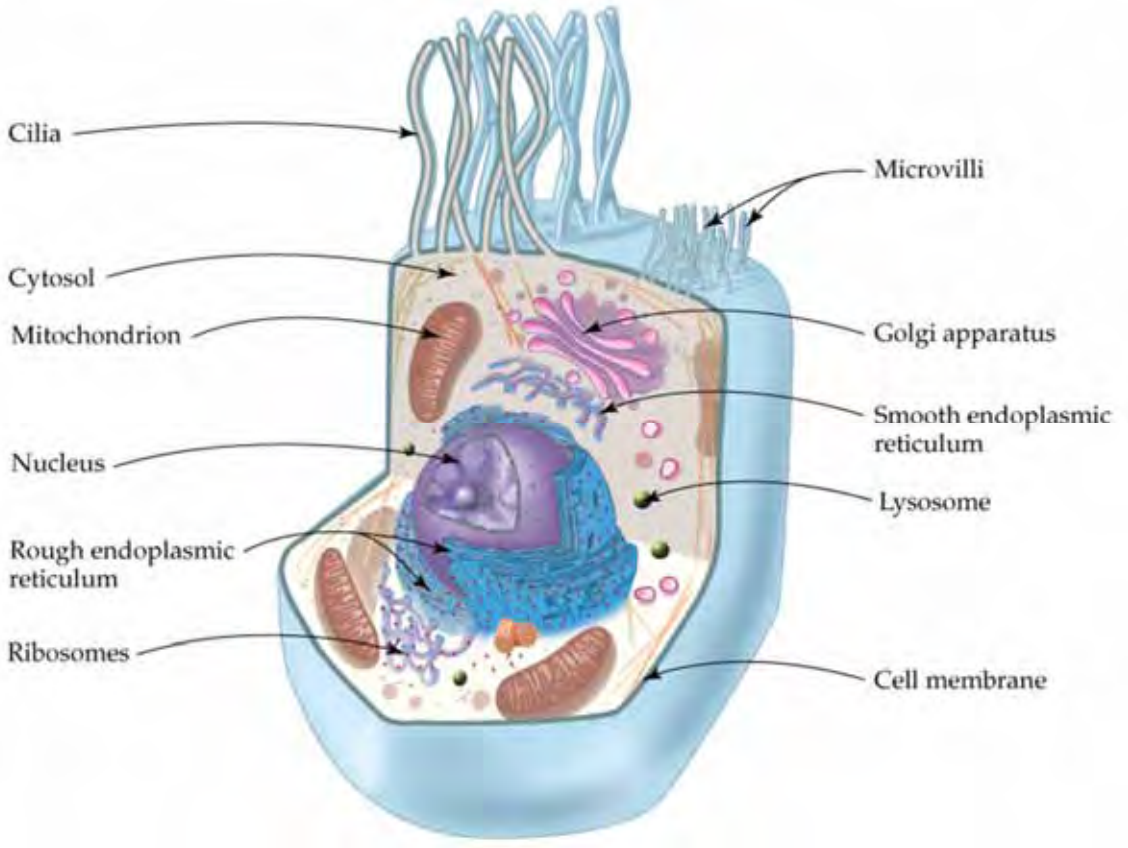

Fig 21.3 A generalized eukaryotic cell.

Cell Membrane

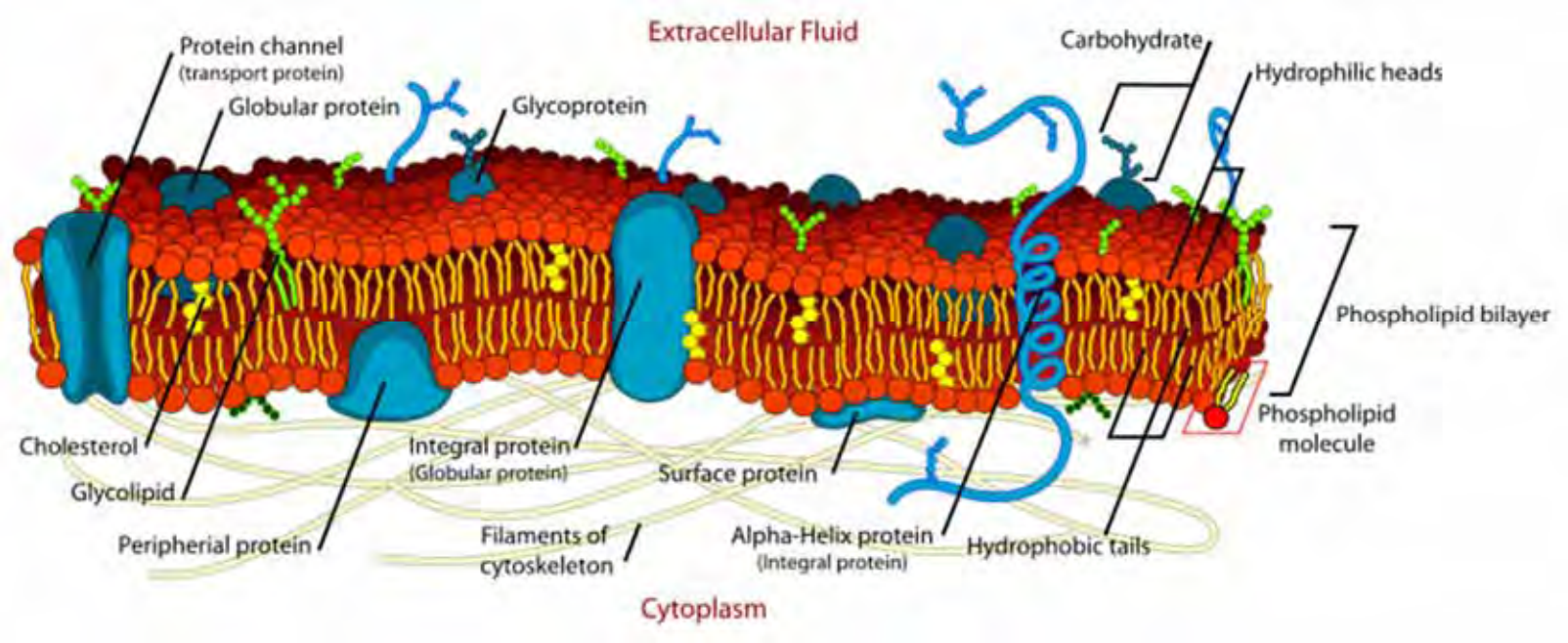

Characteristic diffusivities

Particle	Typical size	Diffusion constant
Solute ion	10^{-1} nm	2×10^3 $\mu m^2/s$
Small protein	5 nm	40 $\mu m^2/s$
Virus	100 nm	2 $\mu m^2/s$
Bacterium	1 μm	0.2 $\mu m^2/s$
Mammalian/human cell	10 μm	0.02 $\mu m^2/s$

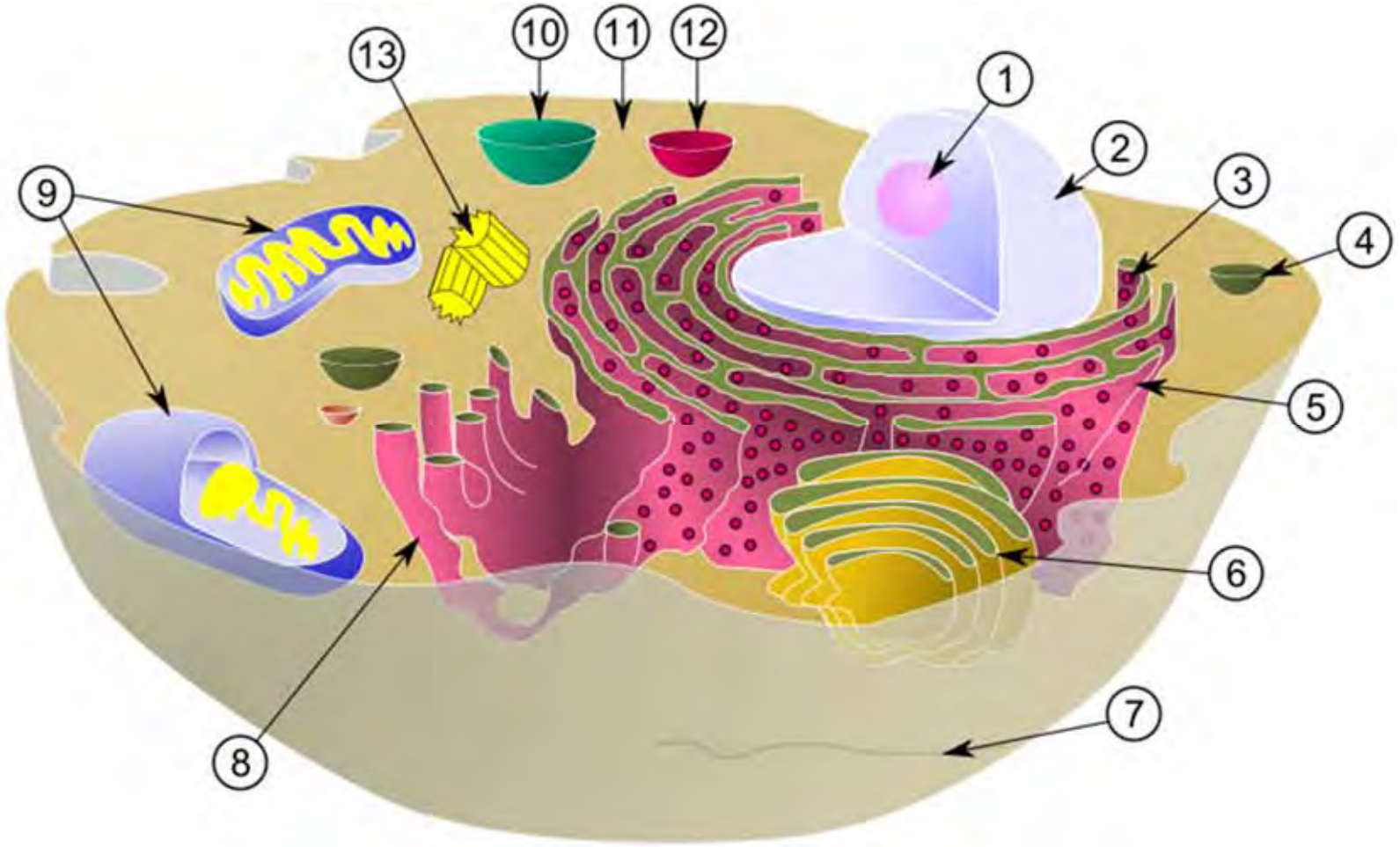

•Schematic showing the cytoplasm, with its components (or *organelles*), of a typical animal cell. Organelles: (1) nucleolus (2) nucleus (3) ribosome (4) vesicle (5) rough endoplasmic reticulum (6) Golgi apparatus (7) cytoskeleton (8) smooth endoplasmic reticulum (9) mitochondria (10) vacuole (11) cytosol (12) lysosome (13) centriole.

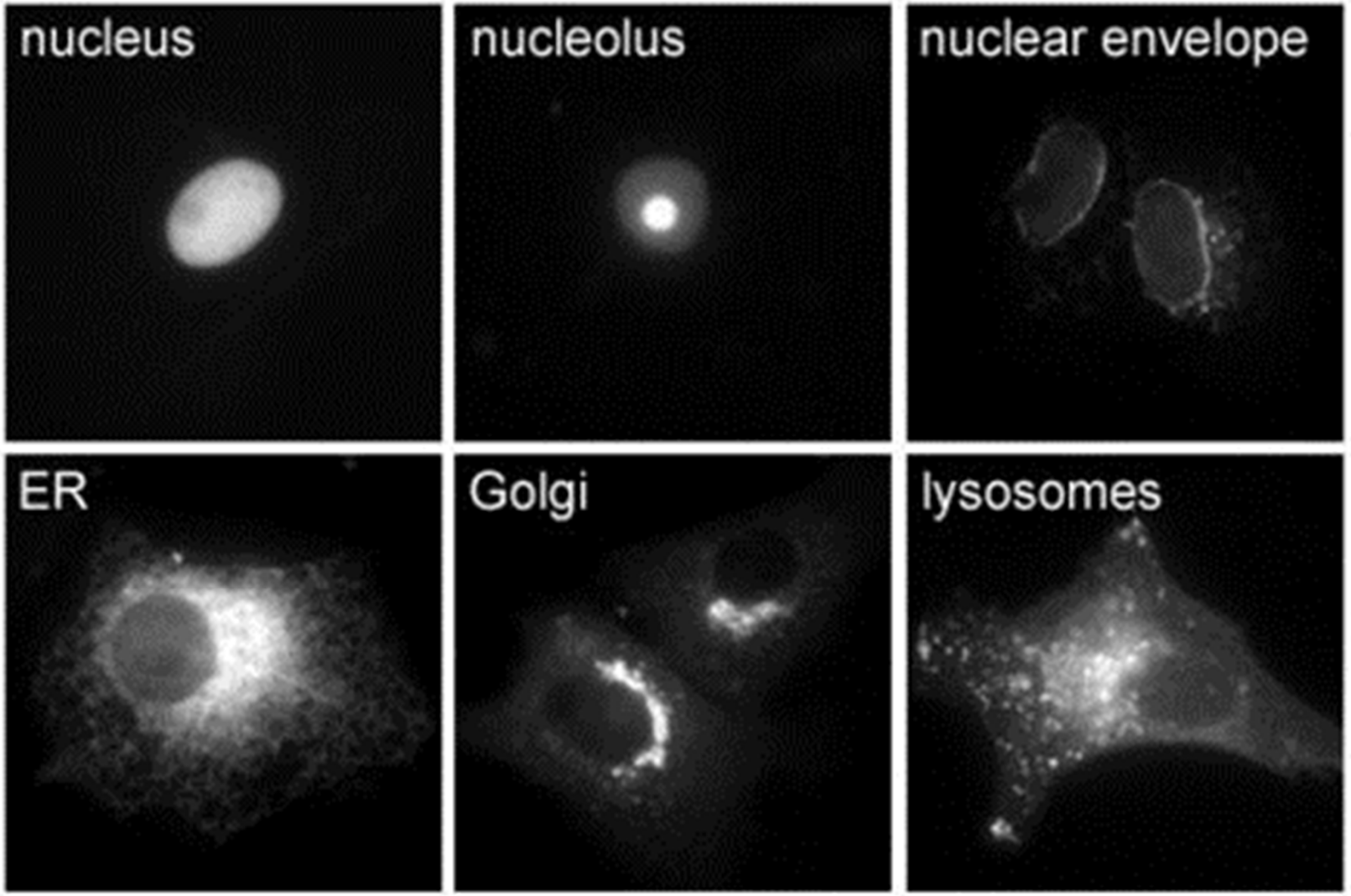
nucleus
nucleolus
nuclear envelope
ER
Golgi
lysosomes

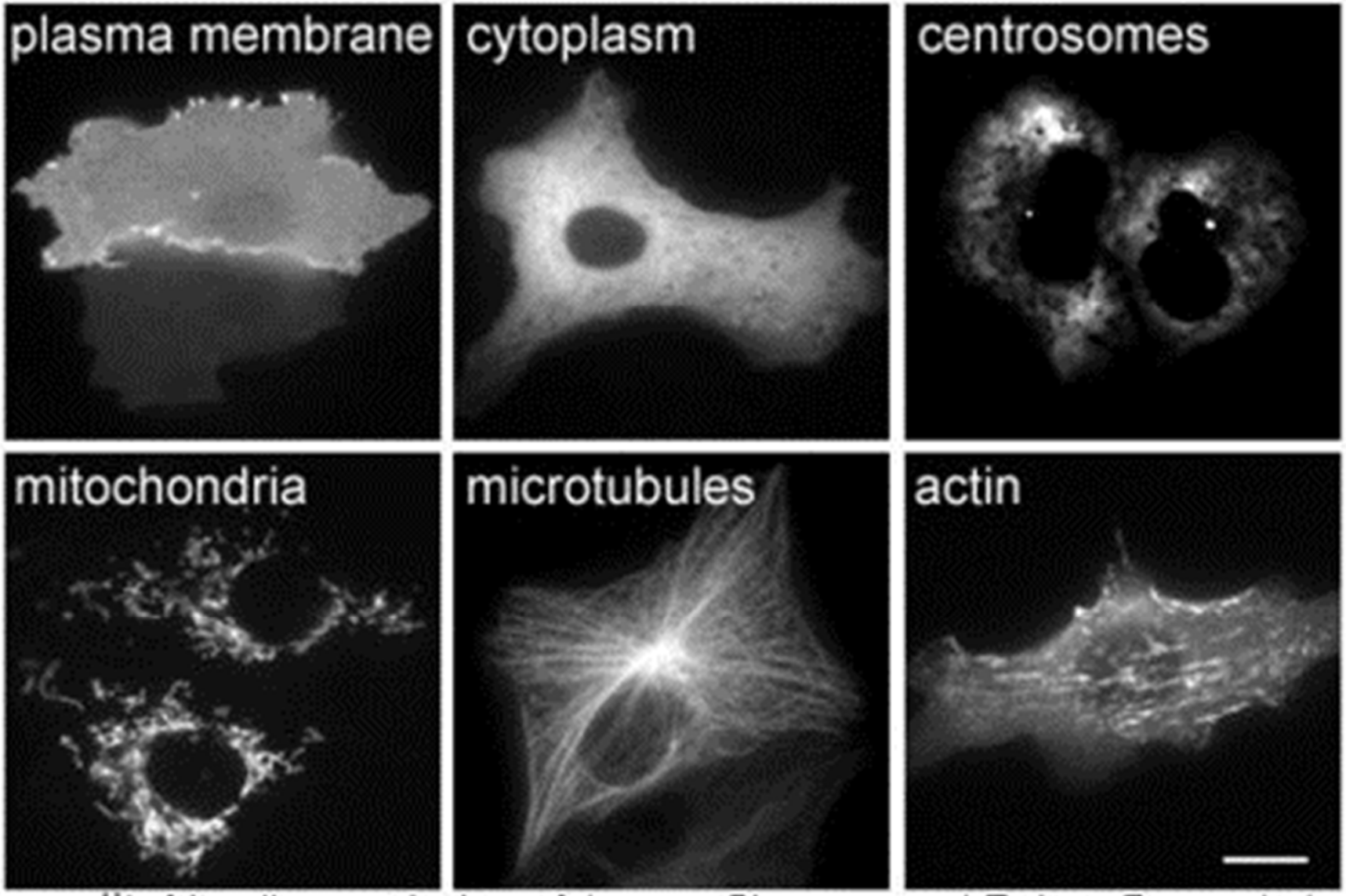

with friendly permission of Jeremy Simpson and Rainer Pepperkok

Nucleus

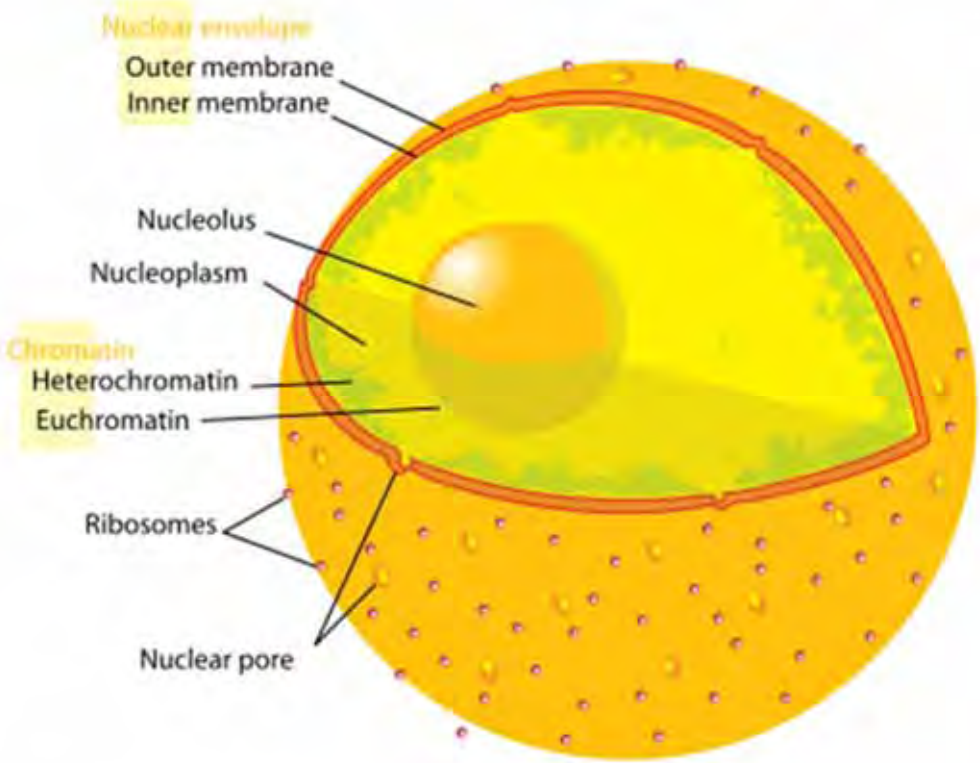

•In cell biology, the **nucleus** is a membrane-enclosed organelle found in most eukaryotic cells. It contains most of the cell's genetic material, organized as multiple long linear DNA molecules in complex with a large variety of proteins such as histones to form chromosomes. The genes within these chromosomes make up the cell's nuclear genome. The function of the nucleus is to maintain the integrity of these genes and to control the activities of the cell by regulating gene expression.

In cell biology, the **nucleolus** (plural *nucleoli*) is a "sub-organelle" of the cell nucleus, which itself is an organelle. A main function of the nucleolus is the production and assembly of ribosome components

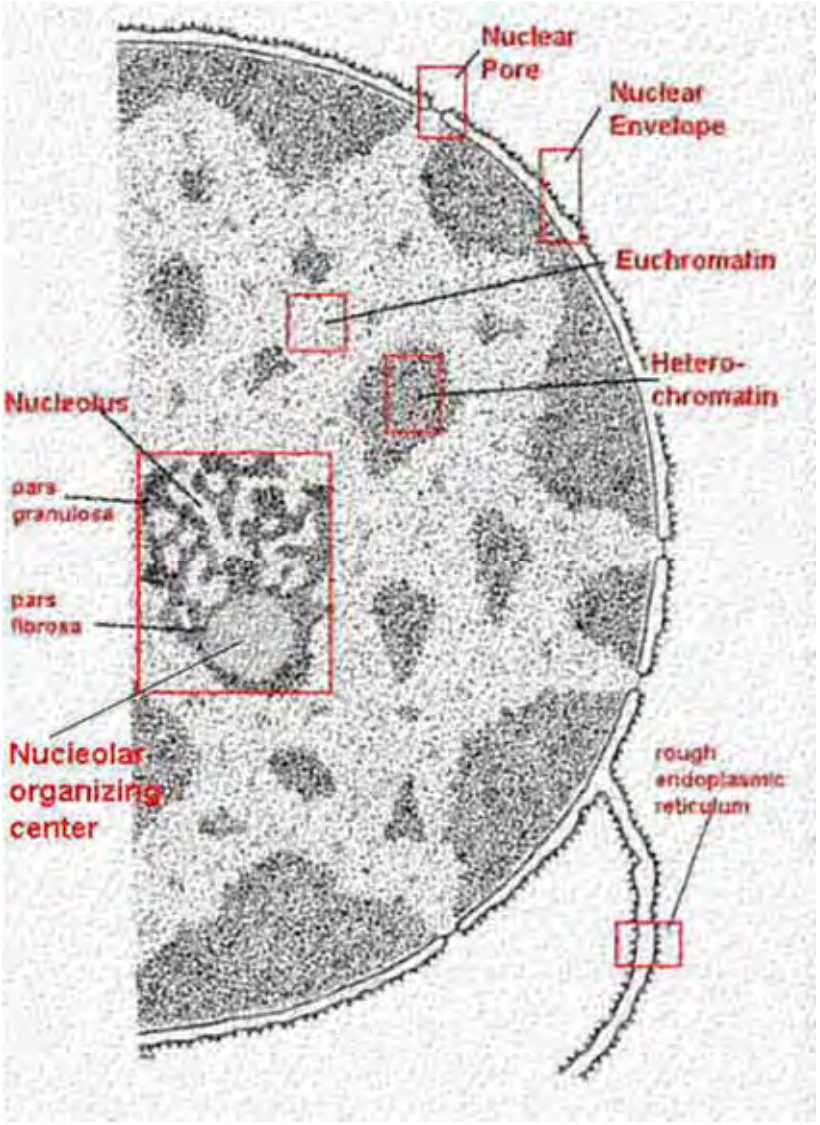

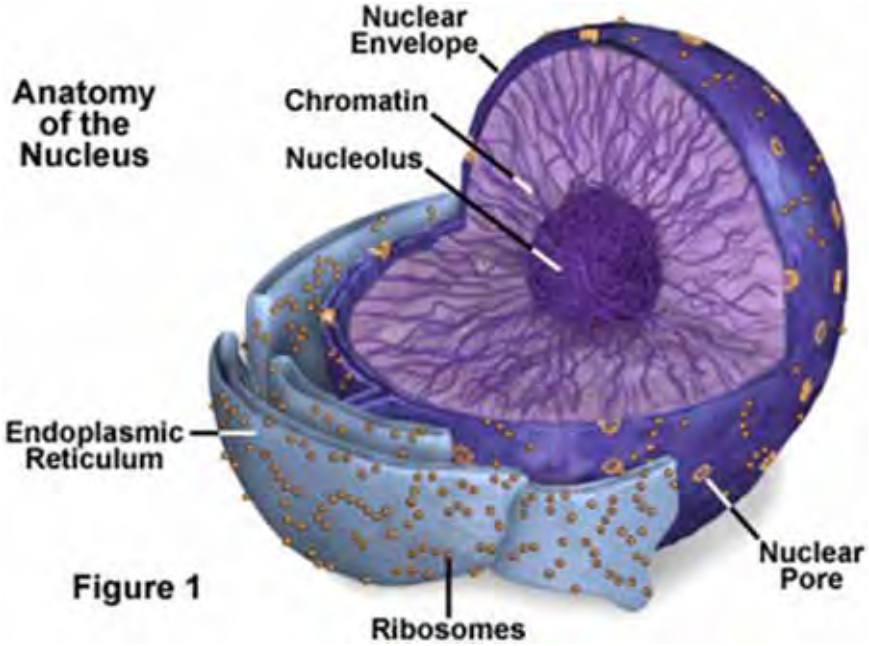

Figure 1

The main roles of the nucleolus are to synthesize rRNA and assemble ribosomes

The main function of the cell nucleus is to control gene expression and mediate the replication of DNA during the cell cycle

Nuclear pores

Nuclear pores, which provide aqueous channels through the envelope, are composed of multiple proteins, collectively referred to as nucleoporins. The pores are 100 nm in total diameter; however, the gap through which molecules freely diffuse is only about 9 nm wide, due to the presence of regulatory systems within the center of the pore. This size allows the free passage of small water-soluble molecules while preventing larger molecules, such as nucleic acids and proteins, from inappropriately entering or exiting the nucleus. These large molecules must be actively transported into the nucleus instead. The nucleus of a typical mammalian cell will have about 3000 to 4000 pores throughout its envelope

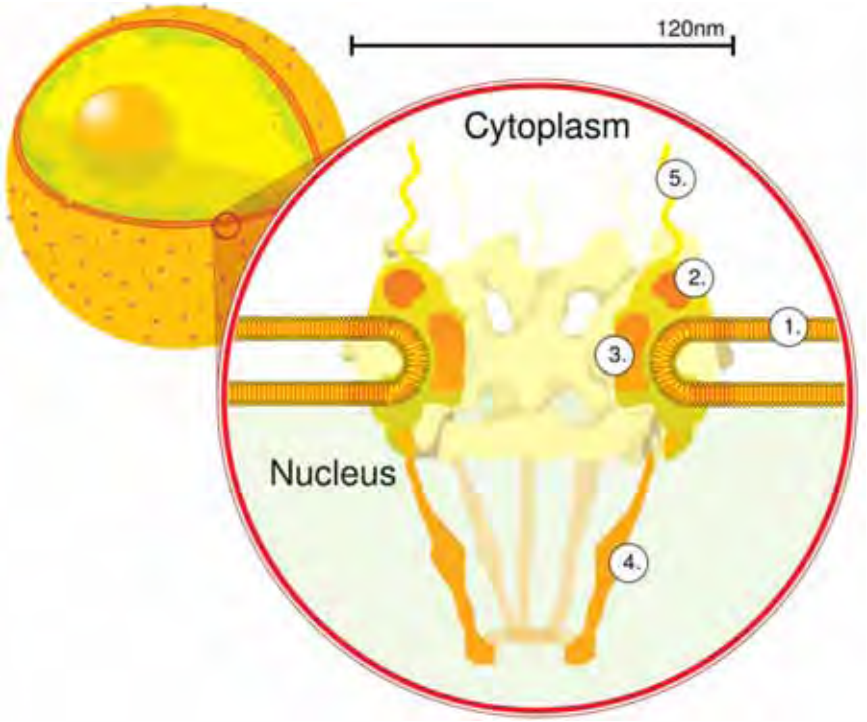

Nuclear localizing sequence (NLS)

- A **nuclear localizing sequence** (**NLS**) is an amino acid sequence which acts like a 'tag' on the exposed surface of a protein. This sequence is used to confine the protein to the cell nucleus through the **Nuclear Pore Complex** and to direct a newly synthesized protein into the nucleus via its recognition by cytosolic nuclear transport receptors. Typically, this signal consists of a few short sequences of positively charged lysines or arginines. Typically the NLS will have a sequence (NH2)-Pro-Pro-Lys-Lys-Lys-Arg-Lys-Val-(COOH).

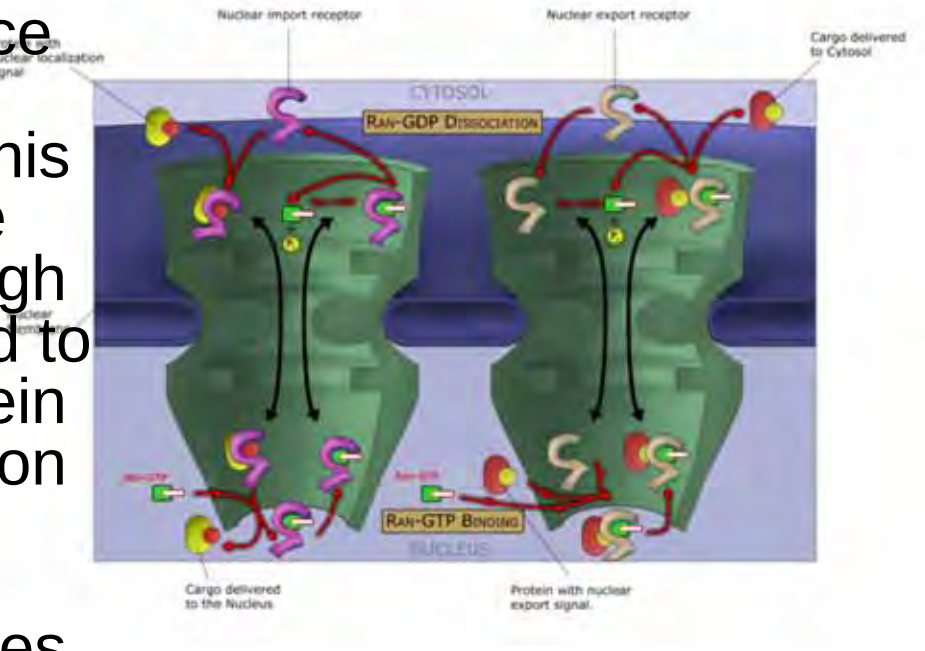

Ribosome

A **ribosome** is a small, dense organelle in cells that assembles proteins. Ribosomes are about 20nm in diameter and are composed of 65% ribosomal RNA and 35% ribosomal proteins (known as a Ribonucleoprotein or RNP). It translates messenger RNA (mRNA) to build a polypeptide chain (e.g., a protein) using amino acids delivered by Transfer RNA (tRNA). It can be thought of as a giant enzyme that builds a protein from a set of genetic instructions. Ribosomes can float freely in the cytoplasm (the internal fluid of the cell) or bound to the endoplasmic reticulum, or to the nuclear envelope.

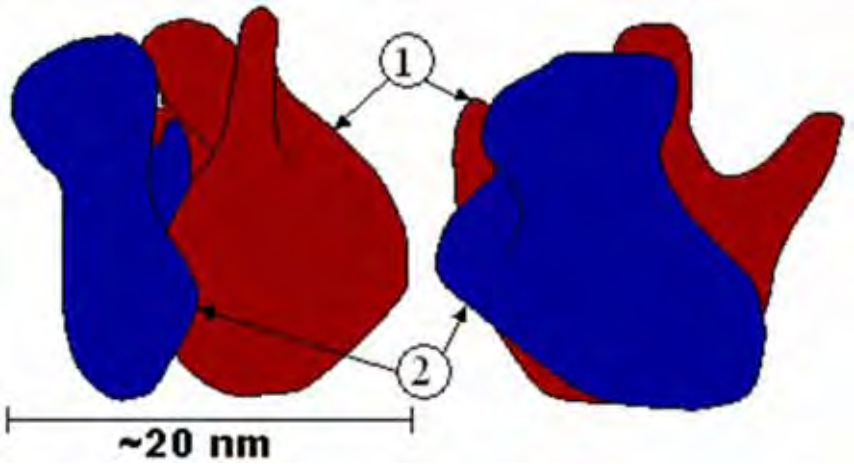

Endoplasmic Reticulum

The **endoplasmic reticulum** or **ER** is an organelle found in all eukaryotic cells that is an interconnected network of tubules, vesicles and cisternae that is responsible for several specialized functions: Protein translation, folding, and transport of proteins to be used in the cell membrane (e.g., transmembrane receptors and other integral membrane proteins), or to be secreted (exocytosed) from the cell (e.g., digestive enzymes); sequestration of calcium; and production and storage of glycogen, steroids, and other macromolecules.[1] The endoplasmic reticulum is part of the endomembrane system. The basic structure and composition of the ER membrane is similar to the plasma membrane.

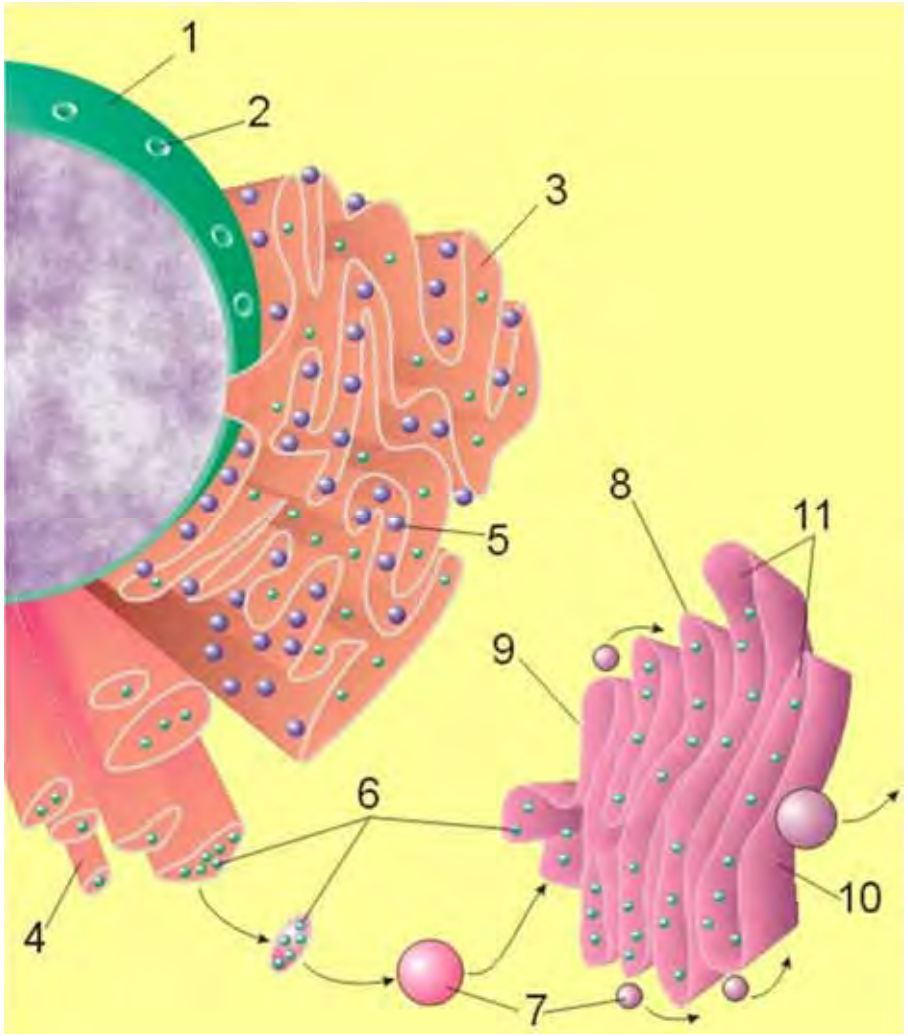

Rough endoplasmic reticulum

- The surface of the rough endoplasmic reticulum is studded with protein-manufacturing ribosomes giving it a "rough" appearance. But it should be noted that these ribosomes are not resident of the endoplasmic reticulum incessantly. The ribosomes only bind to the ER once it begins to synthesize a protein destined for sorting. The membrane of the rough endoplasmic reticulum is continuous with the outer layer of the nuclear envelope. Although there is no continuous membrane between the rough ER and the Golgi apparatus, membrane bound vesicles shuttle proteins between these two compartments. The rough endoplasmic reticulum works in concert with the Golgi complex to target new proteins to their proper destinations

Smooth endoplasmic reticulum

- The smooth endoplasmic reticulum has functions in several metabolic processes, including synthesis of lipids, metabolism of carbohydrates and calcium concentration, and attachment of receptors on cell membrane proteins. It is connected to the nuclear envelope. Smooth endoplasmic reticulum is found in a variety of cell types (both animal and plant) and it serves different functions in each. It consists of tubules and vesicles that branch forming a network. In some cells there are dilated areas like the sacs of rough endoplasmic reticulum. The network of smooth endoplasmic reticulum allows increased surface area for the action or storage of key enzymes and the products of these enzymes. The smooth endoplasmic reticulum is known for its storage of calcium ions in muscle cells.

Golgi apparatus

The **Golgi apparatus** (also called the **Golgi body**, **Golgi complex**, or **dictyosome**) is an organelle found in typical eukaryotic cells. It was identified in 1898 by the Italian physician Camillo Golgi and was named after him. The primary function of the Golgi apparatus is to process and package macromolecules synthesised by the cell, primarily proteins and lipids. The Golgi apparatus forms a part of the endomembrane system present in eukaryotic cells.

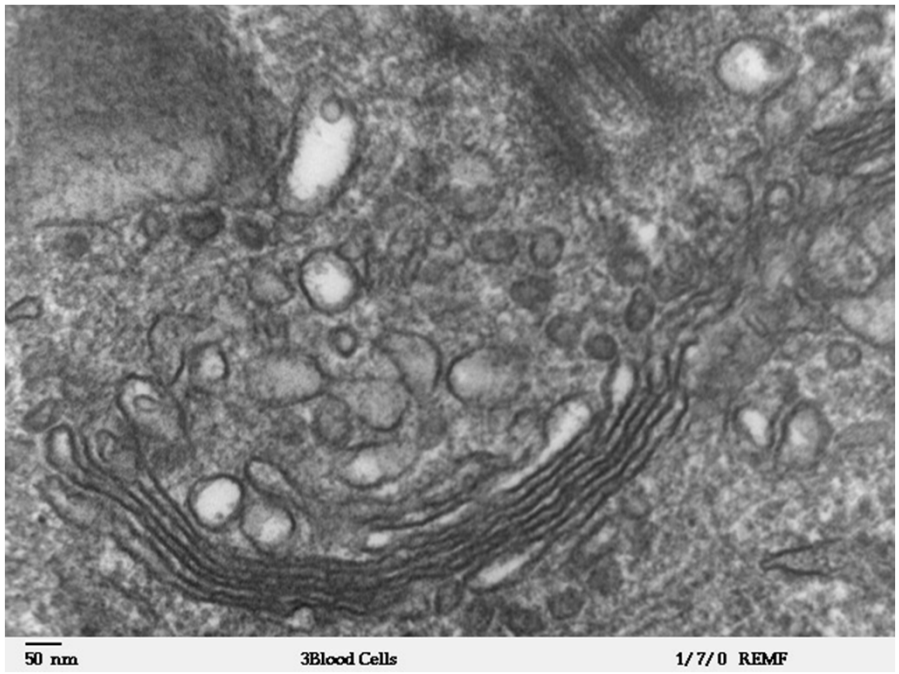

Mitochondrion

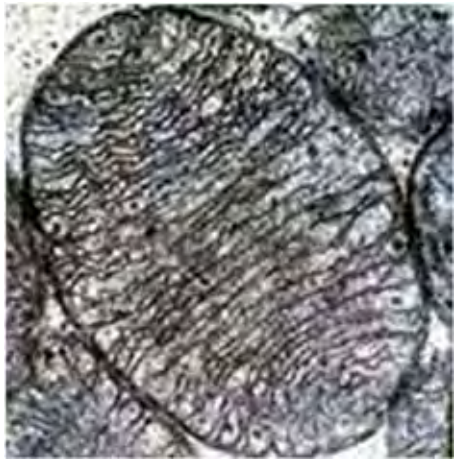

- In cell biology, a **mitochondrion** is a membrane-enclosed organelle, found in most eukaryotic cells.Mitochondria are sometimes described as "cellular power plants," because they convert NADH and NADPH into energy in the form of ATP via the process of oxidative phosphorylation. A typical eukaryotic cell contains about 2,000 mitochondria, which occupy roughly one fifth of its total volume. Mitochondria contain DNA that is independent of the DNA located in the cell nucleus. According to the endosymbiotic theory, mitochondria are descended from free-living prokaryotes.

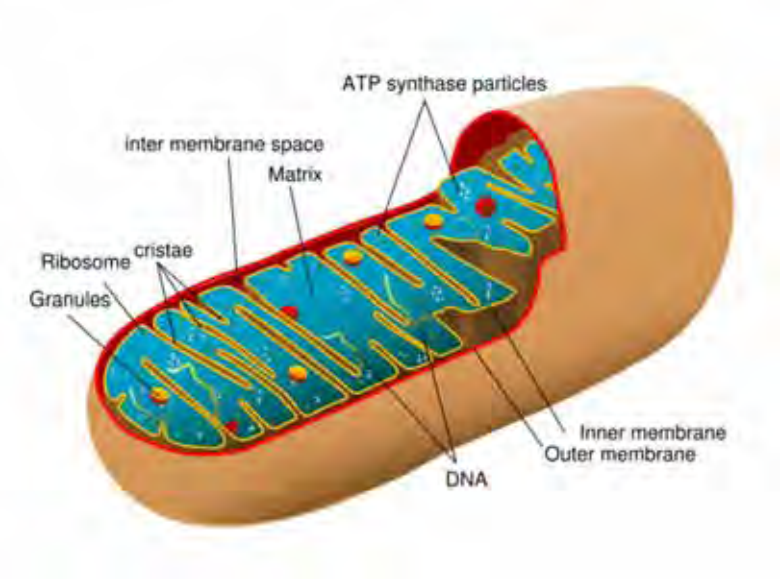

Lysosomes

- **Lysosomes** are organelles that contain digestive enzymes (acid hydrolases). They digest excess or worn out organelles, food particles, and engulfed viruses or bacteria. The membrane surrounding a lysosome prevents the digestive enzymes inside from destroying the cell. Lysosomes fuse with vacuoles and dispense their enzymes into the vacuoles, digesting their contents. They are built in the Golgi apparatus. The name *lysosome* derives from the Greek words *lysis*, which means dissolution or destruction, and *soma*, which means body. They are frequently nicknamed "suicide-bags" or "suicide-sacs" by cell biologists due to their role in autolysis.

Lysosome

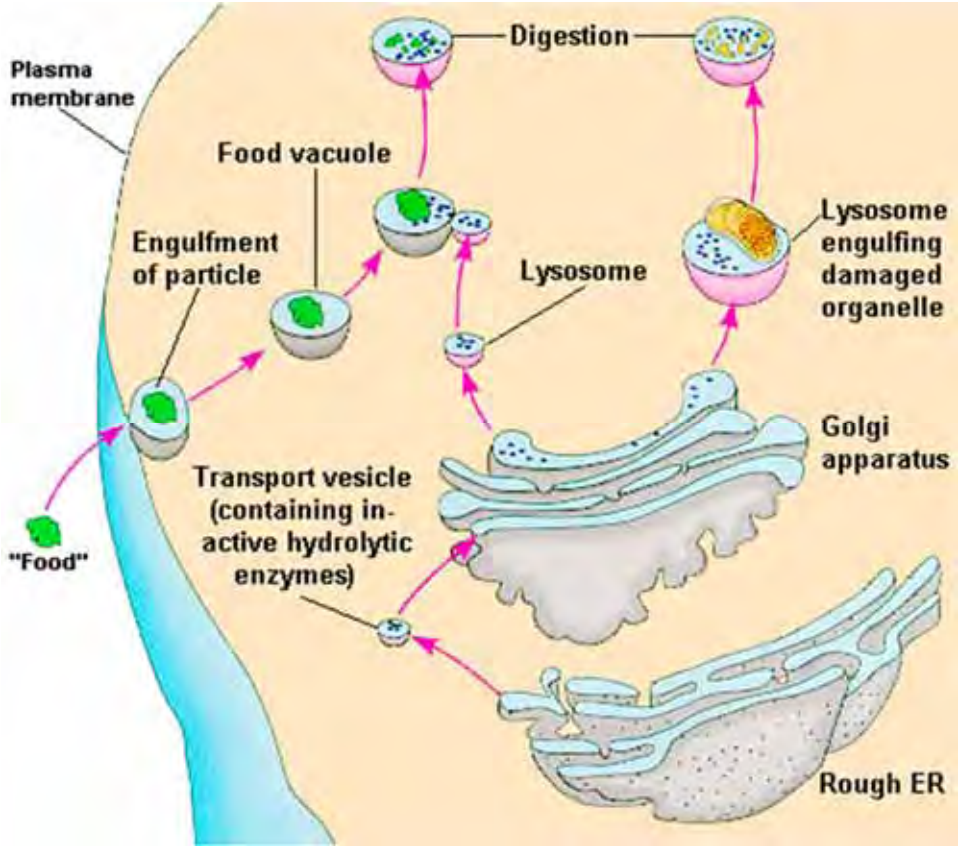

Vedio http://highered.mcgraw-hill.com/olc/dl/120067/bio01.swf

Vesicle

In cell biology, a **vesicle** is a relatively small and enclosed compartment, separated from the cytosol by at least one lipid bilayer. If there is only one lipid bilayer, they are called *unilamellar* vesicles; otherwise they are called *multilamellar*. Vesicles store, transport, or digest cellular products and waste.

This biomembrane enclosing the vesicle is similar to that of the plasma membrane. Because it is separated from the cytosol, the intravesicular environment can be made to be different from the cytosolic environment. Vesicles are a basic tool of the cell for organizing metabolism, transport, enzyme storage, as well as being chemical reaction chambers. Many vesicles are made in the Golgi apparatus, but also in the endoplasmic reticulum, or are made from parts of the plasma membrane.

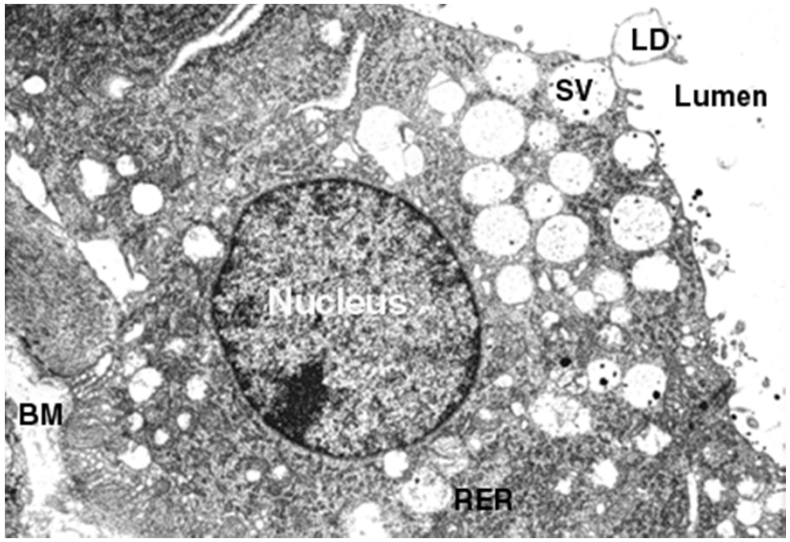

Cytoskeleton

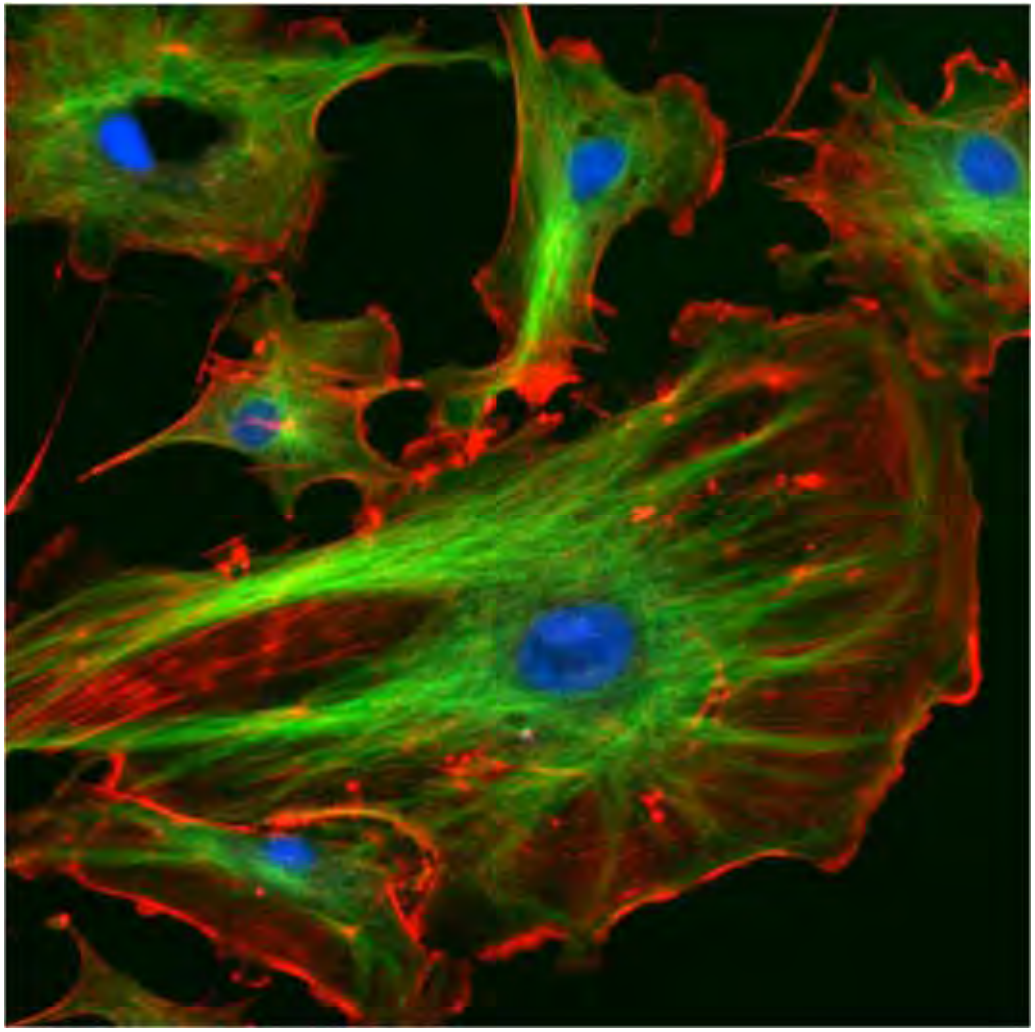

The eukaryotic cytoskeleton. Actin filaments are shown in red, microtubules in green, and the nuclei are in blue.

Actin

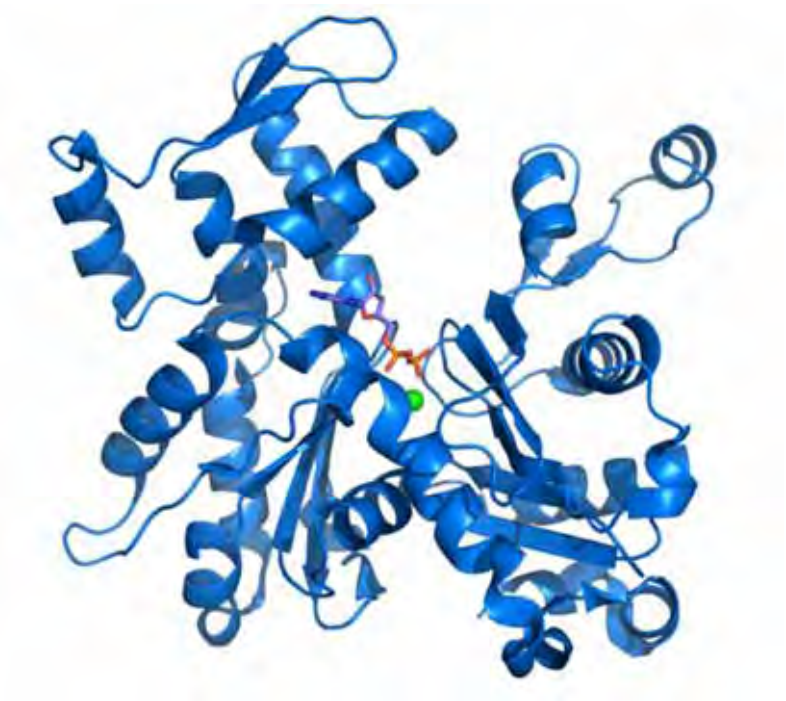

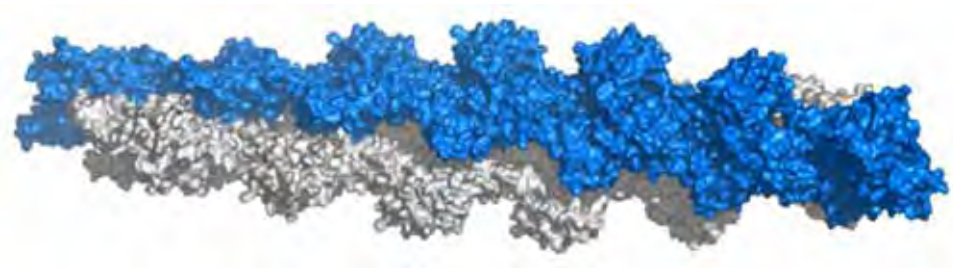

- **Actin** is a globular structural, 42 kDa, protein that polymerizes in a helical fashion to form **actin filaments** (or **microfilaments**). These form the cytoskeleton, a three-dimensional network inside the eukaryotic cell. Actin filaments provide mechanical support for the cell, determine its shape, and enable movement of the cell through lamellipodia, filopodia, or pseudopodia. Actin filaments, along with myosin, have an essential role in muscular contraction. In the cytosol, actin is predominantly bound to ATP, but can also bind to ADP. An ATP-actin complex polymerizes faster and dissociates slower than an ADP-actin complex.

Lamellipodia

- The **lamellipodium** is a cytoskeletal actin projection on the mobile edge of the cell. It contains a two-dimensional actin mesh; the whole structure pulls the cell across a substrate. Within the lamellipodia are ribs of actin called microspikes, which, when they spread beyond the lamellipodium frontier, are called filopodia (Small, et all, 2002). The lamellipodium is born of actin nucleation in the plasma membrane of the cell (Alberts, et al, 2002) and is the primary area of actin incorporation or microfilament formation of the cell. Lamellipodia range from 1μm to 5μm in breadth and are approximately 0.2μm thick.Lamellipodia are found primarily in very mobile cells, crawling at a speeds of 10-20μm/minute over epithelial surfaces..
- The tip of the lamellipodium is the site where exocytosis occurs in migrating mammalian cells as part of their clathrin-mediated endocytic cycle.

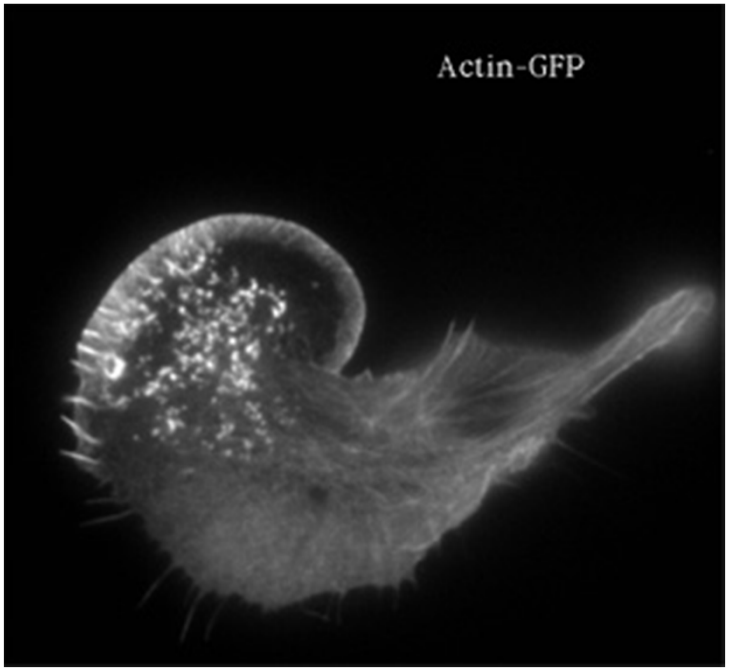

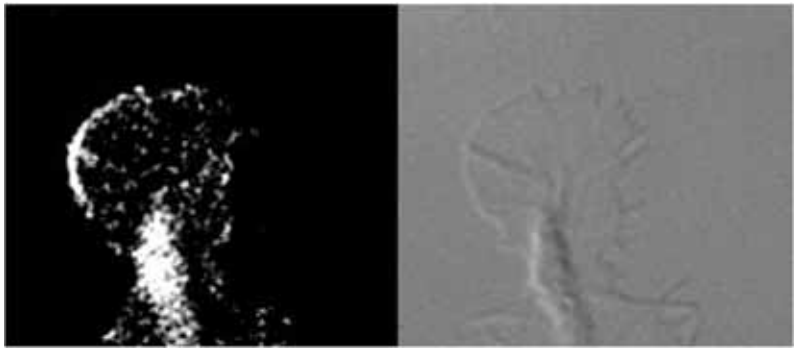

http://www.microscopyu.com/moviegallery/livecellimaging/3t3/t1/3t3-dslwmp1.html

Filopodia

The **filopodia** are slender cytoplasmic projections, similar to lamellipodia, which extend from the leading edge of migrating cells. They contain actin filaments cross-linked into bundles by actin-binding proteins, e.g. fimbrin. Filopodia form focal adhesions with the substratum, linking it to the cell surface. A cell migrates along a surface by extending filopodia at the leading edge. The filopodia attach to the substratum further down the migratory pathway, then contraction of stress fibres retracts the rear of the cell to move the cell forwards.

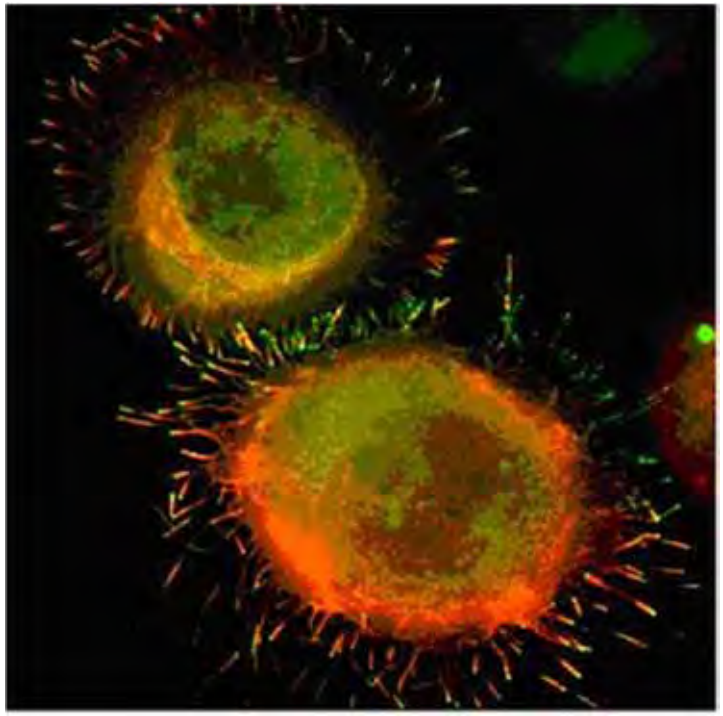

Focal adhesion

- In cell biology, '**Focal Adhesions'** are specific types of large macromolecular assemblies through which both mechanical force and regulatory signals are transmitted. More precisely, **FAs** can be considered as sub-cellular macromolecules that mediate the regulatory effects (e.g. cell anchorage) of extracellular matrix (ECM) adhesion on cell behavior.

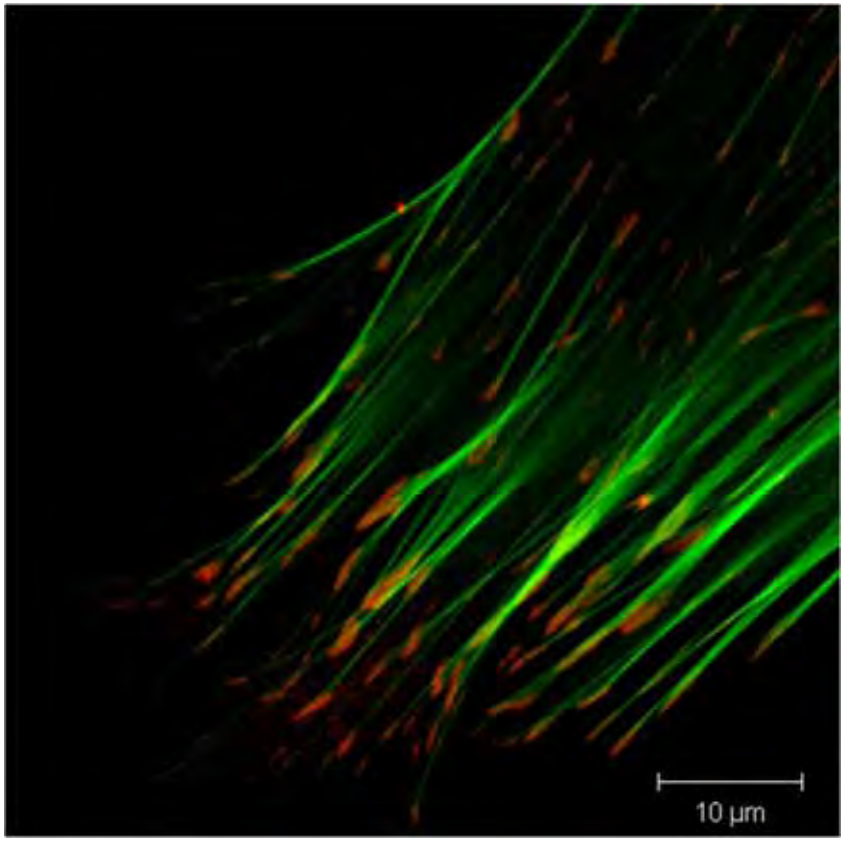

Extra Cellular Matrix

The ECM's main components are various glycoproteins, proteoglycans and hyaluronic acid. In most animals, the most abundant glycoproteins in the ECM are collagens.

ECM also contains many other components: proteins such as fibrin, elastin, fibronectins, laminins, and nidogens, and minerals such as hydroxylapatite, or fluids such as blood plasma or serum with secreted free flowing antigens.

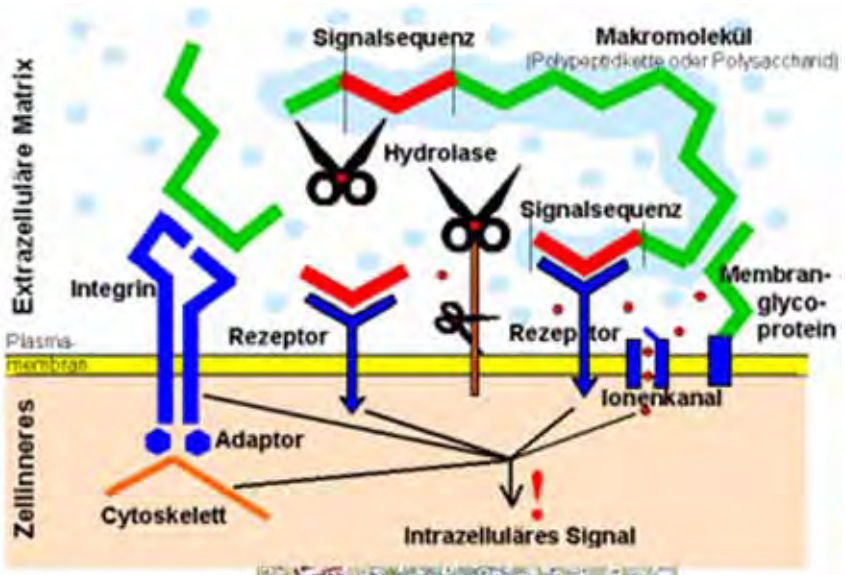

Integrin

An **integrin**, or **integrin receptor**, is an integral membrane protein in the plasma membrane of cells. It plays a role in the attachment of a cell to the extracellular matrix (ECM) and to other cells, and in signal transduction from the ECM to the cell. There are many types of integrin, and many cells have multiple types on their surface. Integrins are of vital importance to all metazoans, from humans to sponges.

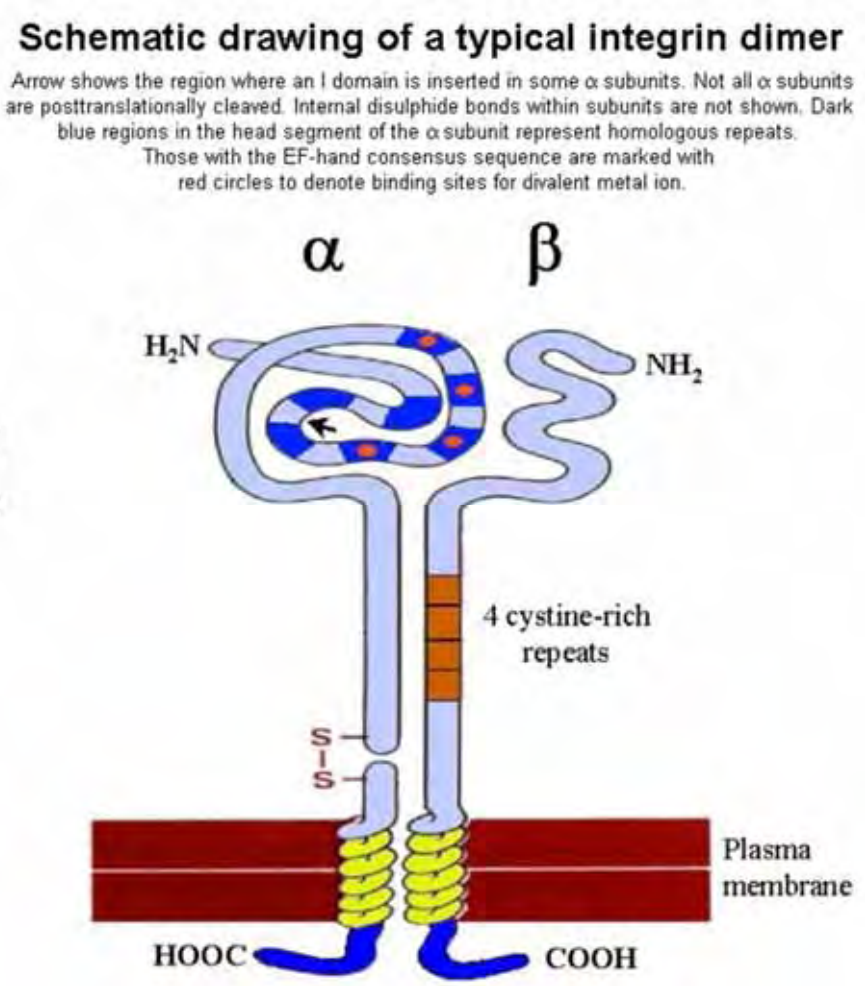

Cell Culture

In the remainder of this section, each step was performed using aseptic technique inside a laminar flow hood (*see* **Note 2**). Ten milliliters of medium was transferred by pipet into each labeled flask. Thawed vials were then sterilized by swabbing with alcohol. The vials were slowly opened, and the medium with the cells was transferred by pipet into the appropriately labeled flask. The flasks were next placed in a 37°C incubator at 5% CO_2, and the cells were allowed to grow until confluent.

Once confluent, the medium was aspirated off and the cells well rinsed with PBS, and then 3 mL of 0.1% trypsin was added. After approx 1 to 2 min, or when the cells began to round up and detach, 3 mL of medium was added to disperse the cells and to inhibit the trypsin (*see* **Note 3**). Cells from each flask were then transferred to an appropriately labeled 50-mL conical tube and centrifuged at 500*g* for 5 min. The supernatant was aspirated off, and the cells were resuspended in fresh medium.

Using a hemacytometer, the cells were counted and their concentration was determined (*see* **Note 4**). The cell solution was next diluted to 1×10^5 cells/mL and 150 µL was added to the glass cover slip of poly-D-lysine-coated sterile MatTek microwell dishes. The cells were incubated at 37°C with 5% CO_2 for 3 h to allow the cells to attach. Once the cells had attached, 2 mL of additional medium was added to the dish. The dishes were then returned to the incubator and allowed to grow for 3 d or until 50% confluent.

Hemacytometer

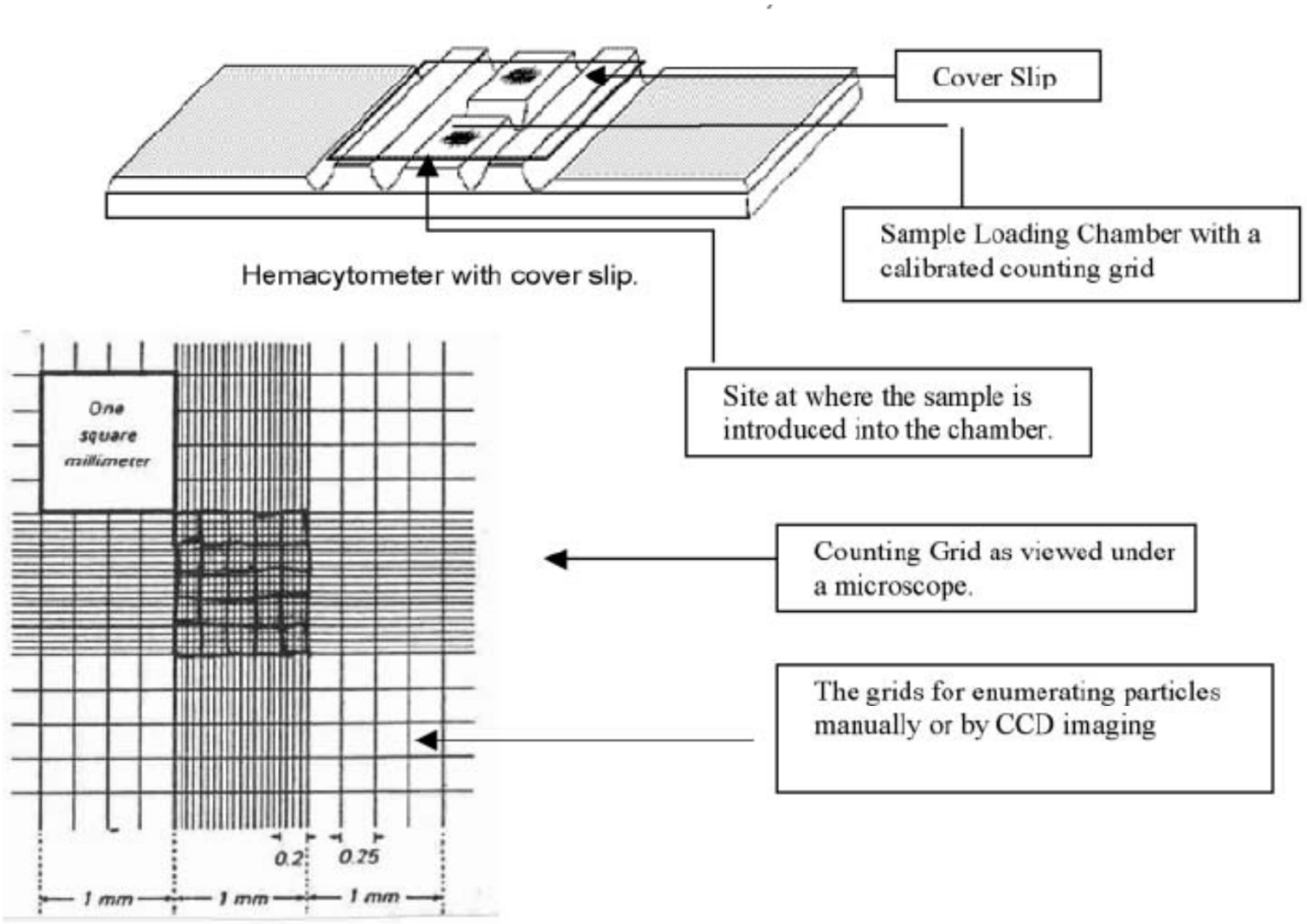

Fig. 3. Layout of hemacytometer.

Cell-Surface Interaction

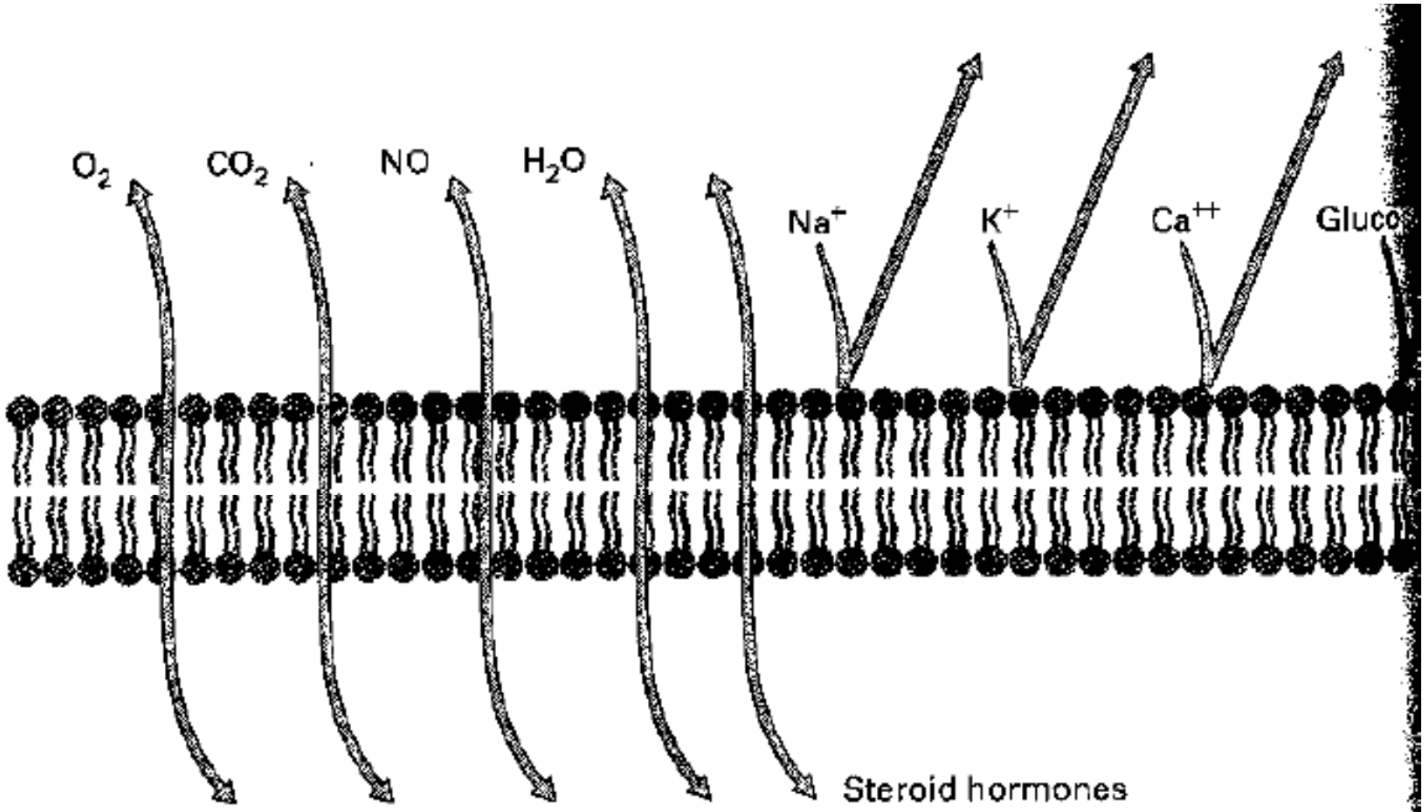

Figure 3.2. Small uncharged molecules can pass through membranes by simple diffusion, but ions can

Endocytosis

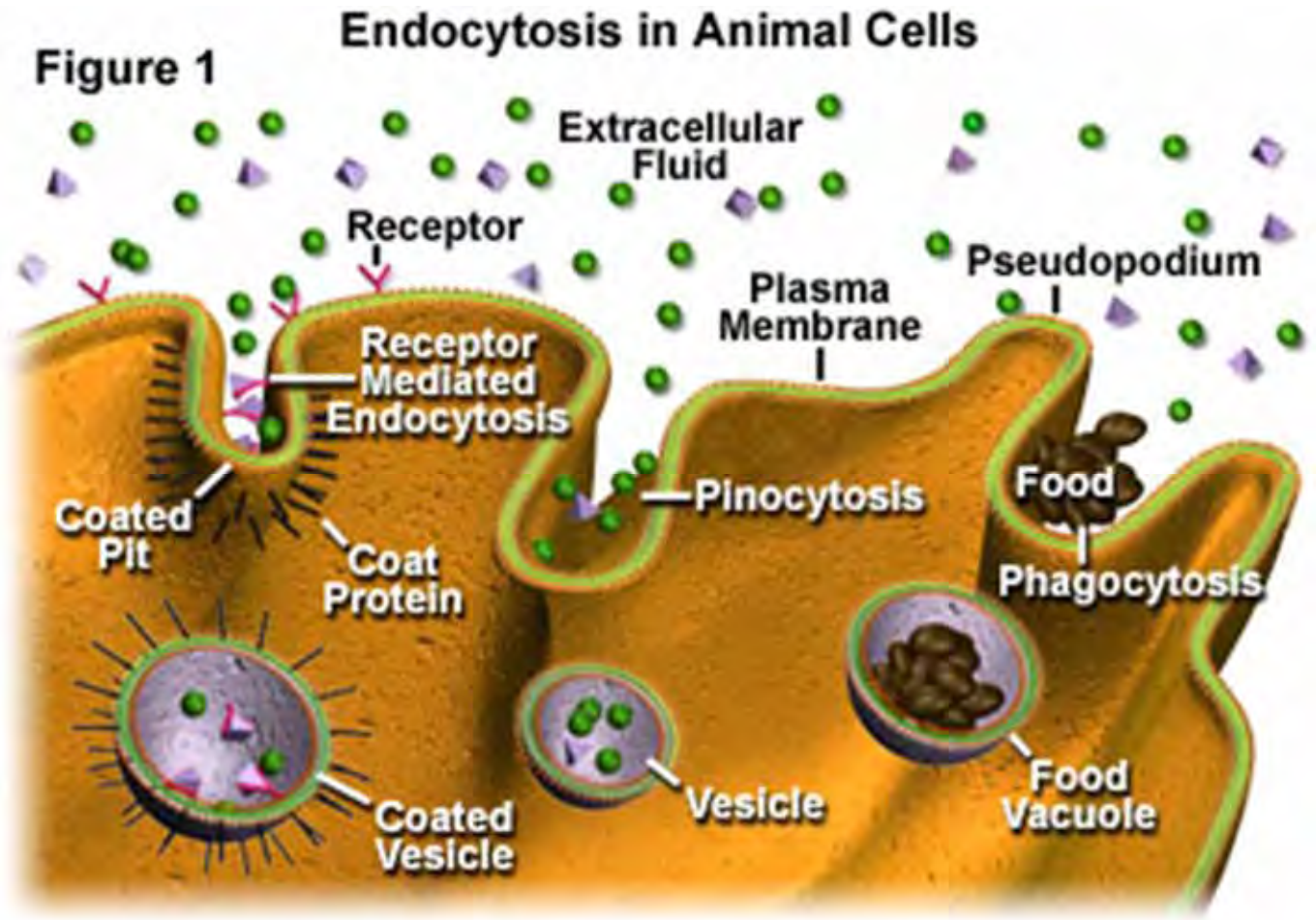

Endocytosis

- Phagocytosis is the process by which cells ingest large objects, such as cells which have undergone apoptosis, bacteria, or viruses. The membrane folds around the object, and the object is sealed off into a large vacuole known as a phagosome.
- Pinocytosis is a synonym for endocytosis. This process is concerned with the uptake of solutes and single molecules such as proteins.
- Receptor-mediated endocytosis is a more specific active event where the cytoplasm membrane folds inward to form coated pits. These inward budding vesicles bud to form cytoplasmic vesicles.

http://highered.mcgraw-hill.com/olc/dl/120068/bio02.swf

Endocytic pathway in mammalian cells

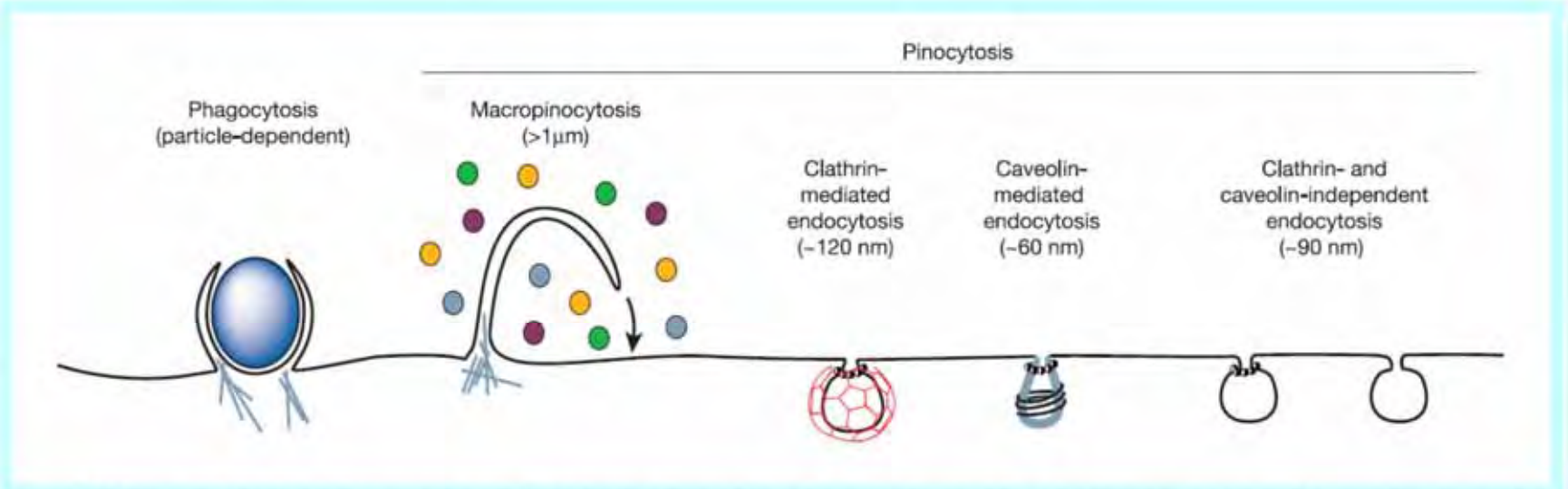

Figure 1 Multiple portals of entry into the mammalian cell. The endocytic pathways differ with regard to the size of the endocytic vesicle, the nature of the cargo (ligands, receptors and lipids) and the mechanism of vesicle formation.

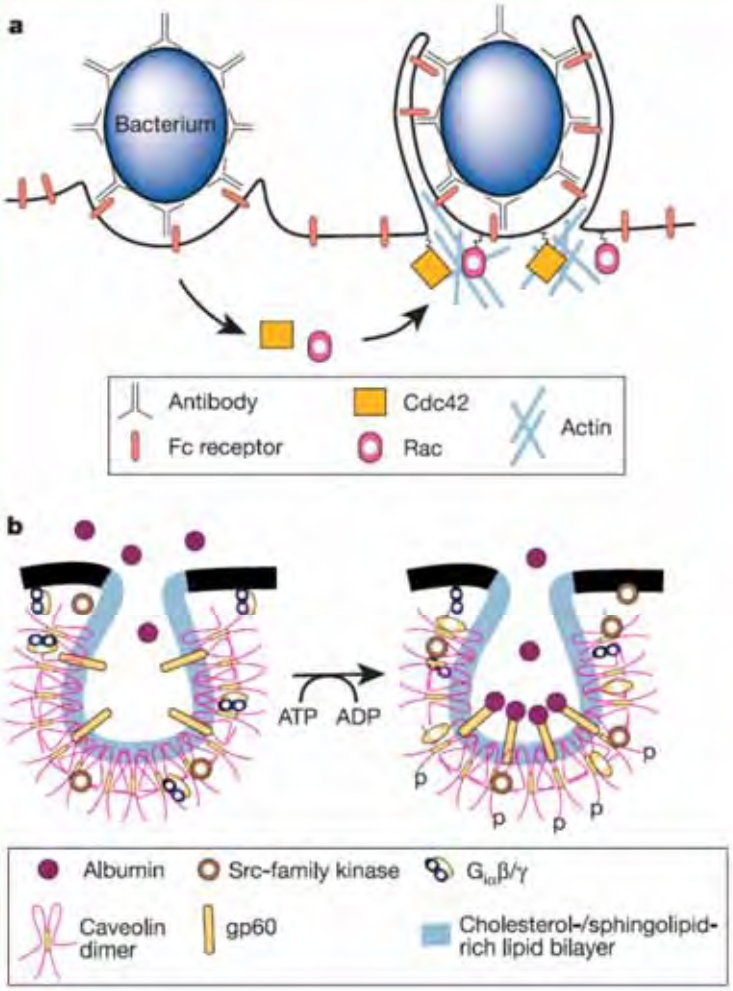

Figure 2 Cargo-stimulated signalling pathways induce uptake by phagocytosis and caveolae. **a**, Fc receptors on the surface of macrophages are activated by immunoglobulin-γ molecules bound to a bacterium. A signalling cascade that involves Rac, Cdc42 and downstream kinases triggers actin rearrangements, protrusion of the membrane around the bacterium, and its engulfment into a phagosome. **b**, Albumin binds to and presumably clusters its receptor, gp60, in caveolae to activate $G_{i\alpha}$ and Src kinases, triggering caveolae endocytosis.

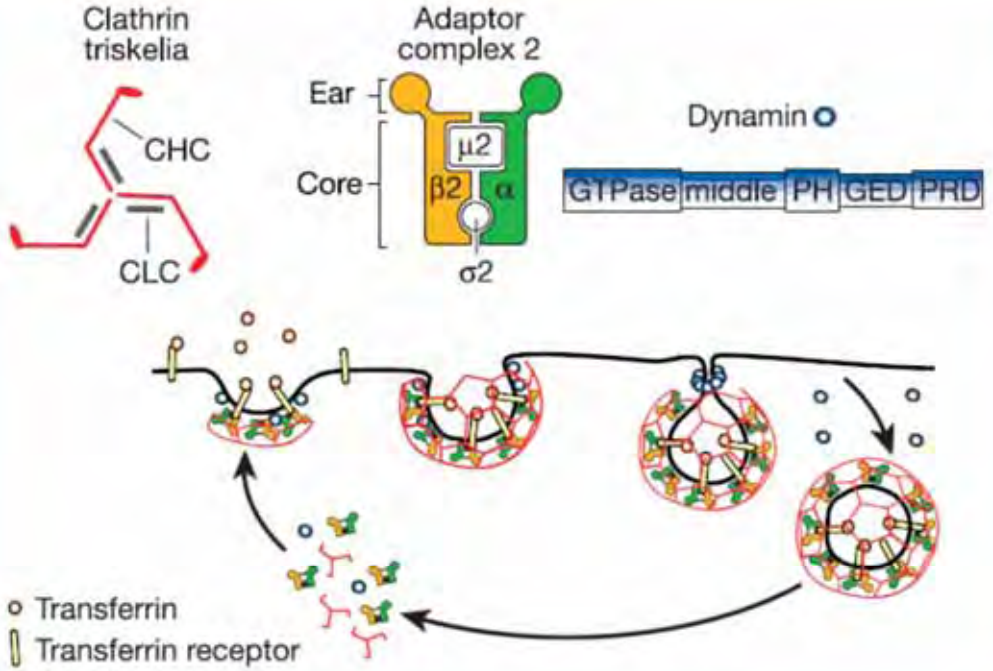

Figure 3 Core components of the machinery driving clathrin-mediated endocytosis. Clathrin triskelions, composed of three clathrin heavy chains (CHC) and three tightly associated light chains (CLC), assemble into a polygonal lattice, which helps to deform the overlying plasma membrane into a coated pit. Heterotetrameric AP2 complexes are targeted to the plasma membrane by the α-adaptin subunits, where they mediate clathrin assembly through the β2-subunit, and interact directly with sorting motifs on cargo molecules through their μ2 subunits. Dynamin is a multidomain GTPase that is recruited to the necks of coated pits, where it can assemble into a spiral or 'collar' to mediate or monitor membrane fission and the release of CCVs (see text for details). A subsequent uncoating reaction recycles the coat constituents for reuse.

Clathrin-mediated endocytosis

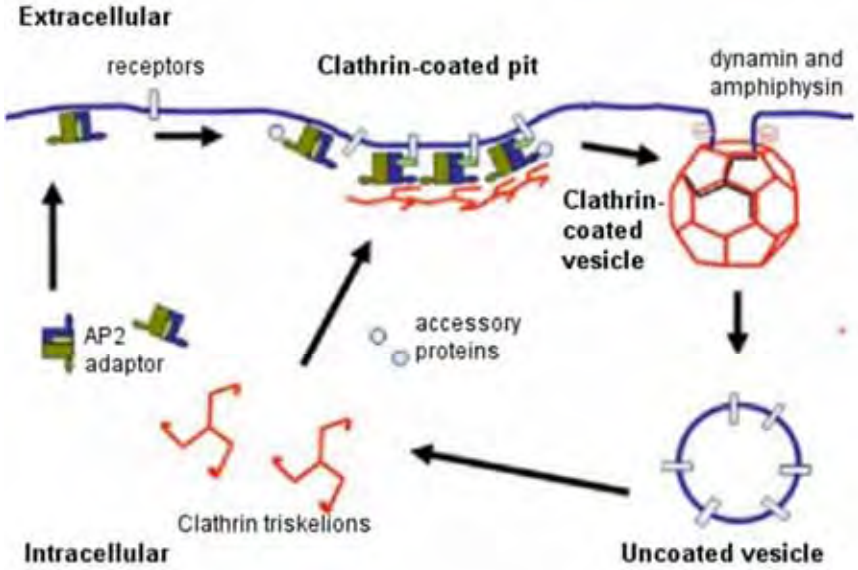

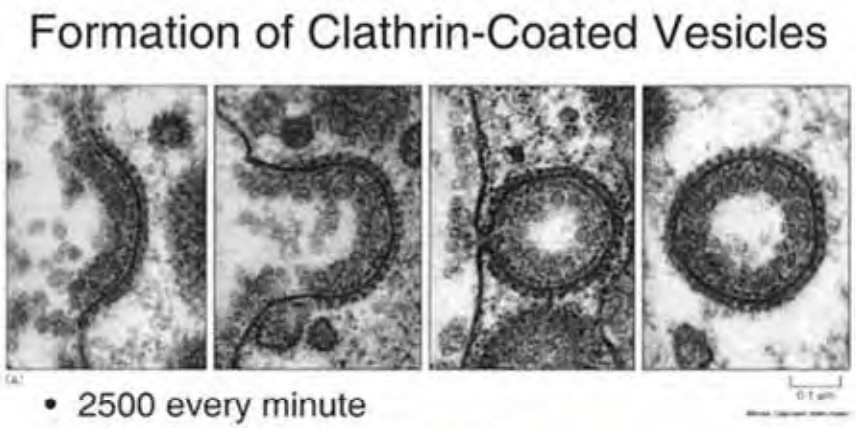

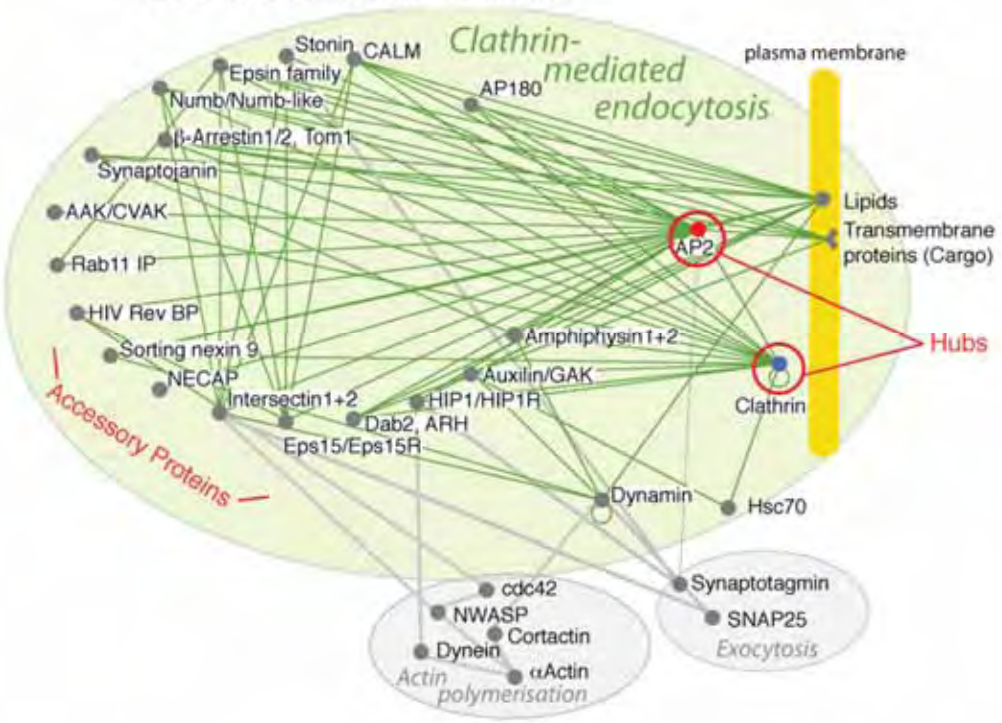

A

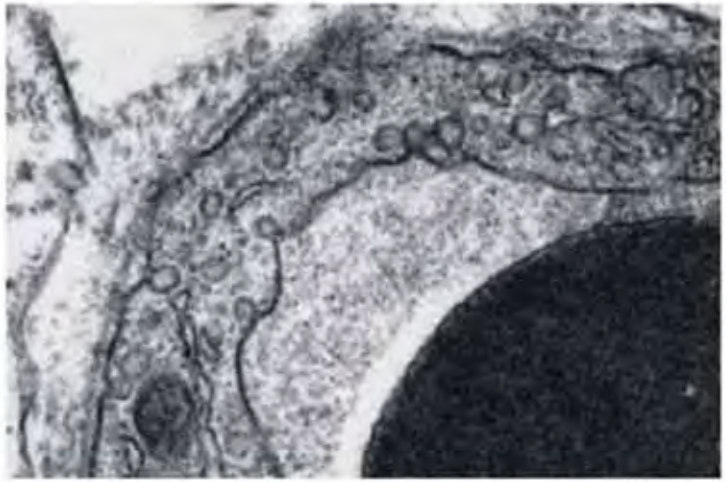

B

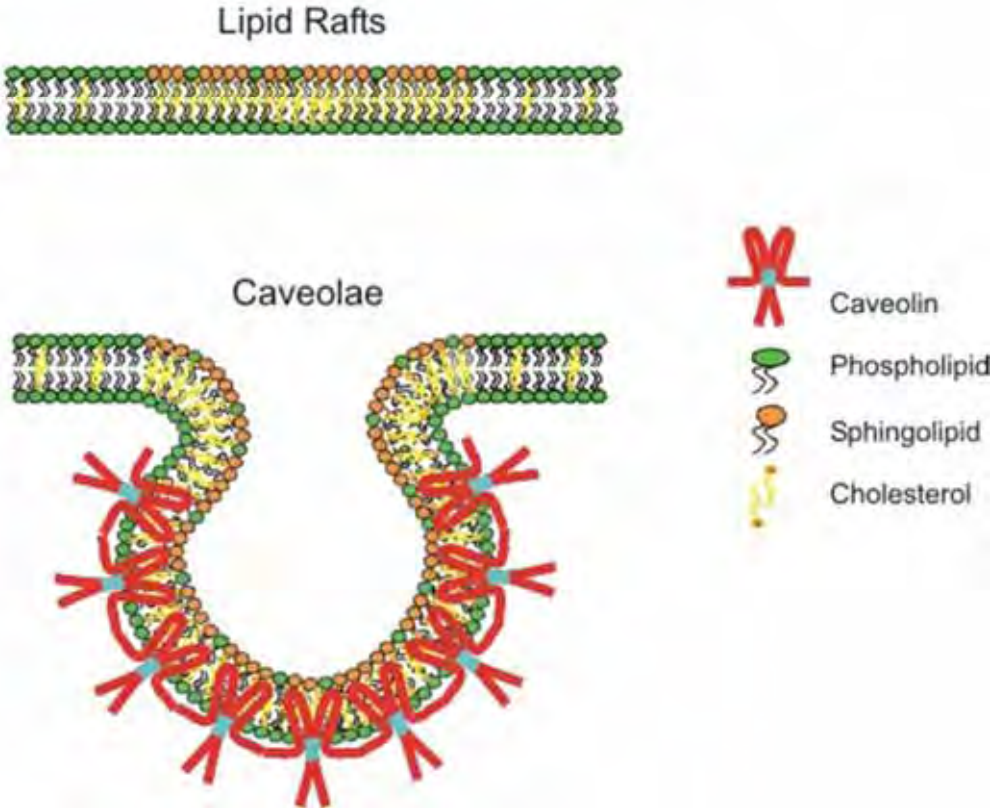
Lipid Rafts
Caveolae
Caveolin
Phospholipid
Sphingolipid
Cholesterol

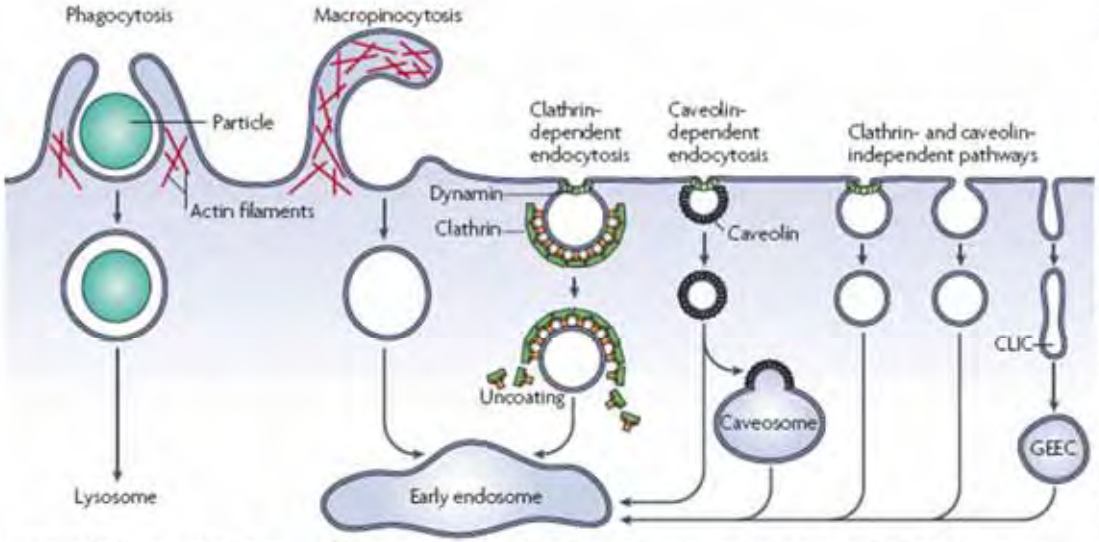

Figure 1 | **Pathways of entry into cells.** Large particles can be taken up by phagocytosis, whereas fluid uptake occurs by macropinocytosis. Both processes appear to be triggered by and are dependent on actin-mediated remodelling of the plasma membrane at a large scale. Compared with the other endocytic pathways, the size of the vesicles formed by phagocytosis and macropinocytosis is much larger. Numerous cargoes (TABLE 1) can be endocytosed by mechanisms that are independent of the coat protein clathrin and the fission GTPase, dynamin. This Review focuses on the clathrin-independent pathways, some of which are also dynamin independent (FIGS 2,3). Most internalized cargoes are delivered to the early endosome via vesicular (clathrin- or caveolin-coated vesicles) or tubular intermediates (known as clathrin- and dynamin-independent carriers (CLICs)) that are derived from the plasma membrane. Some pathways may first traffic to intermediate compartments, such as the caveosome or glycosyl phosphatidylinositol-anchored protein enriched early endosomal compartments (GEEC), *en route* to the early endosome.

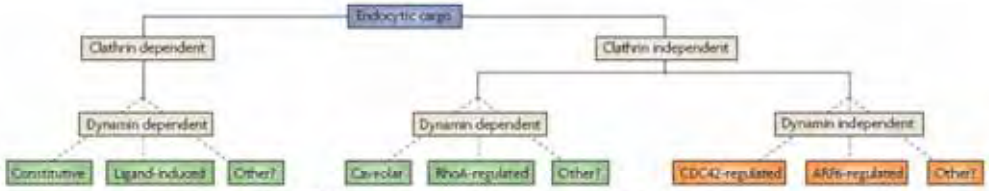

Figure 3 | **Proposed classification system for endocytic mechanisms.** A cargo protein can be endocytosed by either clathrin-dependent or clathrin-independent (CI) mechanisms. We propose that the CI pathways can be further categorized first by their dependence on the large GTPase dynamin, and then by other mechanistic components of the internalization pathway. This system is based on the current literature, which shows that interfering with or modifying the function of a particular GTPase affects the internalization or trafficking of one set of CI endocytic markers but not another. See TABLE 1 for endocytic markers that have been studied. The aim of this classification system for CI pathways is to categorize the molecular machinery that is associated with these pathways in the most parsimonious fashion consistent with the current literature. It is not meant to imply that a given GTPase is directly involved in regulating a particular internalization pathway because many other important cellular functions may also be regulated by that GTPase. There may be other, as-yet-unidentified CI pathways.

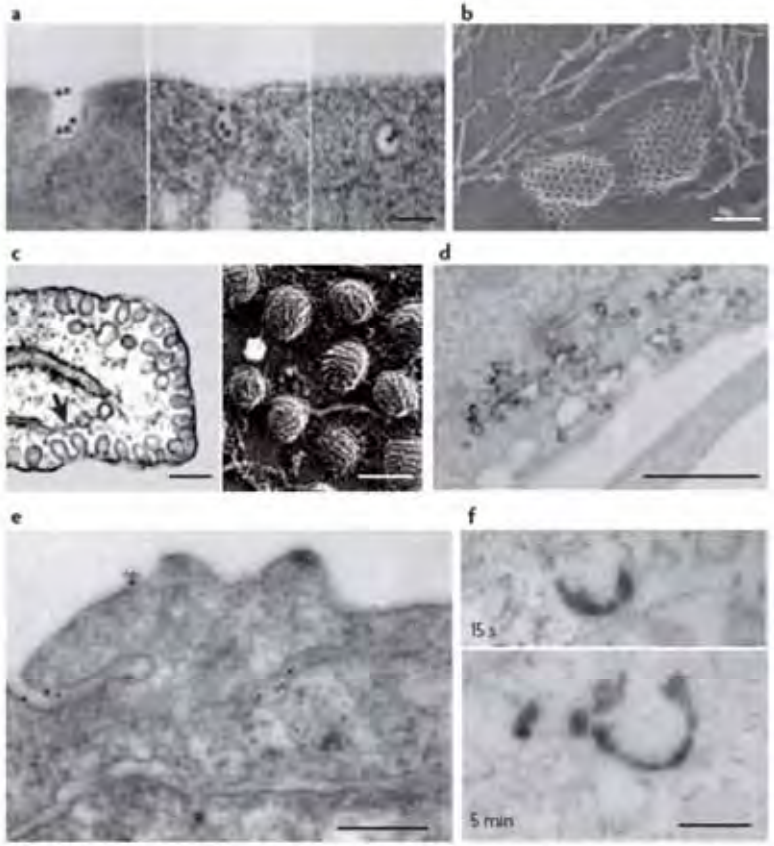

Figure 2 | **Electron micrographs of early intermediates in clathrin-dependent and independent pathways of endocytosis. a** | Thin-section views of reticulocytes incubated with gold-conjugated transferrin (AuTf) for 5 min at 37°C, which shows AuTf clustering into clathrin-coated pits and subsequently being endocytosed via coated vesicles. **b** | Rapid-freeze, deep-etch views of clathrin lattices on the inner surface of a normal chick fibroblast. **c** | Thin-section (left panel) and rapid-freeze, deep-etch images (right panel) of caveolae in endothelial cells. The arrow in the left panel points to the endoplasmic reticulum near deeply invaginated caveolae. **d** | Thin-section surface view of horseradish peroxidase (HRP)-conjugated cholera toxin in the process of internalization via grape-like caveolae in mouse embryonic fibroblasts. **e** | Thin-section images of green fluorescent protein (GFP) with a glycosyl phosphatidylinositol (GPI) anchor expressed in Chinese hamster ovary cells and incubated with gold-conjugated antibodies against GFP. The antibodies show putative sites for clathrin- and dynamin-independent endocytosis. These represent surface-connected tubular invaginations where the gold probe is concentrated with respect to the rest of the plasma membrane. **f** | Thin-section micrographs of internalized HRP-conjugated cholera toxin incubated at 37°C in mouse embryonic fibroblasts, showing early intermediates in clathrin- and caveolin-independent endocytosis. Clathrin- and dynamin-independent carriers (CLICs) are observed after 15 s (top panel) and GPI-anchored protein enriched early endosomal compartments (GEECs) are observed after 5 min (bottom panel). The scale bar in **a** and **b** is 100 nm, in **c** is 200 nm (left panel) and 100 nm (right panel), and in **d**–**f** is 200 nm.

For a cell to move, it must adhere to a substrate and exert traction. Adhesion occurs at specific foci at which the actin cytoskeleton on the inside of the cell is linked via transmembrane receptors (integrins) to the extracellular matrix on the outside. These adhesion sites are composed of complexes of more than 50 different proteins

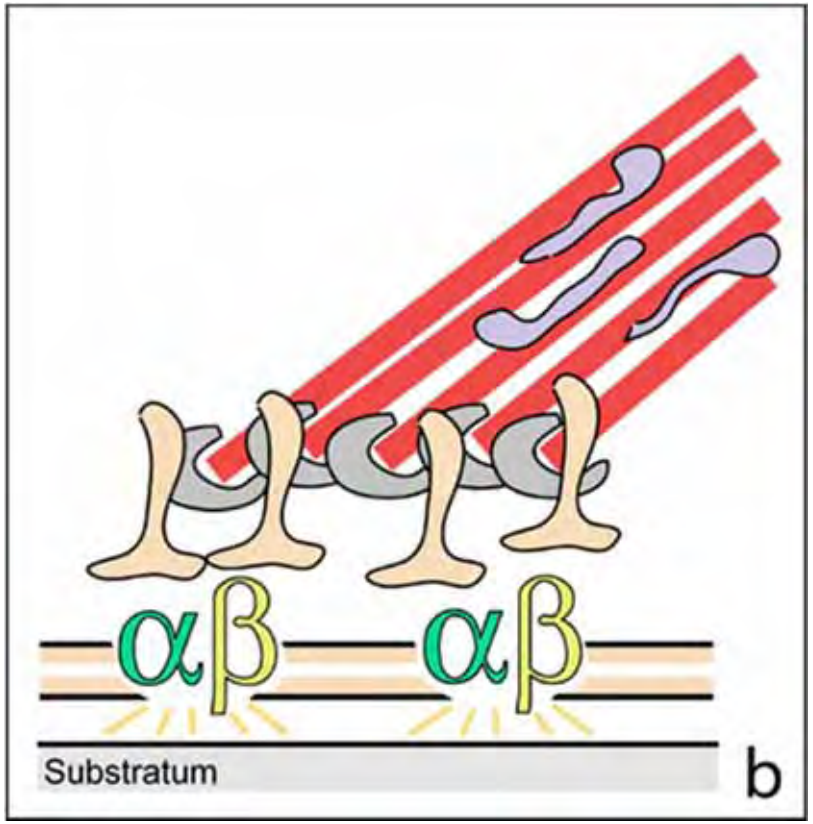

Highly simplified schematic illustration of the organisation of a focal adhesion. Transmembrane integrins (alpha/beta) bind to matrix ligands on the outside of the cell, and to a complex of molecules inside the cell that link to actin filaments. At focal adhesions, the actin filaments are bundled by actin filament cross-linkers, including the contractile protein myosin. Tension in the bundle, generated by myosin, is required to maintain the clustering of integrins and the integrity of focal adhesions

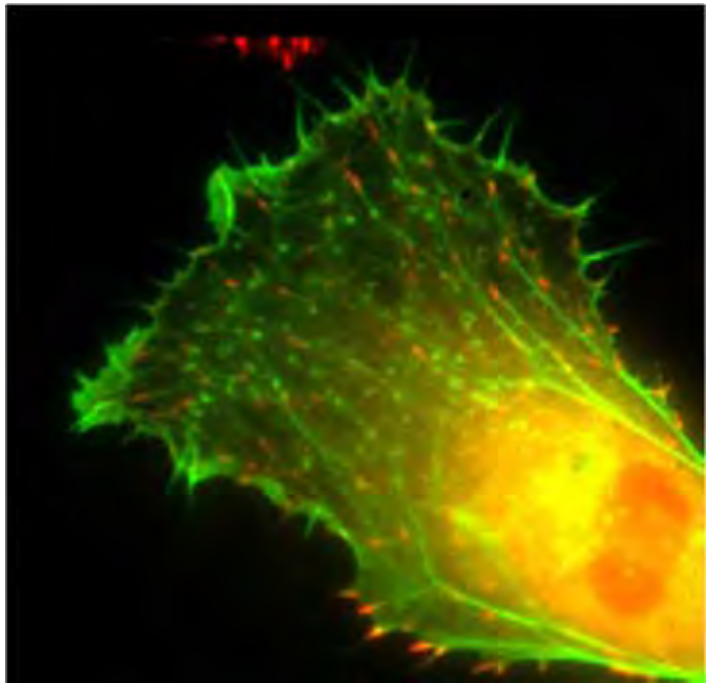

The formation of substrate adhesion sites in a migrating goldfish fibroblast. The cell was transfected with GFP-actin (green) and microinjected with rhodamine-tagged vinculin (an adhesion component; red). The protruding cell front is marked by a diffuse band of actin filaments (the lamellipodium), which contains radial filament bundles (filopodia) that project beyond the cell edge. Different types of adhesion foci (red) can be distiguished: small foci in association with lamellipodia and filopodia (focal complexes) and, behind the lamellipodium, larger foci associated with actin filament bundles (focal adhesions). Focal adhesions are also observed at the periphery of retracting cell edges (bottom region of figure). Focal complexes and focal adhesions in the advancing front remain stationary, relative to the substrate, whereas, focal adhesions at the retracting edges can slide.

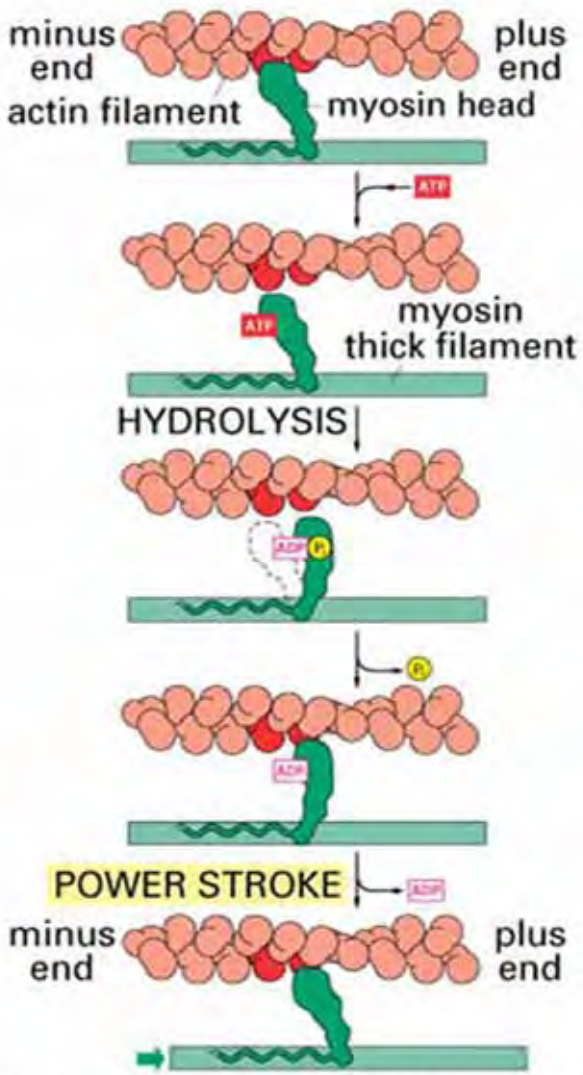

Figure 17-45 Essential Cell Biology, 2/e. (© 2004 Garland Science)

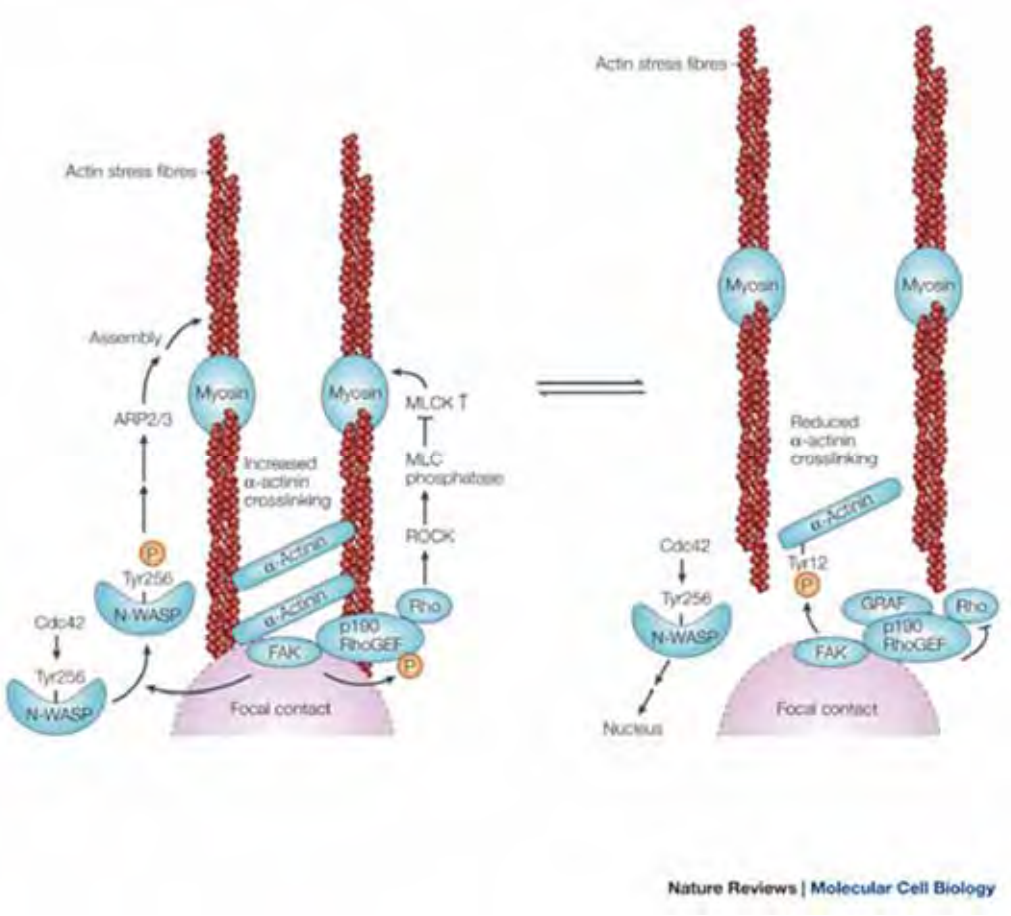

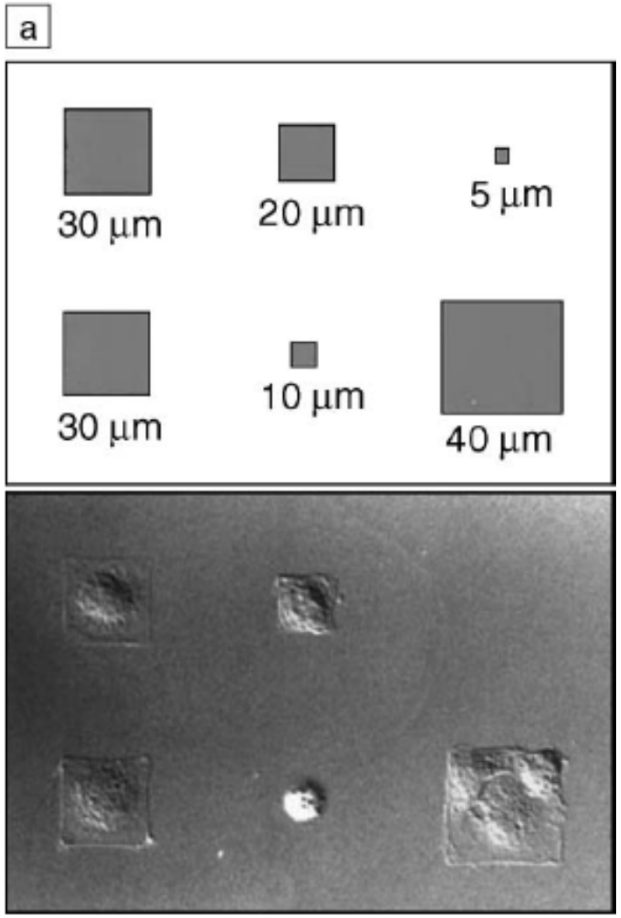

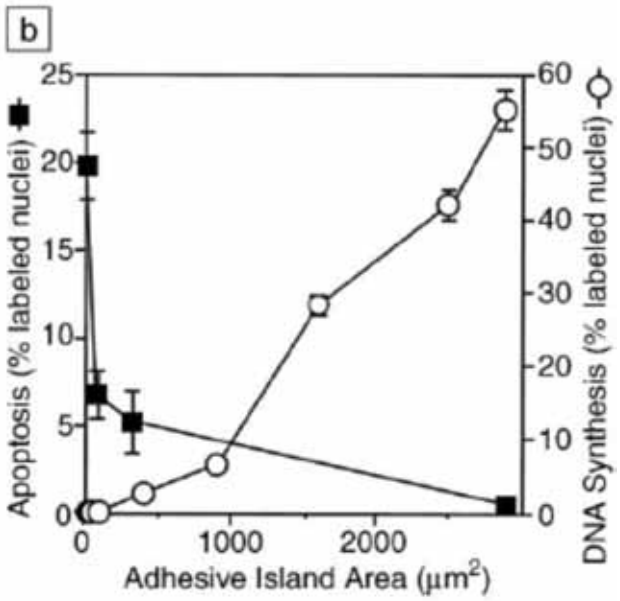

Figure 2. The influence of the footprint of a cell on its choice between growth and apoptosis. (a) (top) Schematic diagram showing the pattern: square islands of self-assembled monolayers (SAMs) to which proteins stick, surrounded by a different SAM to which proteins do not adsorb; (bottom) Nomarski microscopic image of the shapes of bovine adrenal capillary endothelial cells confined to the patterns. Scale labels indicate lengths of the sides of the squares. (b) Changes in cell shape as cells attach, spread, and flatten on an adhesive surface can regulate cell growth and death: apoptotic (cell death) index versus DNA synthesis (cell growth) index after 24 h, plotted as a function of the area of the spread cell.

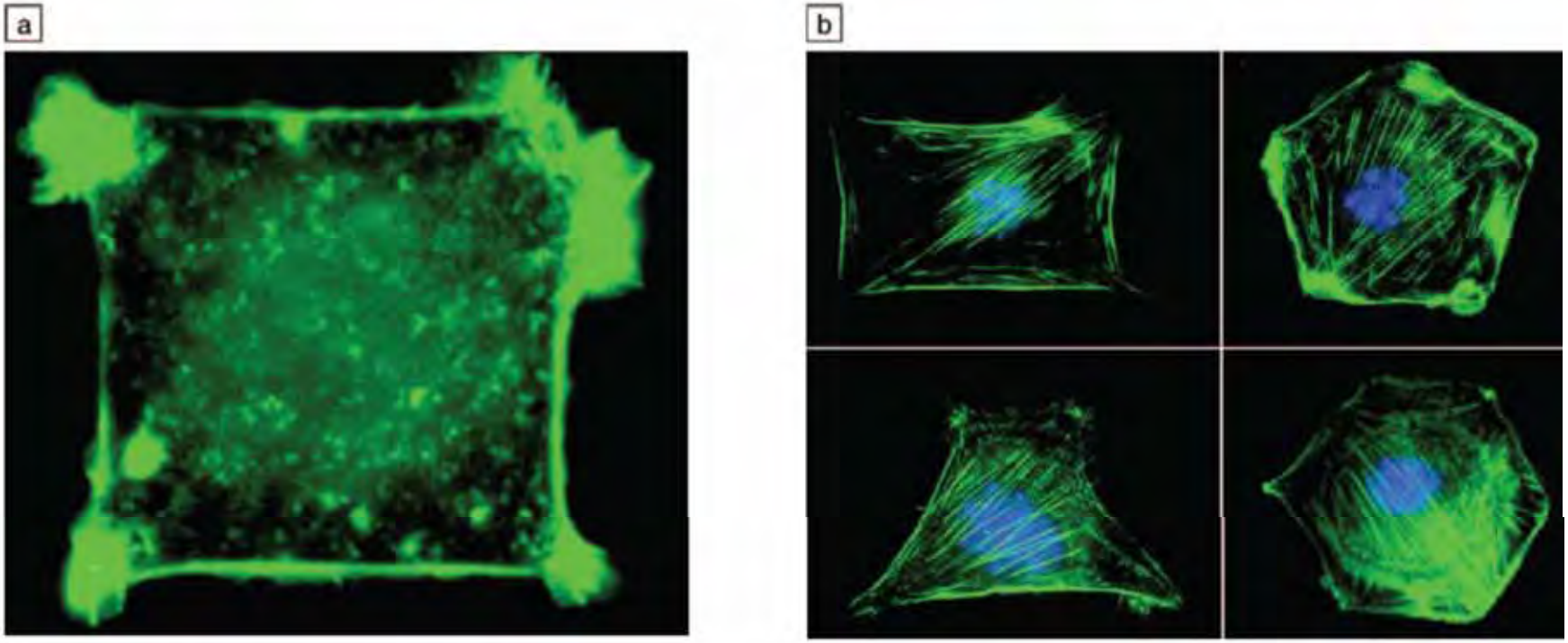

Figure 3. (a) A cell spread on a square 30 μm × 30 μm island; the cell was stimulated with platelet-derived growth factor (PDGF) and stained for F-actin with fluorophore-labeled phalloidin. (b) Cells confined to various shapes (all with areas of 900 μm^2) were stimulated with PDGF and stained with phalloidin and 4′-6-diamidino-2-phenylindole to visualize F-actin (green) and nuclei (blue). Images obtained by fluorescence microscopy.

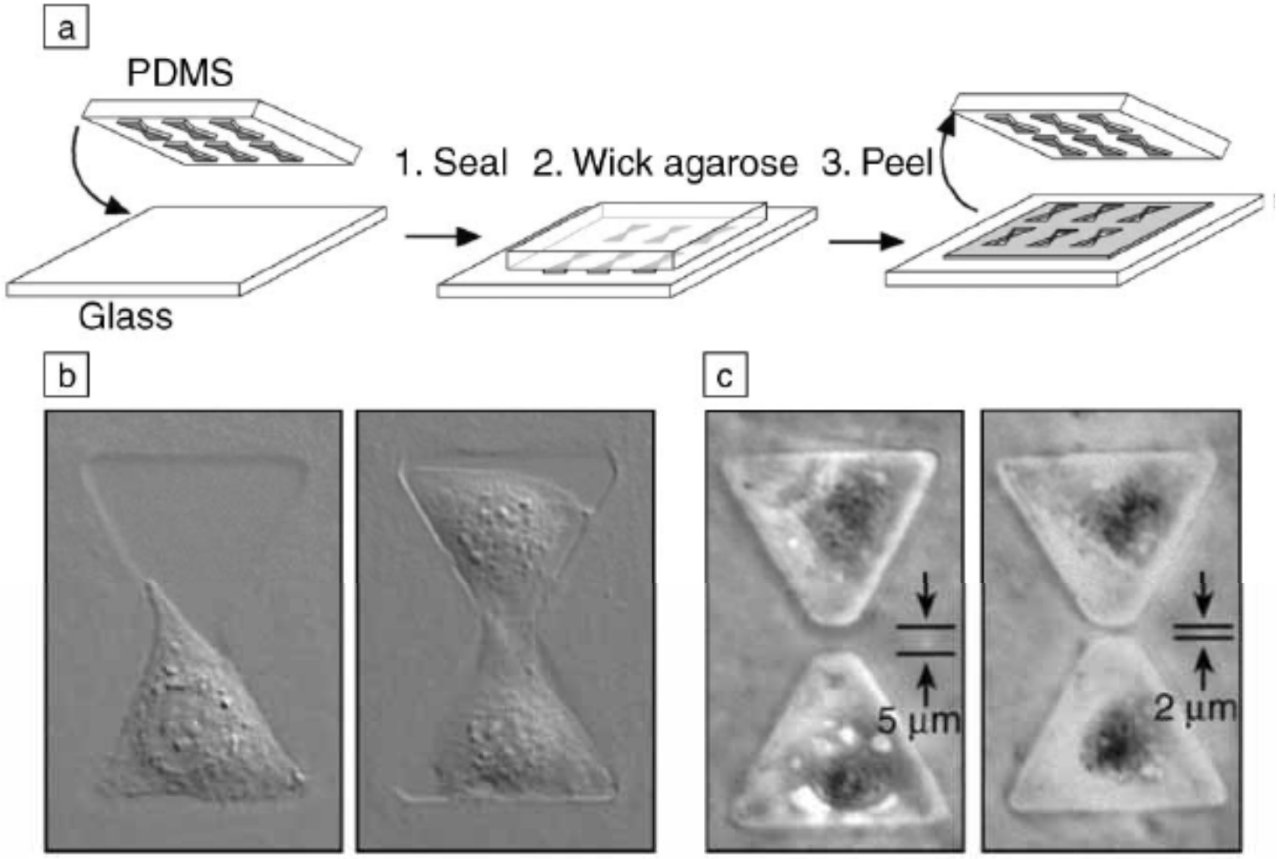

Figure 6. Method to induce cells to culture in pairs with control over the contact between them. (a) Agarose is wicked into channels formed by a poly(dimethylsiloxane) stamp sealed against a glass coverslip and allowed to gel before the stamp is peeled off. (b) When cells are seeded onto these substrates containing bowtie-shaped wells, cells attach and culture as either single cells or pairs. (c) The single cell-to-cell contact formed in these pairs can be blocked by fabricating substrates in which the agarose forms a thin wall, cutting the bowtie-shaped wells into separate, although closely spaced, wells.

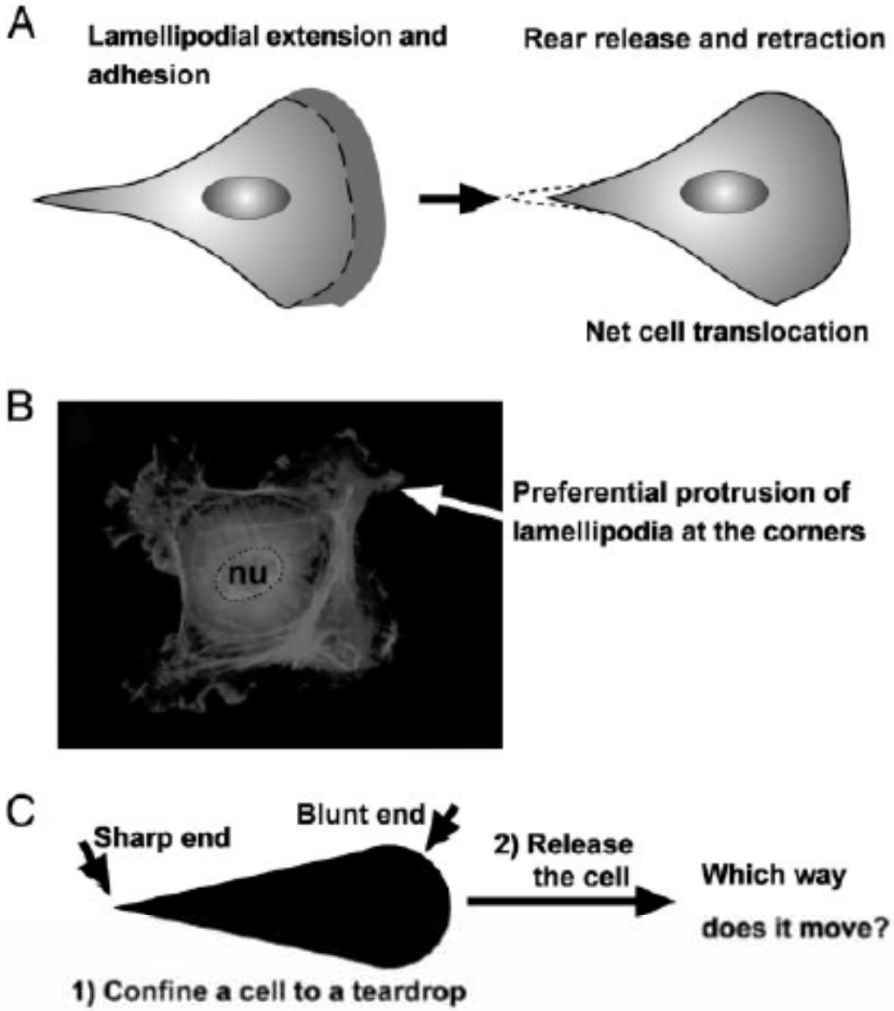

Fig. 1. A problem on cell motility. (*A*) A cartoon illustration of the migration of a typical mammalian cell on a flat surface. This teardrop shape is found in many types of cells. (*B*) Cells confined to squares preferentially extend their lamellipodia from the corners. nu, nucleus. (*C*) If a cell is confined to a shape of teardrop, will the cell preferentially extend its lamellipodia from the sharp end or from the blunt end? If released from confinement, in which direction will it likely move?

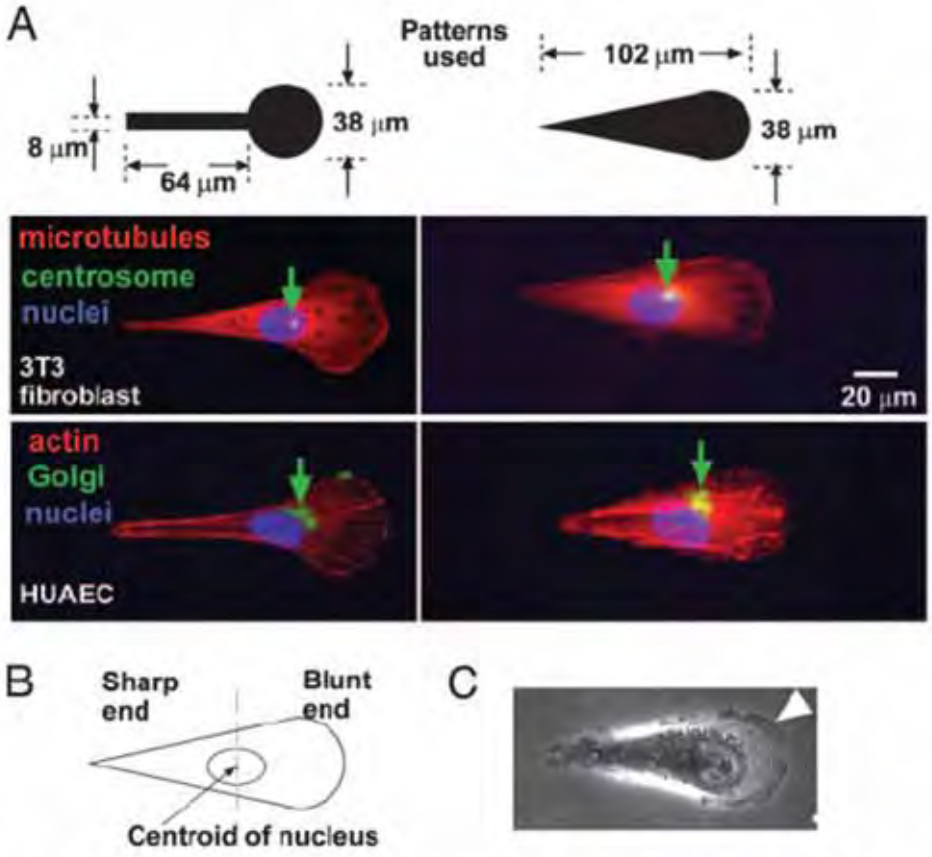

Fig. 2. Asymmetric patterns polarize immobilized cells. (*A*) The Golgi and the centrosome are located closer to the half of a cell with the blunt end. We used phallodin, antigolgin, DAPI, antitubulin, and antipericentrin to identify actin (red), the Golgi (green), the nucleus (blue), microtubules (red), and the centrosome (green), respectively. The green arrows indicate the location of centrosomes in 3T3 cells and Golgi in human umbilical artery endothelial cells (HUAEC). (*B*) We divided the cell into a half with the sharp end and a half with the blunt end by a vertical line drawn at the centroid of the nucleus; >80% ($n = 30$) of the centrosomes and Golgi were localized in the region of the wide end. (*C*) The lamellipodia of immobilized 3T3 cells tended to extend more from the blunt end as well (arrowhead). The dotted line indicates the edges of the adhesive pattern.

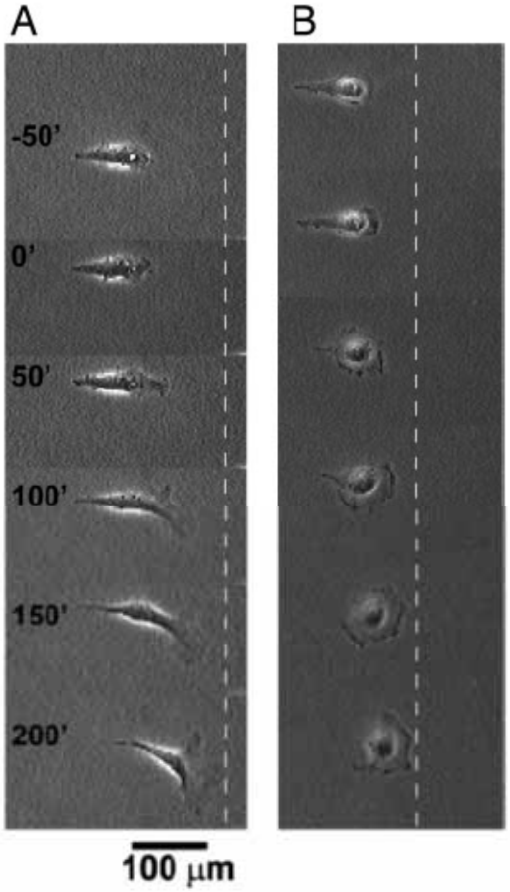

Fig. 3. Time-lapse images (in minutes) show the motility of an initially polarized 3T3 fibroblast after its constraint is released. (*A*) We applied the voltage pulse at time $t = 0$. The dotted line serves as a reference for the location of the cell. (*B*) Another type of cell, COS-7, shows similar behavior.

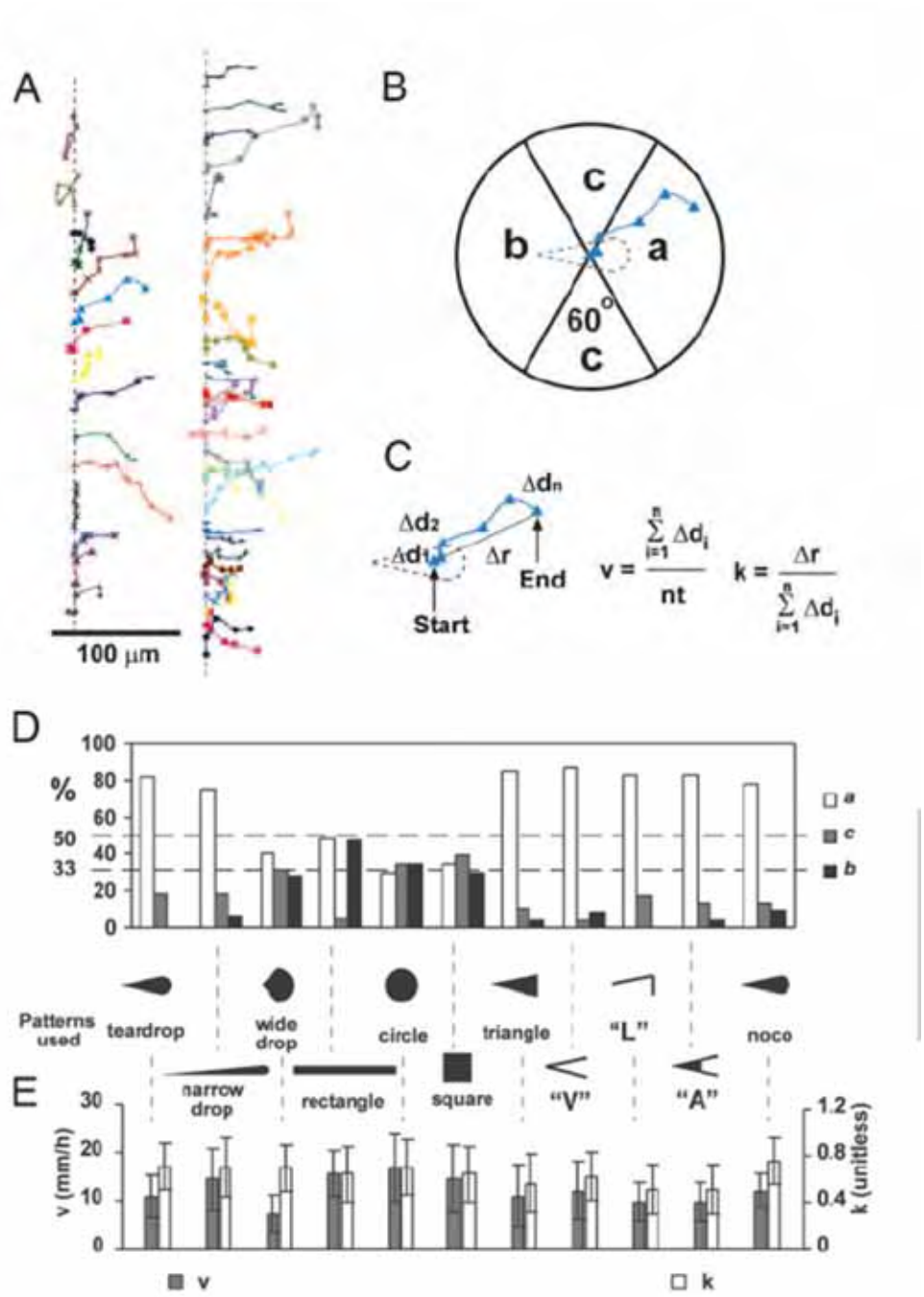

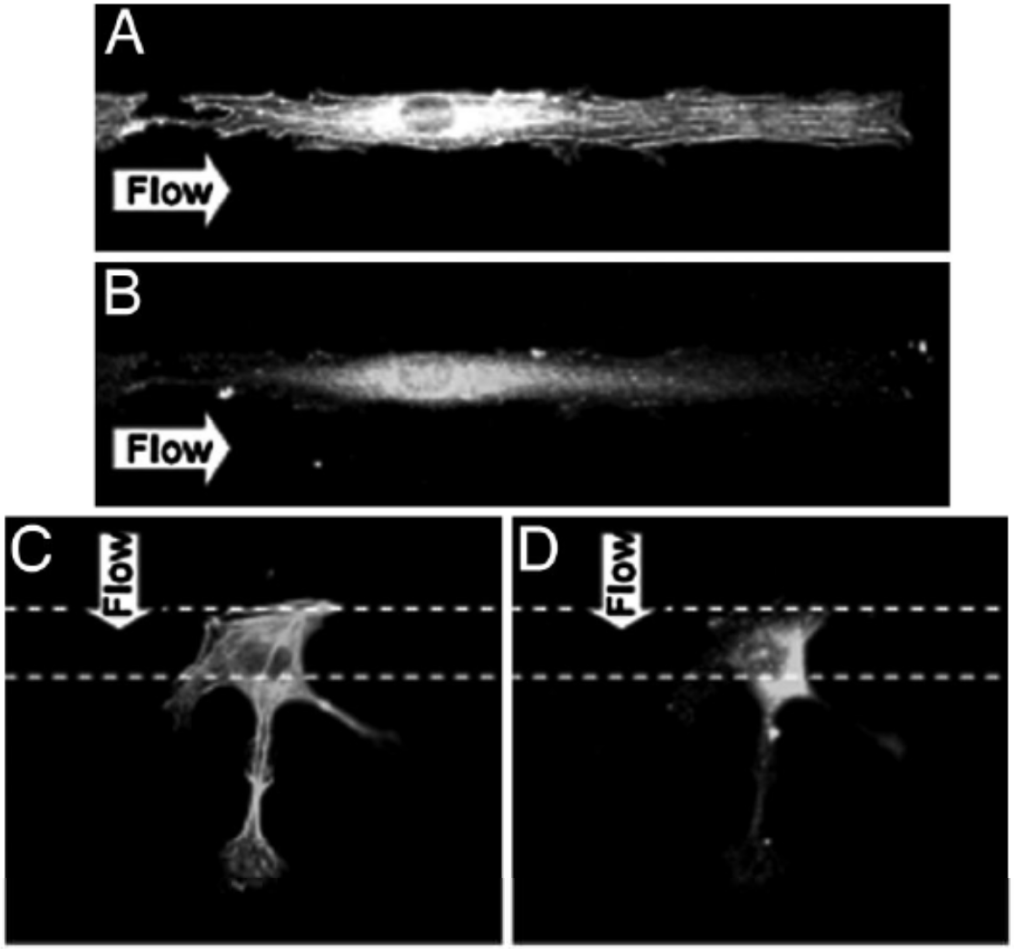

Fig. 3. HUVEC remodeling on MP strips under flow in different directions. Parallel flow increased the stress fiber formation for cytoskeleton remodeling (*A*) and *p*-FAK for the anchoring points at the ends of stress fibers (*B*). In contrast, the perpendicular flow increased the stress fibers (*C*) and *p*-FAK (*D*) in the ineffective NP surface and therefore mitigated the effectiveness of these inductions.

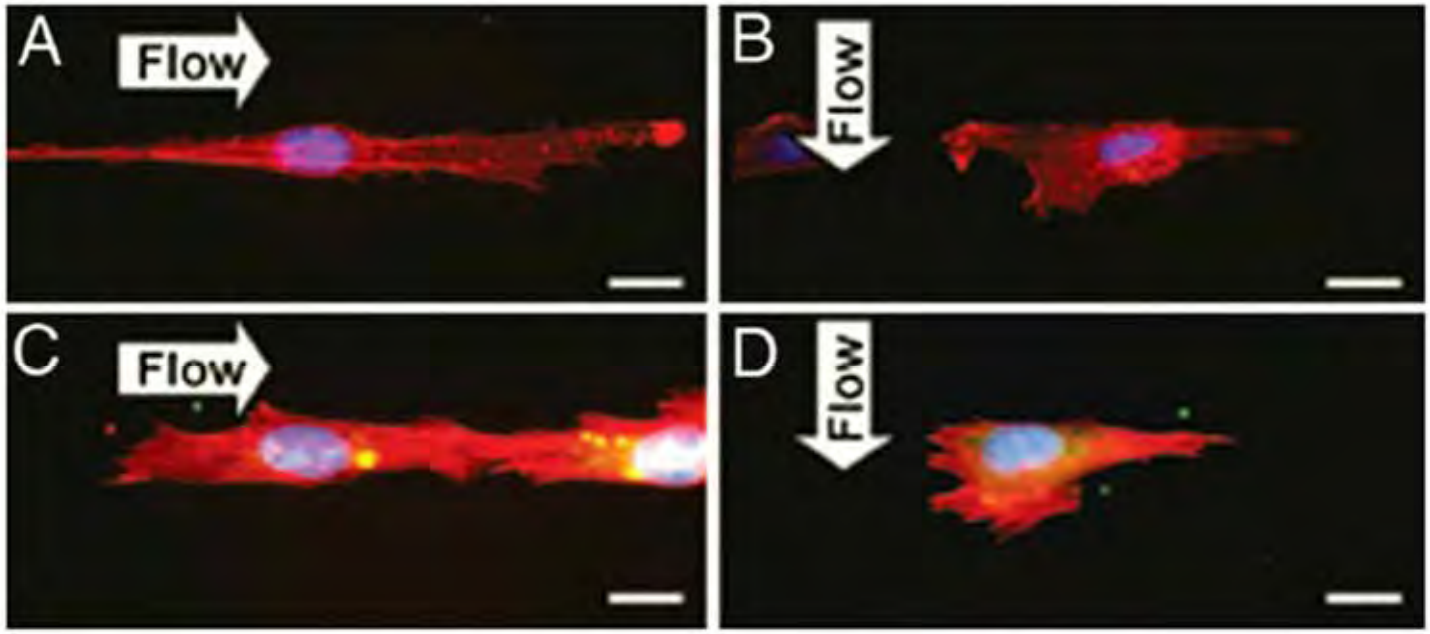

Fig. 6. Rho activities attenuate constraint-induced apoptosis and enable cytoskeleton remodeling independent of flow direction. Shown are images for HUVECs transfected with C3 exoenzyme (*A* and *B*) or RhoV14 (*C* and *D*) on 15-μm strips, and then subjected to parallel (*A* and *C*) or perpendicular (*B* and *D*) flow. The inhibition of Rho activities abolished the antiapoptotic effect of parallel flow and blocked the formation of stress fibers (*A*); RhoV14 attenuated constraint-induced cell apoptosis and restored the actin cytoskeleton under both flow directions (*C* and *D*). Cells were immunostained in the same method as Fig. 4. (Scale bar: 15 μm.)

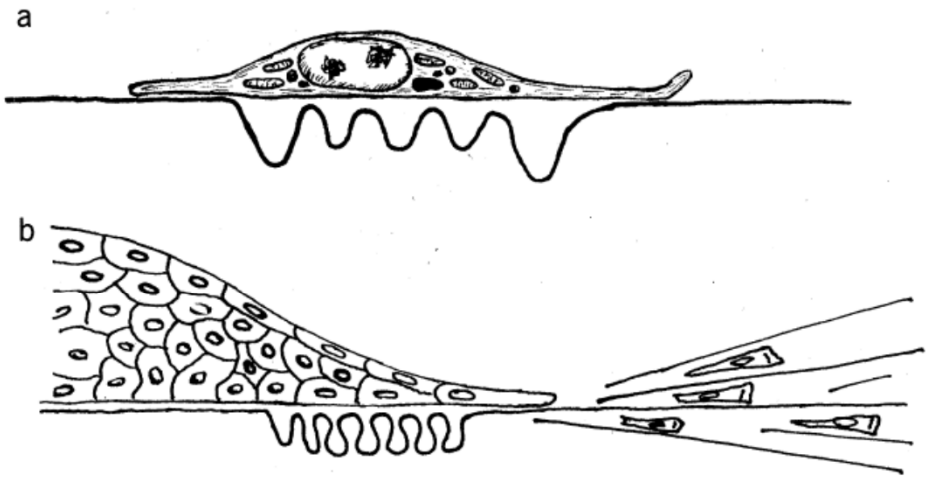

Fig. 1. (a) Diagrammatic side view of an individual cultured fibroblast distorting and wrinkling the elastic silicone substratum upon which it has spread and is crawling. (b) Diagrammatic side view of the margin of an explant whose cells are spreading outward on a silicone rubber substratum. The traction forces exerted by the outgrowing cells compress the rubber sheet beneath the explant and stretch it into long radial wrinkles in the surrounding area.

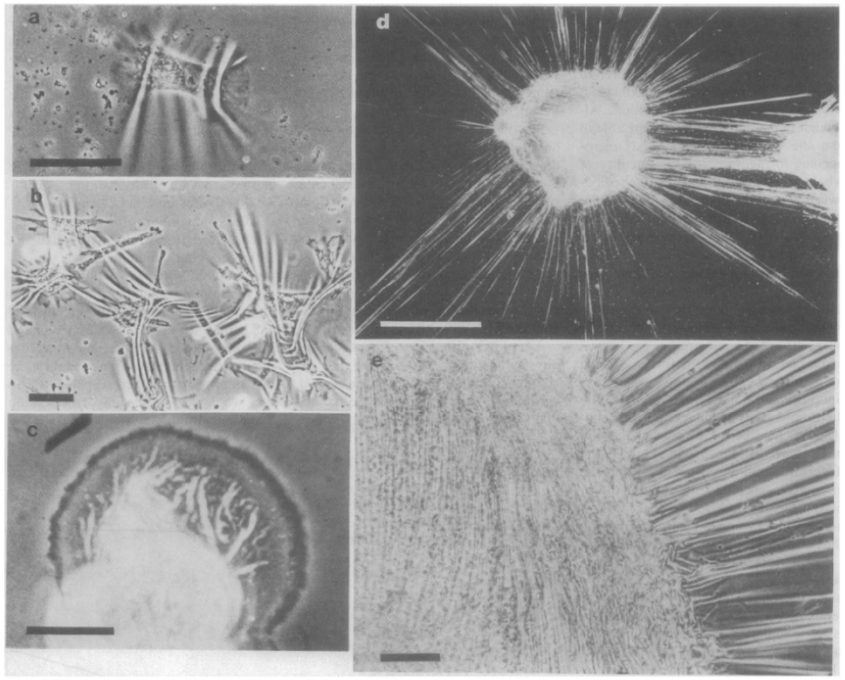

Fig. 2. (a) An individual chick heart fibroblast whose locomotion and contractility have visibly wrinkled the silicone rubber substratum upon which it is crawling (the bar is 50 μm long). (b) Lower magnification view of about a dozen chick heart fibroblasts and the complex pattern of distortions produced in the rubber substratum by their locomotory traction (the bar is 100 μm). (c) Higher magnification view of an individual PTK-1 cell just beginning to spread onto a silicone rubber sheet after trypsinization. Ruffling activity is seen as a dark band around the periphery, while the wrinkles being generated in the substratum are seen as irregular white bands beneath the cell body (from an individual frame of a 16-mm time-lapse film; the bar is 20 μm long). (d) Very low magnification, dark-field illumination view of a chick heart explant that had been spreading on a silicone rubber substratum for 48 hours. The bright radiating lines are stress wrinkles. Notice the "two-center effect" of wrinkles running between the large central explant and the smaller one at the edge of the photograph at the right (the bar is 1 mm long). (e) Higher magnification, phase-contrast view of the marginal outgrowth zone of the same explant as shown in (d). The compression folds beneath the explant are seen on the left and the radial stress wrinkles around it are on the right (the bar is 100 μm long).

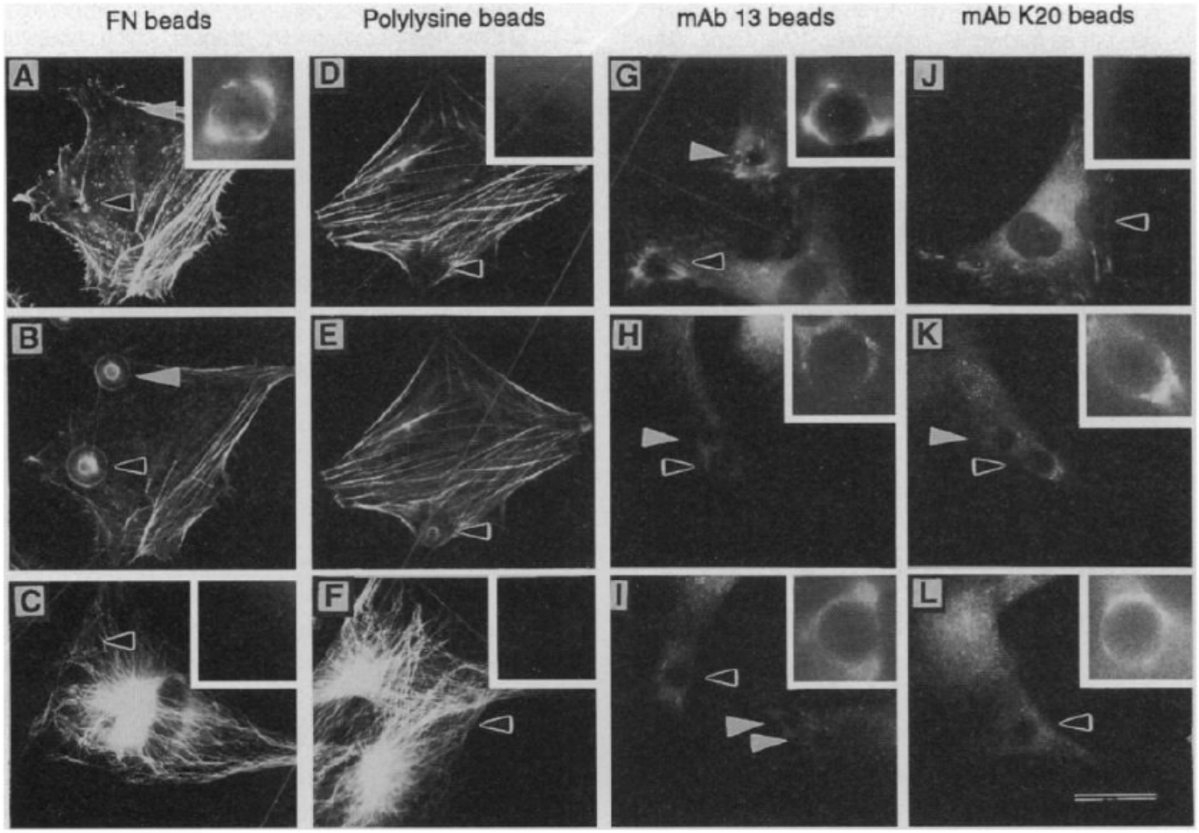

Fig. 1. Immunofluorescence for juxtamembrane accumulation of cytoskeletal proteins and FAK induced by beads coated with ligands or antibodies to integrin (*4*). Each inset shows a higher-magnification view, focusing on the equator of the bead marked by a highlighted black arrowhead; white arrowhead indicates a second bead bound to the cell. (**A** to **C**) Fibronectin-coated beads. Localization of F-actin as detected by rhodamine-labeled phalloidin (A), compared with combined transmitted light and fluorescence to illuminate the bead (B); no tubulin immunolocalization was detected adjacent to these beads (C). Lack of F-actin adjacent to polylysine-coated beads (**D**), and transmitted light to illuminate the bead (**E**); absence of tubulin immunolocalization (**F**). Effects of beads coated with adhesion-blocking mAb 13 (**G** to **I**) or noninhibitory mAb K20 (**J** to **L**) (both mAbs bind the β_1 subunit) on immununolocalization of paxillin (G and J), tensin (H and K), and FAK (I and L). Scale bar, 20 μm.

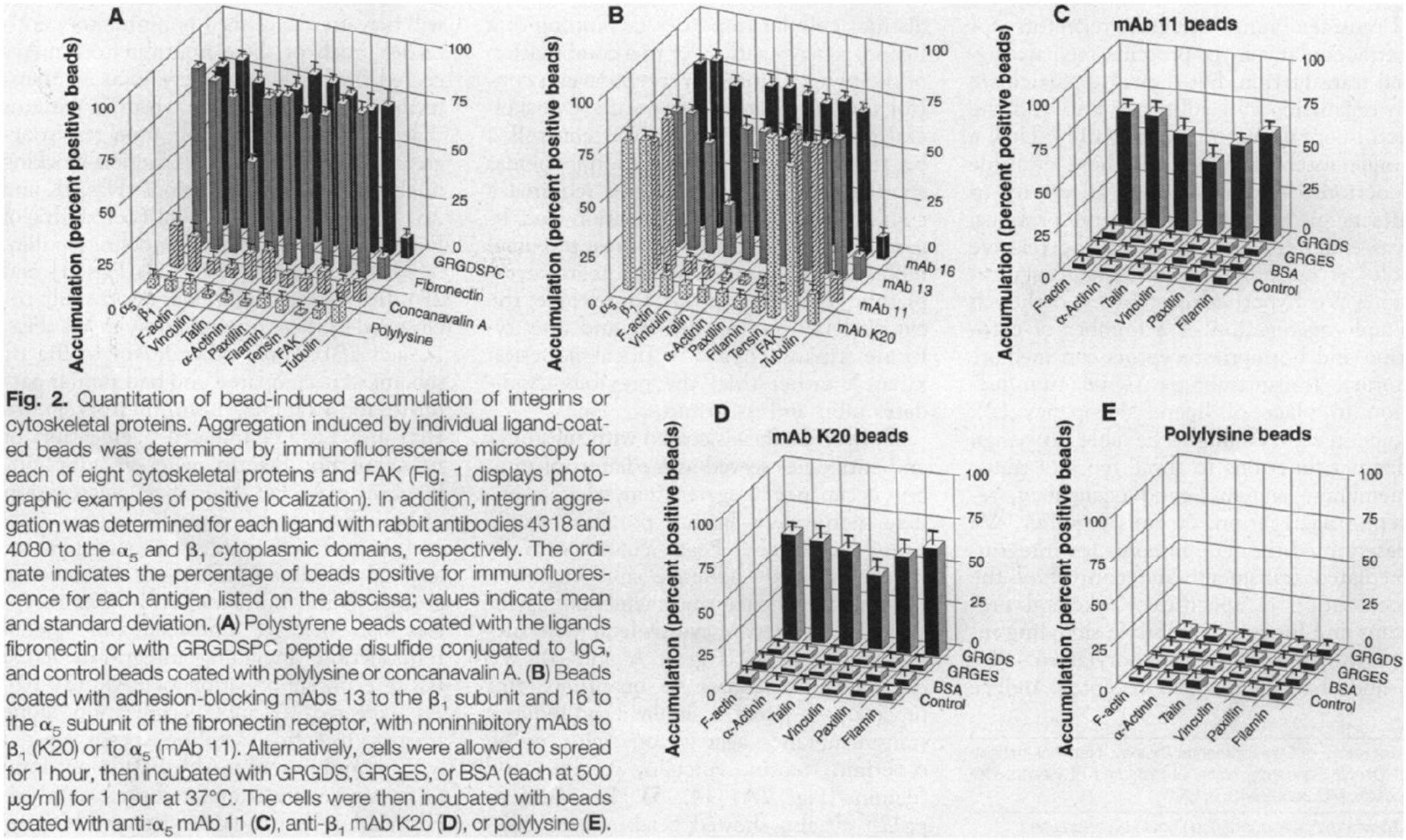

Fig. 2. Quantitation of bead-induced accumulation of integrins or cytoskeletal proteins. Aggregation induced by individual ligand-coated beads was determined by immunofluorescence microscopy for each of eight cytoskeletal proteins and FAK (Fig. 1 displays photographic examples of positive localization). In addition, integrin aggregation was determined for each ligand with rabbit antibodies 4318 and 4080 to the α_5 and β_1 cytoplasmic domains, respectively. The ordinate indicates the percentage of beads positive for immunofluorescence for each antigen listed on the abscissa; values indicate mean and standard deviation. (**A**) Polystyrene beads coated with the ligands fibronectin or with GRGDSPC peptide disulfide conjugated to IgG, and control beads coated with polylysine or concanavalin A. (**B**) Beads coated with adhesion-blocking mAbs 13 to the β_1 subunit and 16 to the α_5 subunit of the fibronectin receptor, with noninhibitory mAbs to β_1 (K20) or to α_5 (mAb 11). Alternatively, cells were allowed to spread for 1 hour, then incubated with GRGDS, GRGES, or BSA (each at 500 μg/ml) for 1 hour at 37°C. The cells were then incubated with beads coated with anti-α_5 mAb 11 (**C**), anti-β_1 mAb K20 (**D**), or polylysine (**E**).

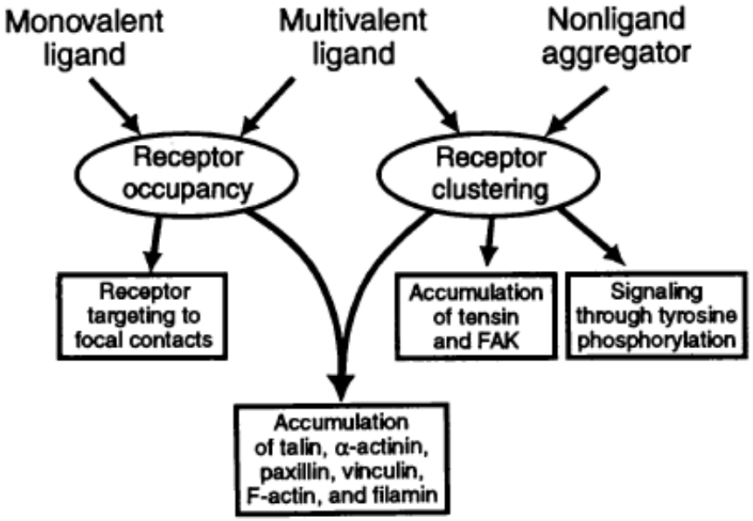

Fig. 4. Diagram summarizing proposed roles of receptor occupancy and receptor clustering in integrin responses to extracellular ligands. Unlike soluble growth factors and hormones, extracellular matrix molecules often exist as multivalent ligands immobilized in matrices or fibrils (*16*). Their functions in inducing ligand occupancy and formation of receptor clustering can be separated experimentally by the use of the monovalent peptide ligand GRGDS or beads coated with noninhibitory antibodies to integrin (nonligand aggregator), respectively. Each activating stimulus produces specific effects, and their actions synergize to induce accumulation of most cytoskeletal proteins examined. Extracellular matrix aggregates or matrix-coated beads produce all sets of responses because they induce both ligand occupancy and receptor clustering as a result of their multivalency.

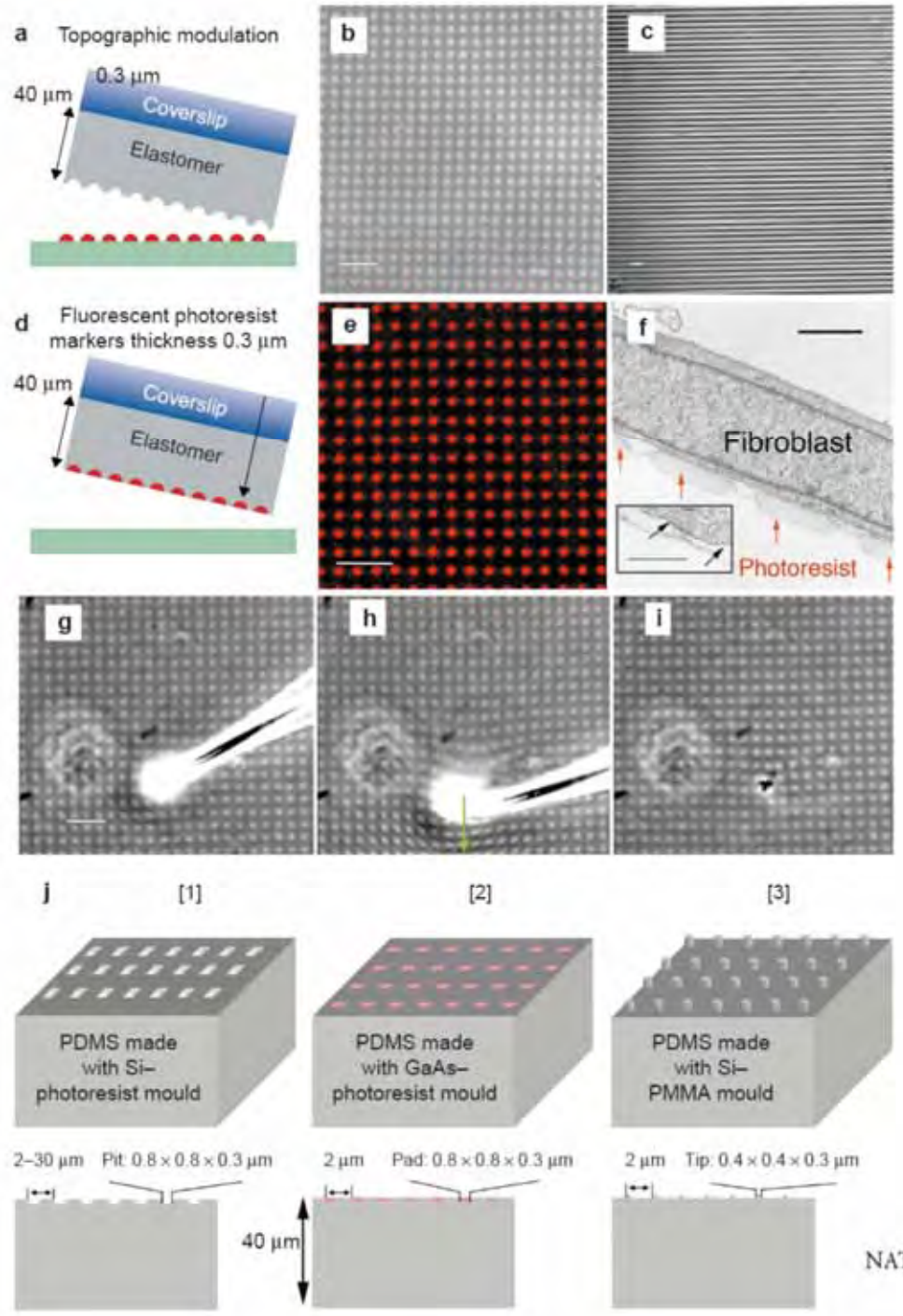
a
Topographic modulation
0.3 µm
40 µm
Coverslip
Elastomer
b
c
d
Fluorescent photoresist markers thickness 0.3 µm
40 µm
Coverslip
Elastomer
e
f
Fibroblast
Photoresist
g
h
i
j
[1]
[2]
[3]
PDMS made with Si–photoresist mould
PDMS made with GaAs–photoresist mould
PDMS made with Si–PMMA mould
2–30 µm
Pit: 0.8 × 0.8 × 0.3 µm
2 µm
Pad: 0.8 × 0.8 × 0.3 µm
2 µm
Tip: 0.4 × 0.4 × 0.3 µm
40 µm

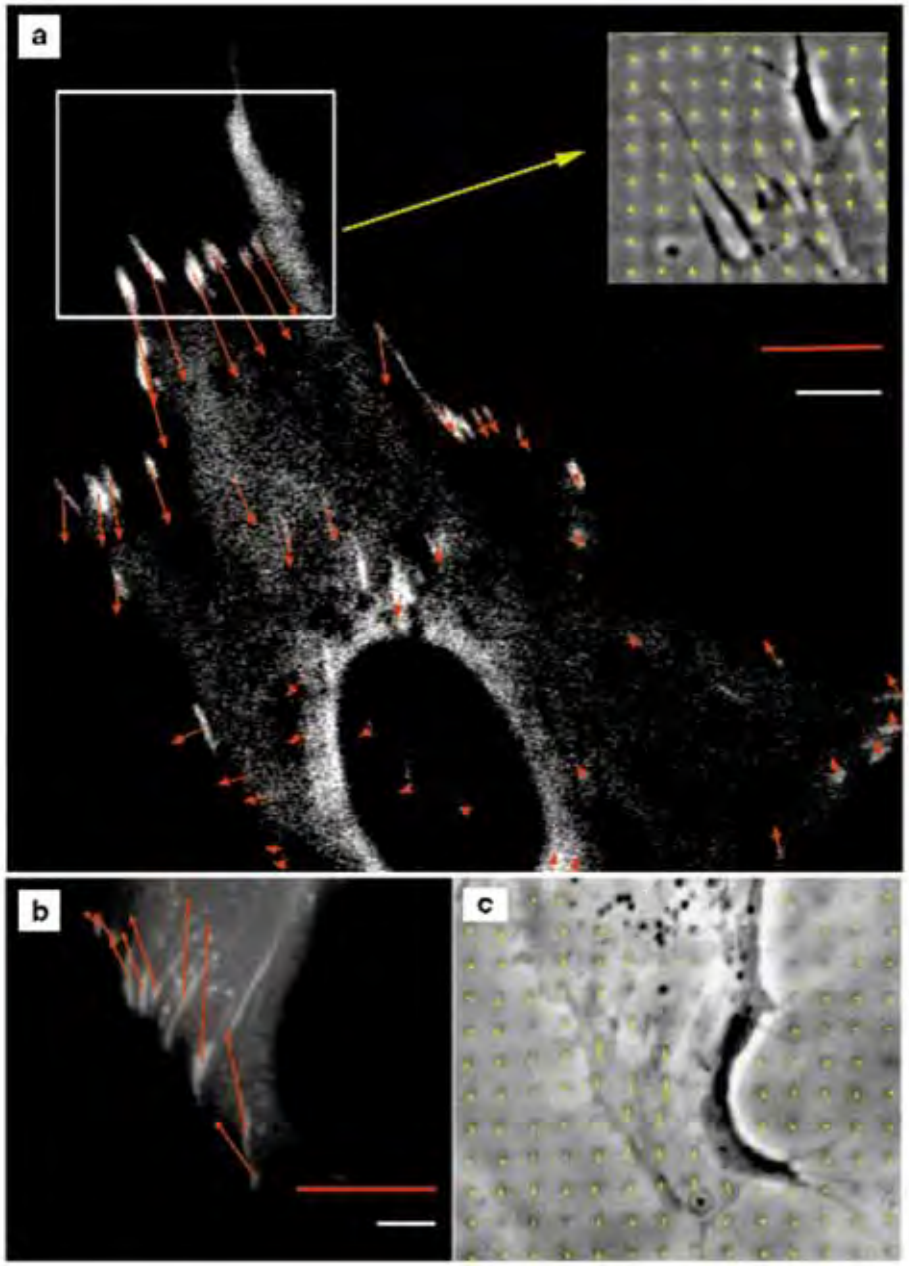

Figure 3 **Visualization of forces and focal adhesions. a**, Fluorescence image of a human foreskin fibroblast expressing GFP–vinculin, which localizes to focal adhesions. Red arrows correspond to forces extracted from the displacements of the patterned elastomer (Young's modulus = 18 kPa). Note the alignment of force with the direction of elongation of large focal adhesions. Inset, phase-contrast image of the upper part of the cell (white rectangle), showing displacements of the dots (green arrows); the pattern consists of small square pits (see Fig. 1j, 1). **b**, Fluorescence image of a human foreskin fibroblast stained with antibodies against paxillin, which also localizes at focal adhesions. Red arrows correspond to forces extracted from the displacements of the patterned elastomer (Young's modulus = 21 kPa); the pattern consists of small tips formed by electron-beam lithography (see Fig. 1j, 3). **c**, Phase-contrast image of the same cell immediately before fixation. White scale bars represent 4 μm; red scale bars represent 30 nN.

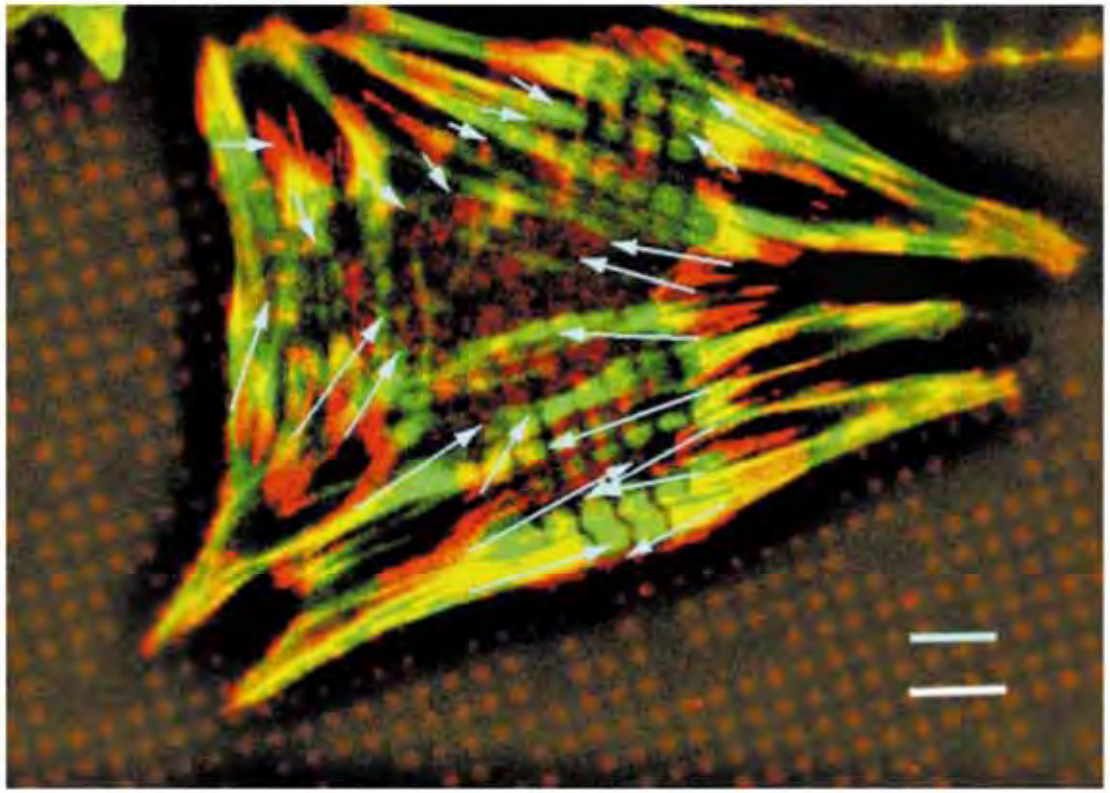

Figure 4 **Distribution of forces in a cardiac myocyte.** After recording the displacements of the pattern caused by beating (Fig. 2c, d), the cardiac myocytes are stained for vinculin (red) to visualize the sites of force transmission, and for actin (green). Yellow regions correspond to overlap of actin and vinculin. The light-blue arrows denote the forces applied to the substrate at the vinculin-rich areas. White bar = 6 μm; blue bar = 70 nN.

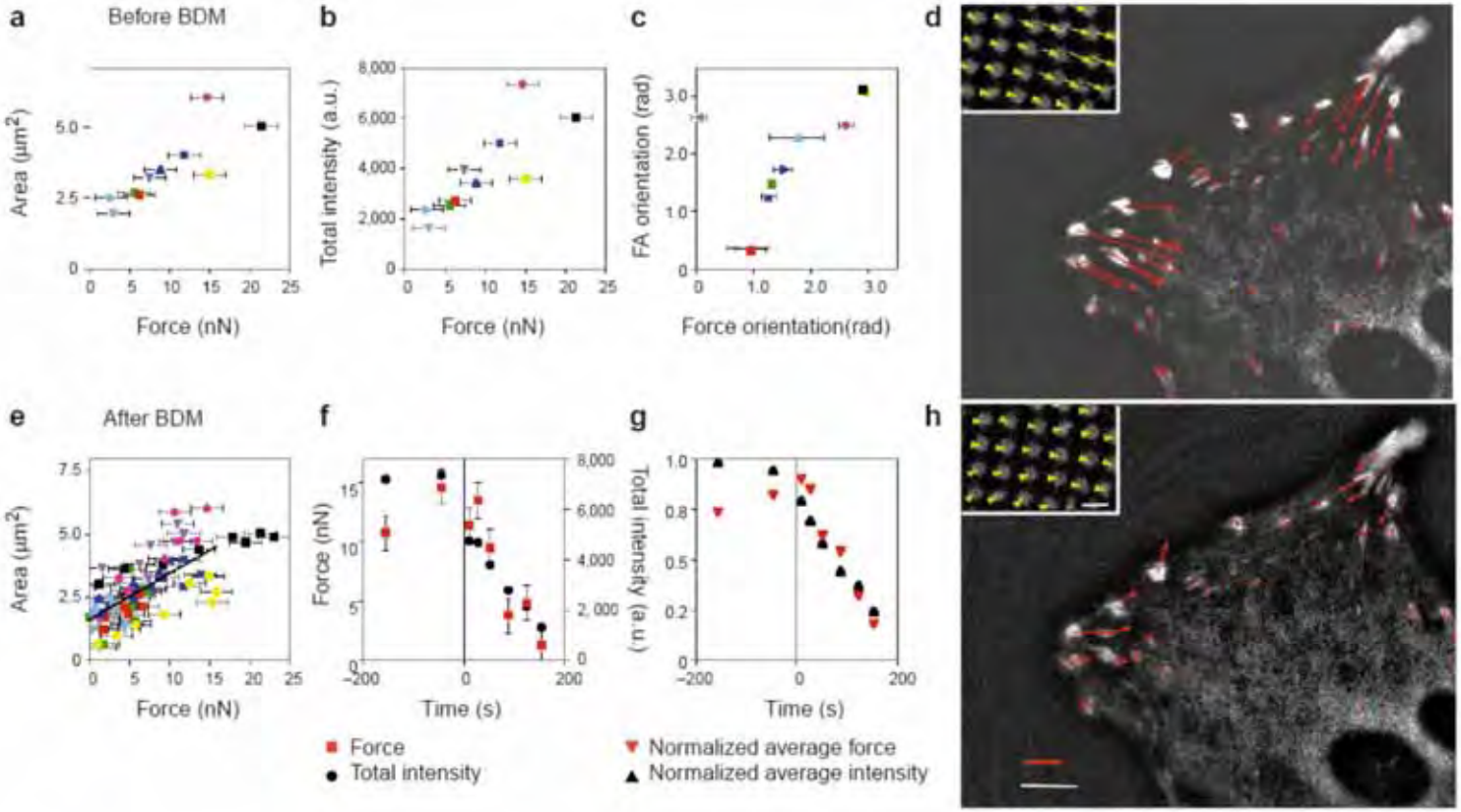

Figure 5 **Correlation between force and focal adhesion structure. a–d**, Before the addition of BDM. **a**, Correlation between force and area of single focal adhesions. **b**, Correlation between force and total fluorescence intensity of single focal adhesions. **c**, Correlation between the direction of the force and the elongation of the focal adhesion. The angles (in radians) were measured relatively to the x axis of the pictures. Each point represents a single focal adhesion from Fig. 5d. Absence of error bars indicates an error below the size of the symbol. **d**, Fluorescence image of a human foreskin fibroblast expressing GFP–vinculin, which localizes to the focal adhesions. The red arrows show the forces transmitted at the focal adhesions. Inset: fluorescence image of the pattern of dots below the left-hand side of the cell; green arrows denote displacements. **e–h**, After the addition of 15 mM 2,3-butanedione monoxime (BDM). **e**, Correlation between the area and force of the focal adhesions of the cell shown in Fig. 5d, at all time points. Each different symbol represents a different focal adhesion. The black line is the correlation line of the linear part of the plot. Its slope defines a stress of 5.5 ± 2 nN μm^{-2} at the focal adhesions. **f**, Time dependence of the relaxation of force (red squares) and total GFP–vinculin intensity (black dots) of a single focal adhesion. **g**, Time dependence of the relaxation of force and total intensity as a normalized average over all focal adhesions. Notice the close correlation between force and total intensity, as both decrease with time. **h**, Same cell as in **d** 2 min after BDM treatment. White bar = 4 μm; red bar = 10 nN; Young's modulus = 12 kPa.

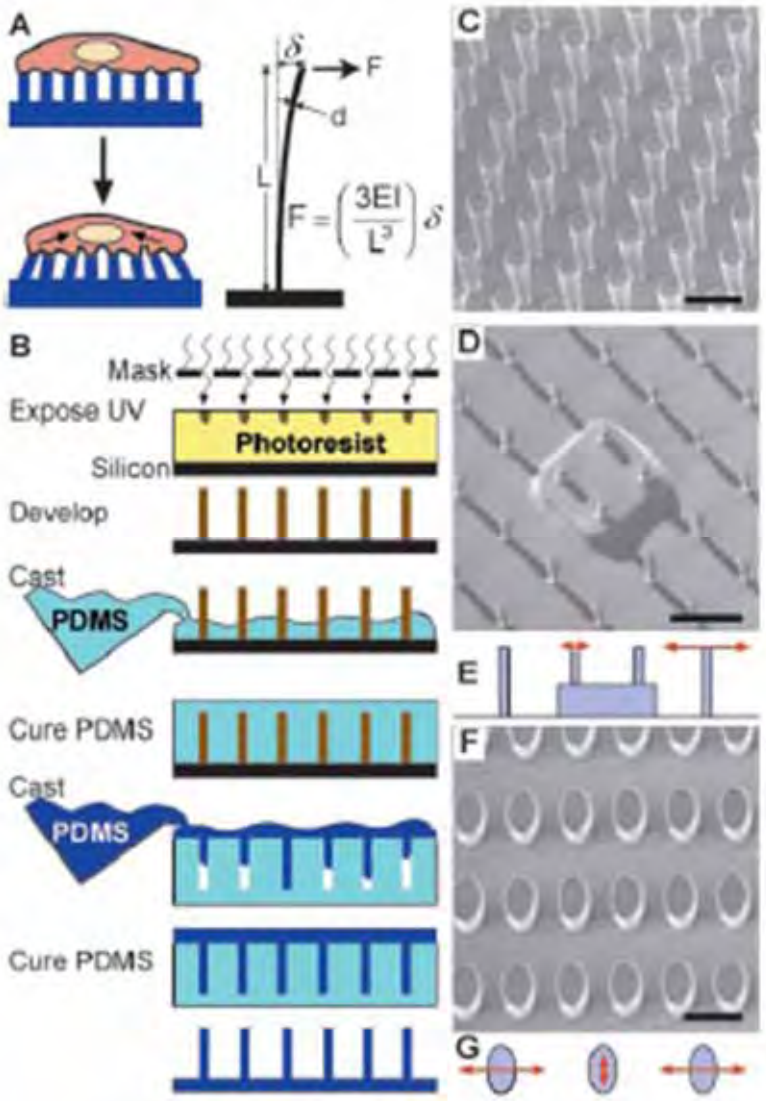

$$F = \left(\frac{3EI}{L^3}\right)\delta,$$

and δ are the bending force. You

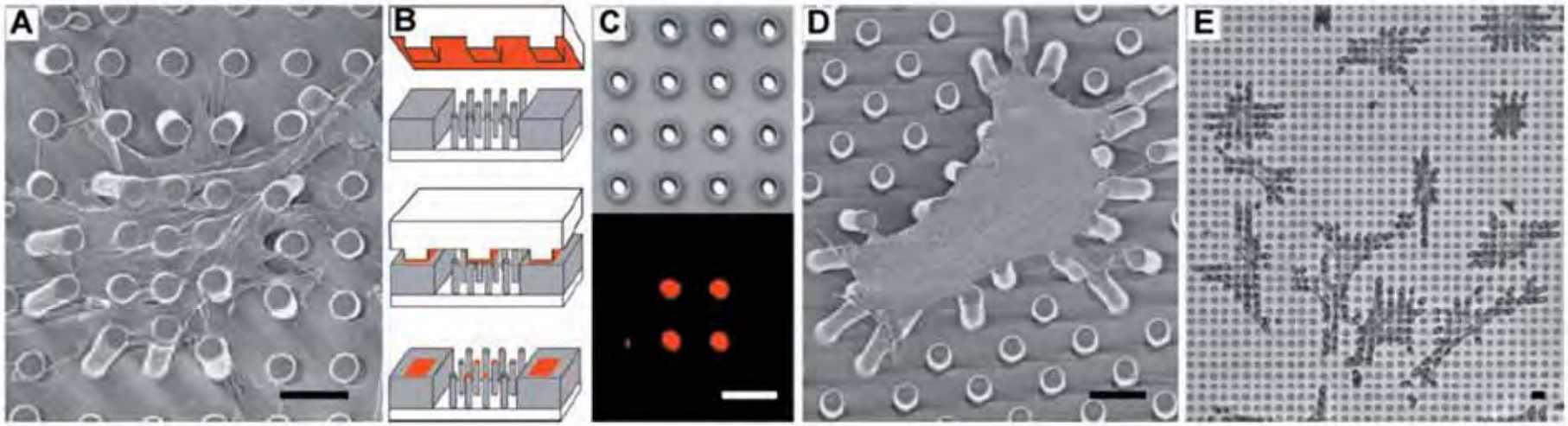

Fig. 2. Cell culture on arrays of posts. (*A*) Scanning electron micrograph of a representative smooth muscle cell attached to an array of posts that was uniformly coated with fibronectin. Cells attached at multiple points along the posts as well as the base of the substrates. (*B*) Schematic of microcontact printing of protein (red), precoated on a PDMS stamp, onto the tips of the posts (gray). (*C*) Differential interference contrast (*Upper*) and immunofluorescence (*Lower*) micrographs of the same region of posts where a 2 × 2 array of posts has been printed with fibronectin. (*D* and *E*) Scanning electron micrograph (*D*) and phase-contrast micrograph (*E*) of representative smooth muscle cells attached to posts where only the tips of the posts have been printed with fibronectin by using a flat PDMS stamp. Cells deflected posts maximally during the 1- to 2-h period after plating, were fully spread after 2 h, and were fixed and critical point dried 4 h after plating. (Scale bars indicate 10 μm.)

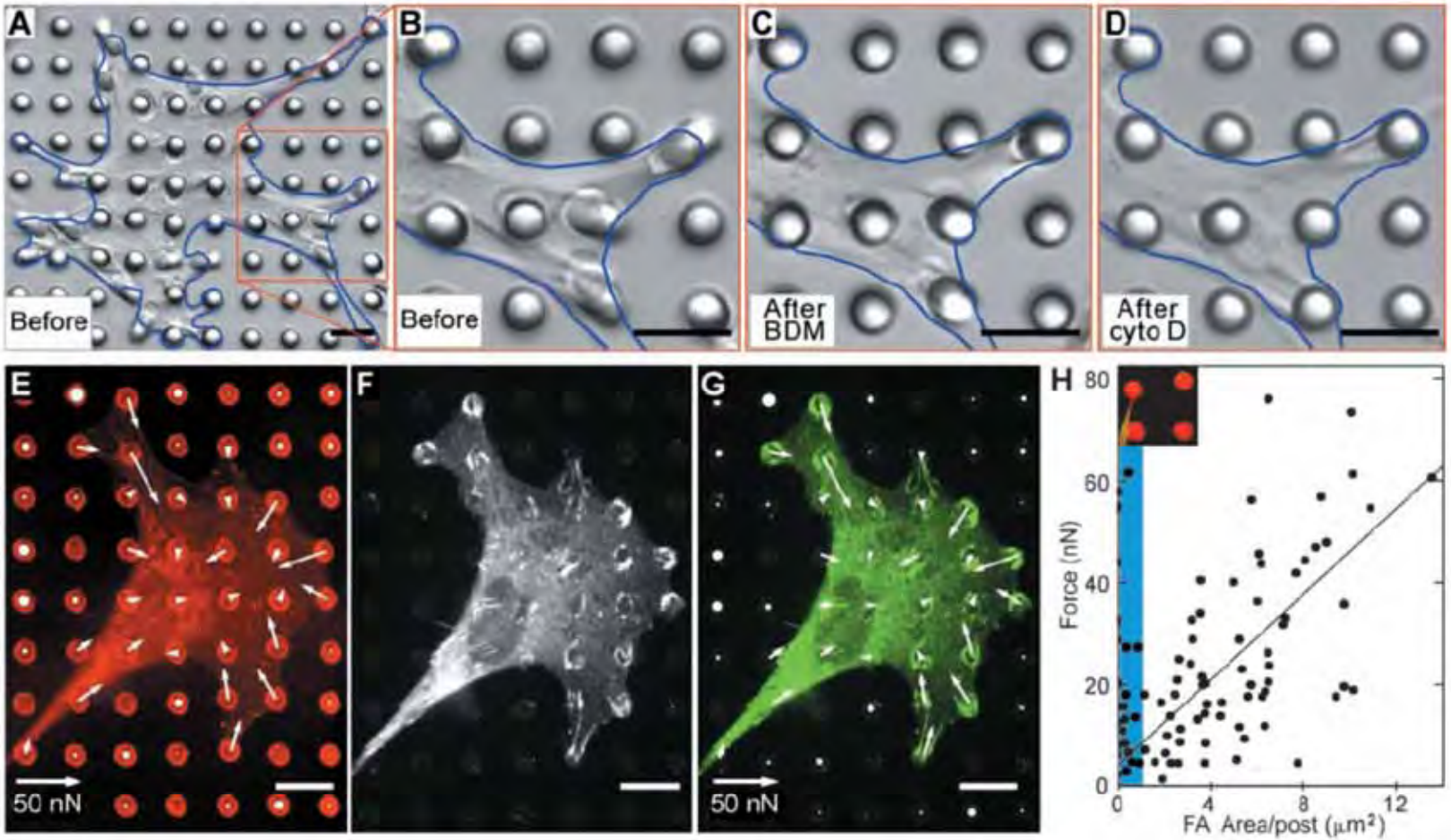

Fig. 3. Measurement of contractile forces in cells. (*A–D*) Differential interference contrast micrographs of a smooth muscle cell (outlined in blue) cultured for 2 h on an array of posts in 10% serum (*A* and *B*), 20 min after 20 mM 2,3-butanedione monoxime (BDM) was added to the culture to inhibit myosin contractility (*C*), and after 2 μg/ml cytochalasin D (cyto D) was added to the same culture for an additional 10 min to disrupt the actin cytoskeleton (*D*). In each case, longer treatments did not result in additional loss of contractility. (*E–G*) Confocal images of immunofluorescence staining of a smooth muscle cell on posts. Position of fibronectin (*E*, red) on the tips of the posts was used to calculate force exerted by cells (white arrows). The force map was spatially correlated to immunofluorescence localization of the focal adhesion protein vinculin (*F*, white; *G*, green). A similar correlation in the orientation and the quantity of focal adhesion with the traction forces was observed in all cells examined ($n > 10$). The lengths of arrows indicate the magnitude of the calculated force (top right arrow indicates 50 nN); white circles on undeflected posts depict the background error in the force measurement, where the diameter of the circle (same length scale as the arrows) indicates the magnitude of calculated force on each post not attached to a cell. (Scale bars indicate 10 μm.) (*H*) Plot of the force generated on each post as a function of total area of focal adhesion staining per post. Each point represents the force and area of vinculin staining associated with each post; focal adhesions from five cells were analyzed. The shaded region (blue) indicates the adhesions smaller than 1 μm^2. (*Inset*) Image of a typical small adhesion ($<1\ \mu m^2$) formed by a cell (green) generating substantial force on a post (red).

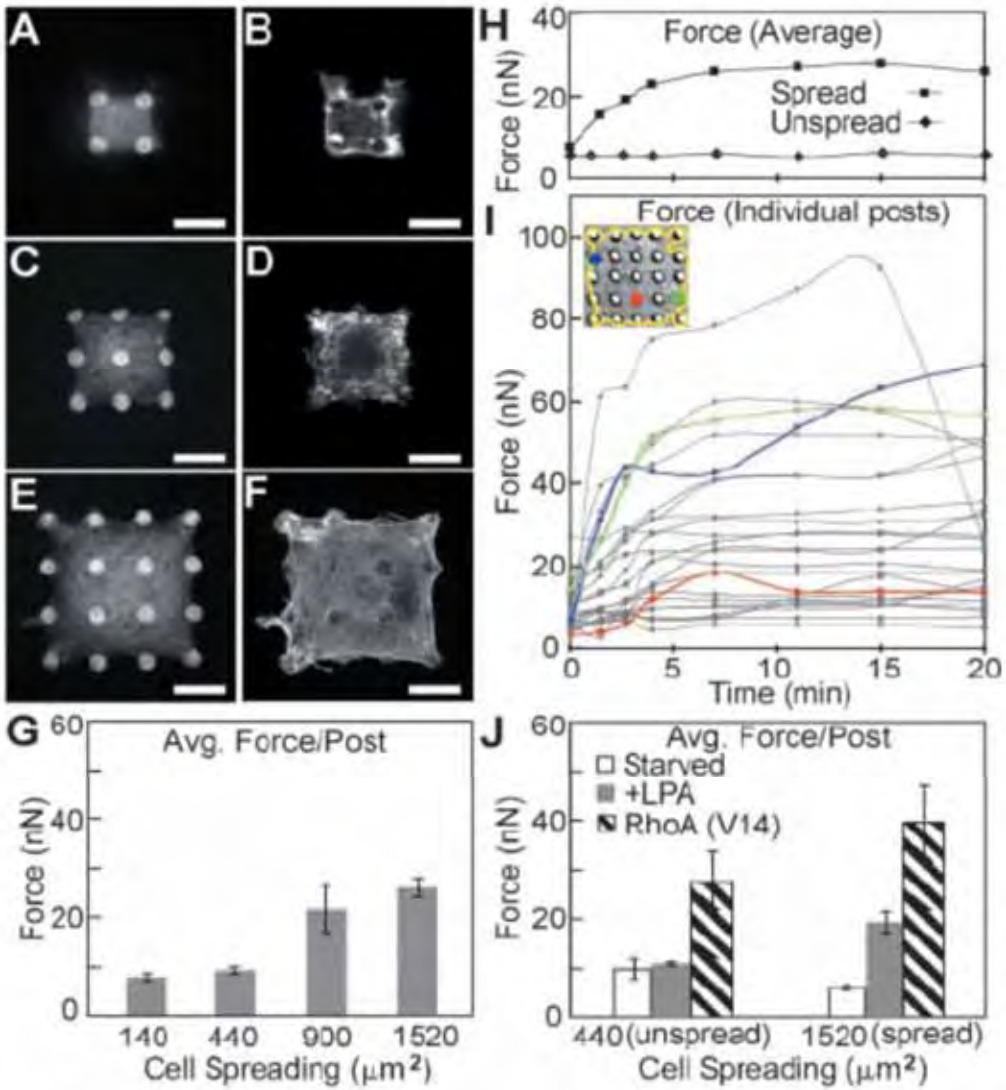

Fig. 4. Role of cell spreading in regulating contractile forces. (*A–F*) Confocal micrographs of smooth muscle cells attached onto different-sized sets of fibronectin-coated posts. Cells attached to 2 × 2 (*A* and *B*), 3 × 3 (*C* and *D*), or 4 × 4 (*E* and *F*) sets of posts were costained for fibronectin (*A*, *C*, and *E*) and filamentous actin (*B*, *D*, and *F*). (Scale bars indicate 10 μm.) (*G*) Plot of average force generated per post for cells spread to different degrees (140, 440, 900, or 1,520 μm^2) on arrays of posts (2 × 2, 3 × 3, 4 × 4, or 5 × 5, respectively) for 20 h in standard culture media. (*H*) Plot of average force generated per post over time for a cell cultured on either a 5 × 5 ("spread") or 3 × 3 ("unspread") set of posts. Cells were serum-starved for 12 h on the posts and were exposed to LPA (10 μg/ml) at time 0. (*I*) Plot of force exerted on each of the 25 posts over time for the spread cell plotted in *H* and shown as the *Inset*. The forces exerted on the posts colored in the *Inset* are indicated by line plots of the same color. (*J*) Plot of average force exerted per post for cells cultured on 5 × 5 (spread) or 3 × 3 (unspread) posts and were serum-starved, exposed to LPA for 12 min, or transfected with constitutively active RhoA. A total of 18 cells in *G* and 25 cells in *J* were analyzed across three independent experiments; error bars indicate standard error of the mean.

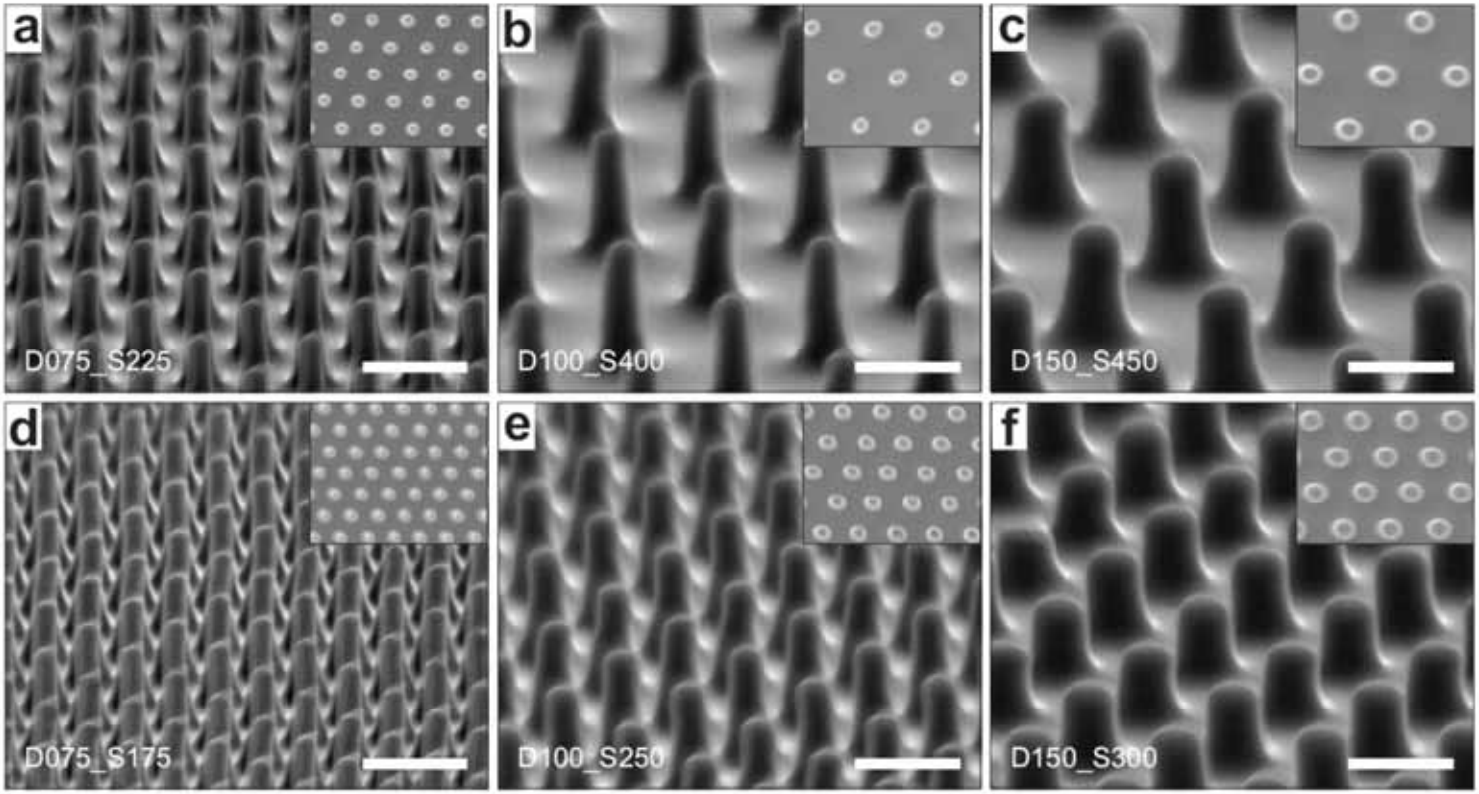

g

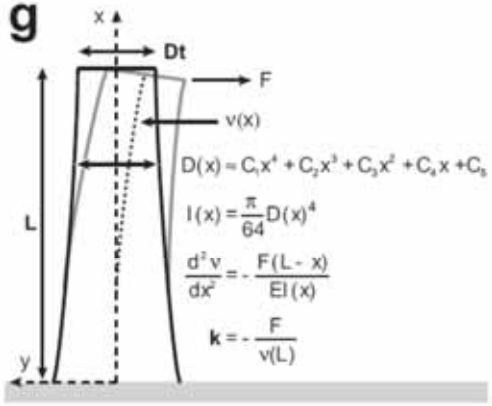

h

Array Designation	Shown in Figure	Target Post Diameter (μm)	Center-to-Center Spacing (μm)	Actual Tip Diameter **Dt** (μm)	Height **L** (μm)	Post Stiffness **k** (nN/μm)
D075_S175	2d	0.75	1.75	0.67	3.10	8
D075_S225	2a	0.75	2.25	0.67	3.29	7
D100_S200	1c	1.00	2.00	0.81	2.00	37
D100_S250	2e	1.00	2.50	0.83	3.09	28
D100_S400	2b	1.00	4.00	0.83	3.36	16
D150_S300	2f	1.50	3.00	1.32	2.07	231
D150_S450	2c	1.50	4.50	1.31	3.21	135

Figure 2. Characterization of elastomeric nanopost arrays. a–f) SEM images of PDMS nanopost arrays. Insets show top-down images of arrays. Scale bar is 3 μm. g) Calculation of post stiffness for a post with varying cross-sectional diameter. h) Table summarizing post measurements and calculated stiffness for different post array geometries.

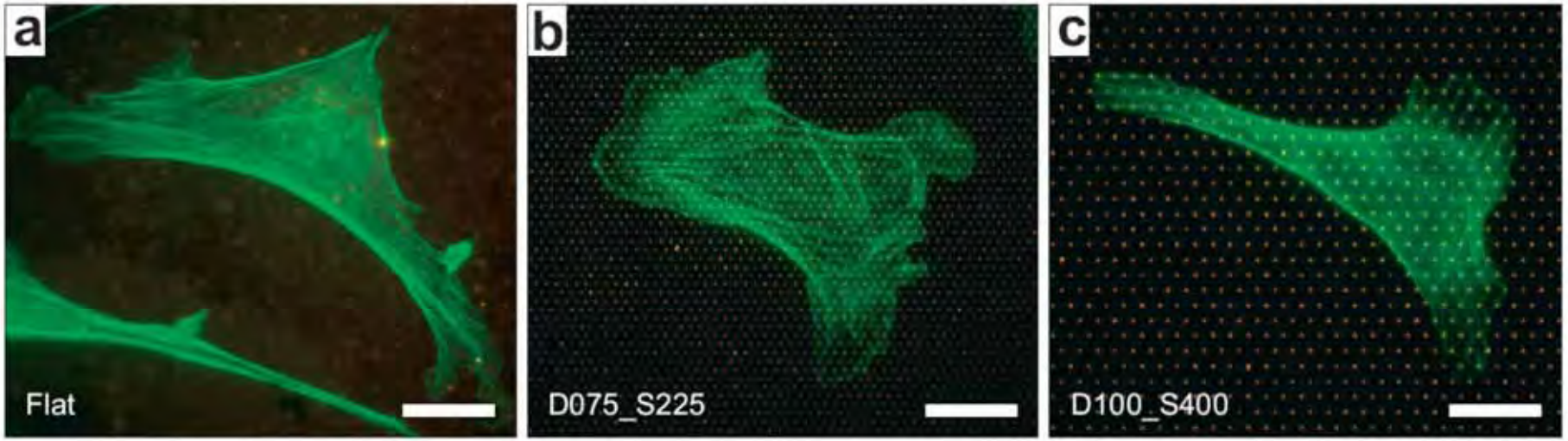

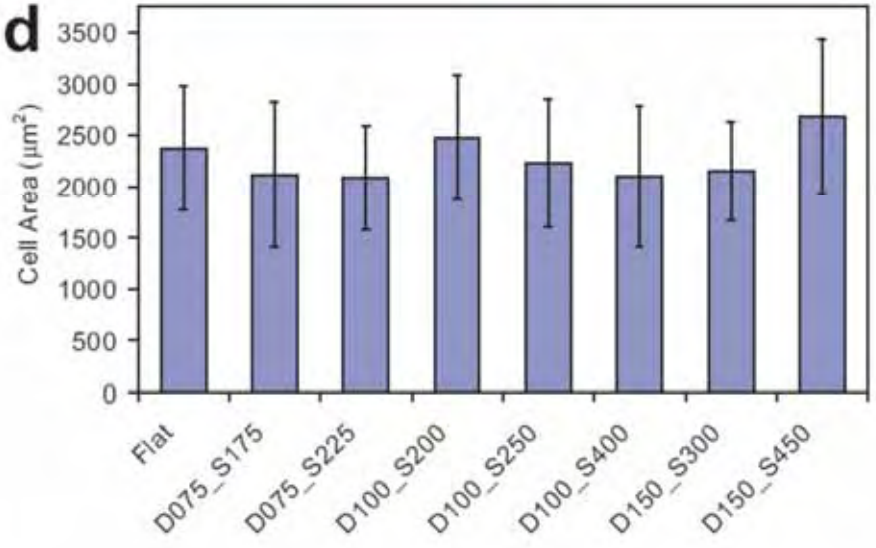

Figure 3. Cell spreading on nanopost arrays. a–c) Representative images of cells, stained for F-actin, on flat and nanopost surfaces. Scale bars are 20 μm. d) Graph of the average cell area on the flat surface and seven nanopost arrays. Error bars indicate standard deviation of the mean.

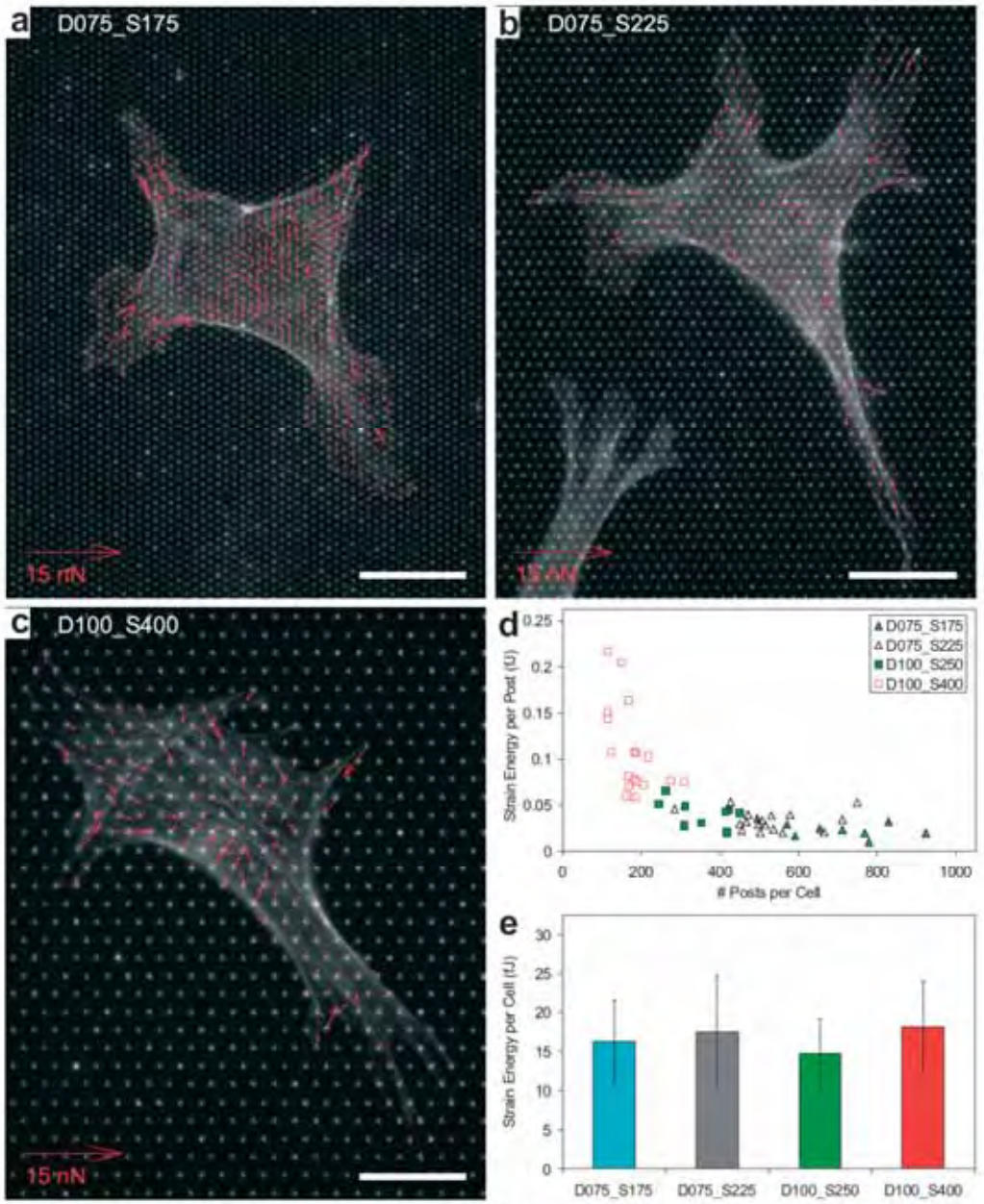

igure 4. Traction force measurement on nanopost arrays. a–c) Representative force vector plots overlayed on cells spread on different nanopost array eometries. White scale bars are 20 μm. d) Graph of the strain energy per post versus the number of posts per cell. e) Graph of the average strain ener- y per cell on four nanopost arrays. Error bars indicate standard deviation of the mean.

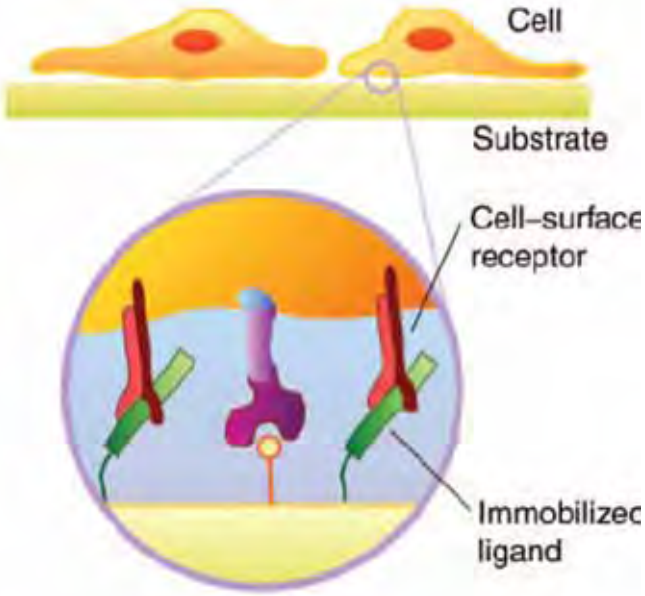

Figure 1. Most cells are adherent and must attach and spread on a matrix. The interaction of a cell with the substrate relies on the binding of cell–surface receptors with ligand proteins that are adsorbed to the material.

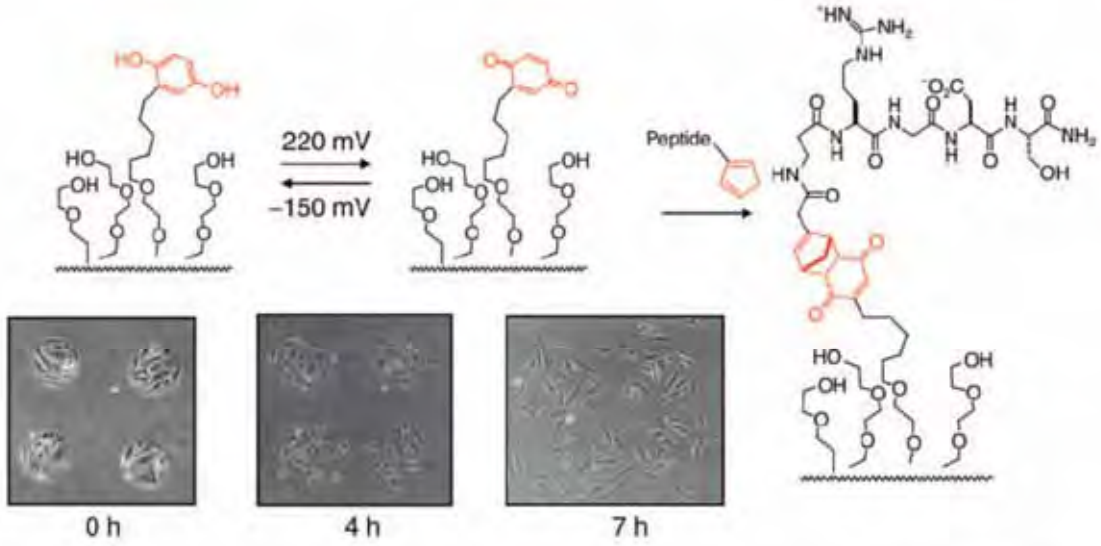

Figure 3. Design of a substrate that electrically turns on the immobilization of a ligand. An electrical potential converts a hydroquinone group to benzoquinone, which serves to immobilize a peptide ligand. The dynamic surfaces can initiate the migration of cells that are originally confined to 200 μm circular regions on the substrate.

Using electroactive substrates to pattern the attachment of two different cell populations

5992–5996 | PNAS | May 22, 2001 | vol. 98 | no. 11

Muhammad N. Yousaf, Benjamin T. Houseman, and Milan Mrksich*

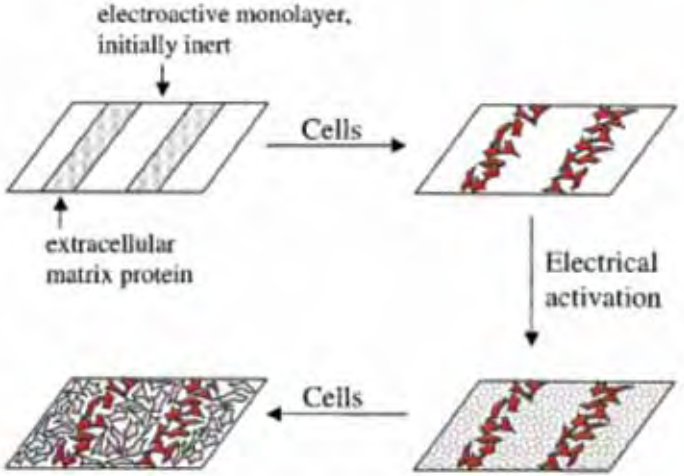

Fig. 1. Strategy for patterning two different cell types to a substrate. The method starts with a surface that is patterned into regions that promote cell attachment (i.e., regions coated with extracellular matrix proteins) and regions that are inert to cell attachment, but that can be converted to promote attachment by the application of an electrical potential. After cells attach to the first set of regions, the inert set of regions can be activated electrically so that a second cell population can attach, generating a patterned coculture.

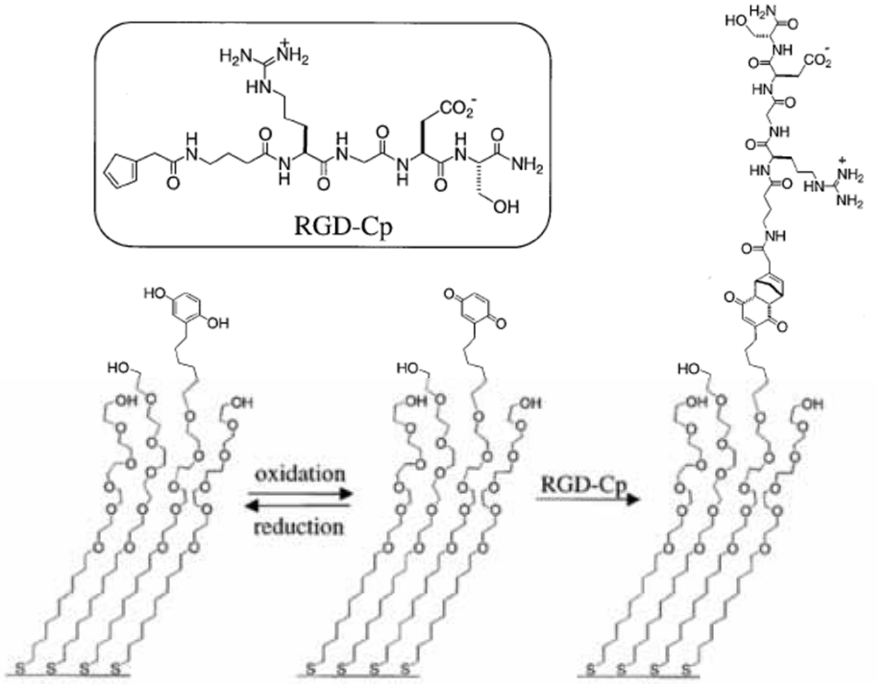

Fig. 2. Molecular strategy for creating substrates that can be electrically switched to permit cell attachment. A monolayer presenting a mixture of hydroquinone groups and penta(ethylene glycol) groups (Left) is converted to a monolayer presenting the corresponding quinone groups (Center) by application of a potential to the underlying gold (500 mV versus Ag/AgCl). Both monolayers are inert to the attachment of cells. Addition of a conjugate of cyclopentadiene and the peptide Gly-Arg-Gly-Asp-Ser-NH_2 (RGD-Cp) to the monolayer presenting the quinone group results in the Diels–Alder-mediated immobilization of peptide (*Right*). 3T3 fibroblasts attach and spread on the resulting surface. Monolayers presenting the hydroquinone group are unaffected by the treatment with RGD-Cp and remain inert to cell attachment.

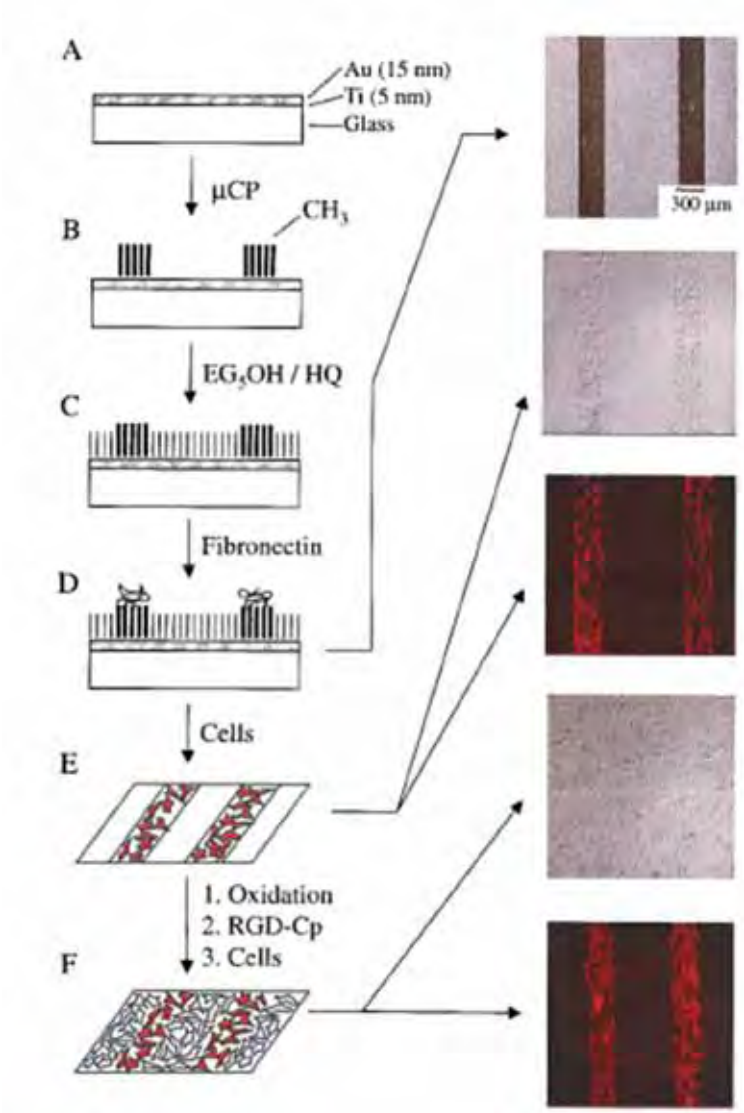

Fig. 3. Use of an electroactive substrate to pattern two cell populations into a coculture. (*A*) Substrates were prepared by evaporating titanium (5 nm) and then gold (15 nm) onto glass coverslips. (*B*) Microcontact printing was used to pattern hexadecanethiolate into lines that are 300 μm wide and separated by 800 μm. (*C*) A second monolayer was assembled on the remaining regions of gold by immersing the substrate into a solution of hydroquinone-terminated alkanethiol (HQ) and penta(ethylene glycol)-terminated alkanethiol (EG_5OH). (*D*) The substrate then was immersed in a solution of fibronectin in PBS for 4 h. A scanning electron micrograph shows that protein adsorbed only to the methyl-terminated regions of the monolayer. (*E*) 3T3 fibroblasts attached only to the regions presenting fibronectin, and when cultured in serum-containing media, divided to fill these regions entirely. The surrounding inert monolayer strictly confined the cell to the rectangular regions. (*F*) Electrochemical oxidation of the monolayer in the presence of media containing RGD-Cp (2 nM) led to the immobilization of the peptide. Fluorescence microscopy shows that the two cell populations are patterned on the substrate. All micrographs were taken by ×5 magnification.

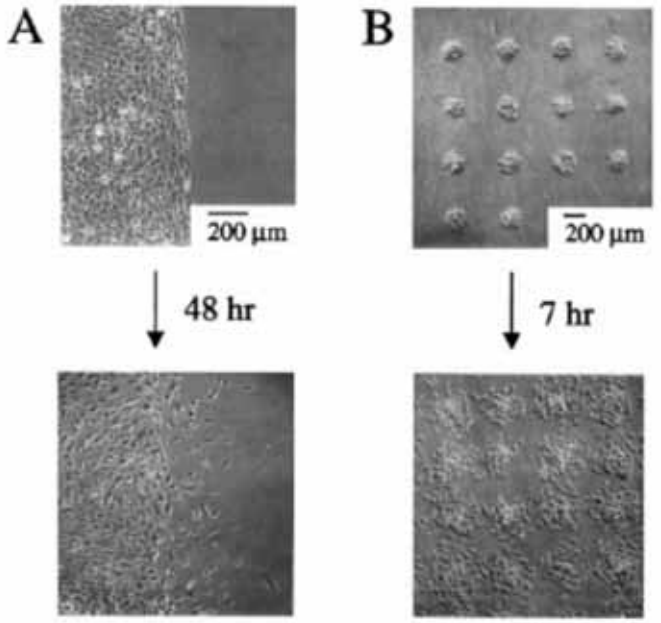

Fig. 4. The onset of migration into the second set of regions after electrochemical activation and peptide immobilization depends on the geometric features of the pattern. Cells patterned along a straight edge (*A*) showed little migration after 48 h, whereas cells patterned to 200-μm circles showed extensive migration after only 7 h (*B*). All micrographs were taken at ×5 magnification.

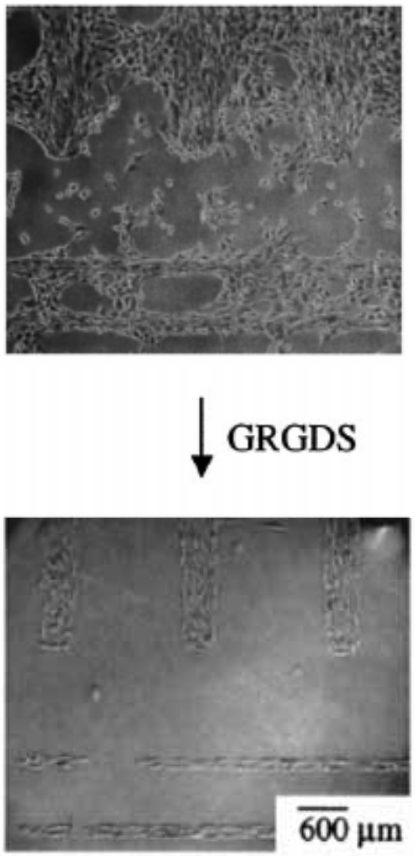

Fig. 5. Selective detachment of cells adhered to regions of the substrate presenting the RGD peptide among penta(ethyene glycol) groups. A patterned coculture was prepared as described in Fig. 3 *Left*. Addition of soluble peptide (GRGDS, 2 mM for 1 h) resulted in the detachment of cells only from the regions of the monolayer presenting peptide conjugates, indicating the specificity of the cell-substrate interaction. Micrographs were taken at ×5 magnification.

Electrochemical Desorption of Self-Assembled Monolayers Noninvasively Releases Patterned Cells from Geometrical Confinements

procedure uses microcontact printing (μCP) and readily available thiols—$HS(CH_2)_{11}(OCH_2OCH_2)_3OH$ ($C_{11}EG_3$) and $HS(CH_2)_{17}CH_3$ (C_{18})—to confine cells into patterns; these methods are well established.[1,2] EG_3-terminated SAMs resist the adsorption of

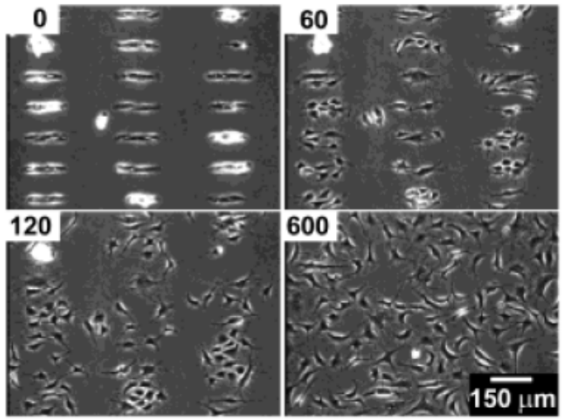

Figure 1. BCE cells were allowed to attach to a surface patterned with $C_{11}EG_3$ and C_{18}. Application of a cathodic voltage pulse (−1.2 V for 30 s in this case) released the cells from the microislands. The numbers indicate the time elapsed (in minutes) after the voltage pulse.

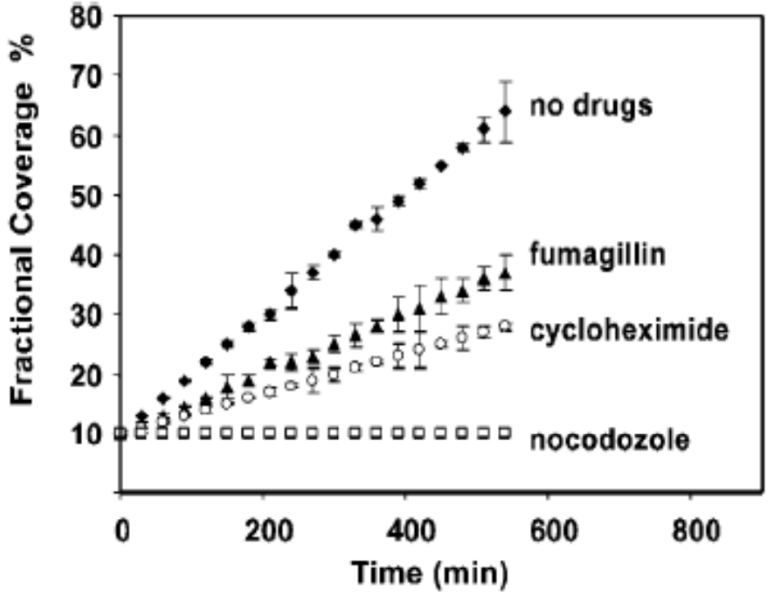

Figure 3. A cell-based screening assay. A summary of the influence of drugs on the motility of BCE cells after application of a voltage pulse (−1.2 V, 30 s). Each datum represents the average of eight fields of cells. Error bars represent one standard deviation from the mean. See Supporting Information for the calculation of the Fractional Coverage.

Electrically Driven Conformational Switching

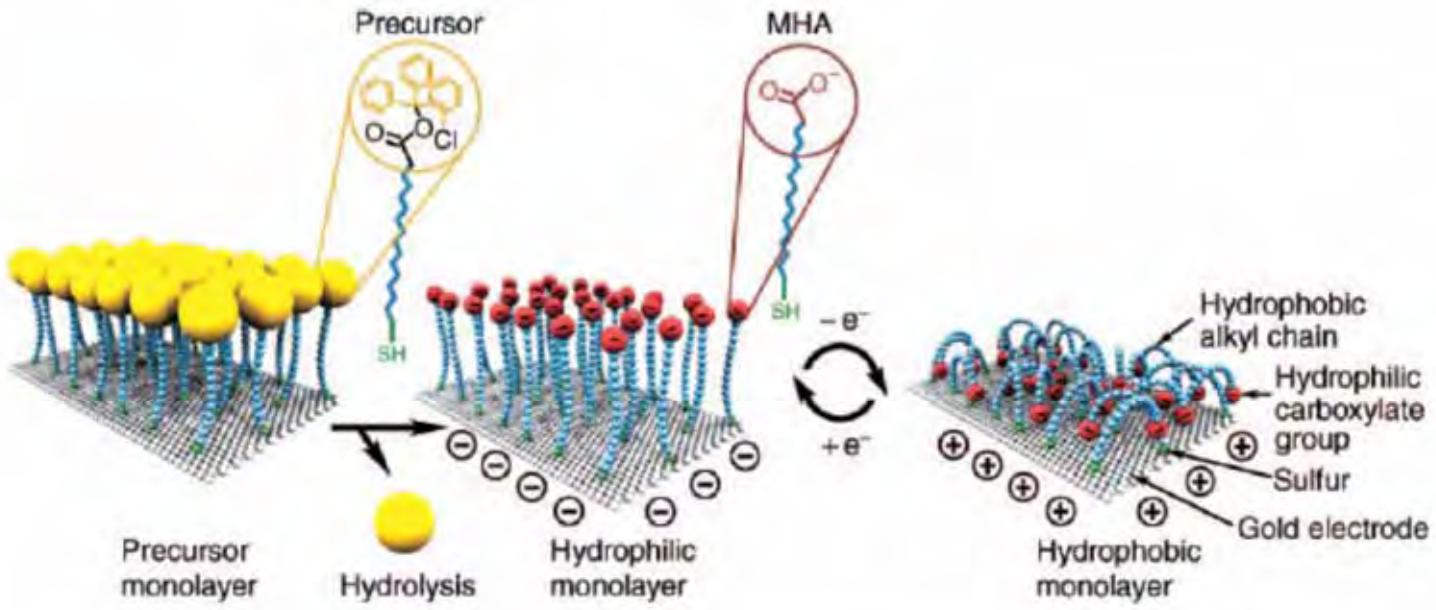

Figure 1. Idealized representation of the transition between straight (hydrophilic) and bent (hydrophobic) molecular conformations. Ions and solvent molecules are not shown. MHA is 16-mercapto-hexadecanoic acid. (Reproduced with permission from Reference 38.)

Temperature Responsive Surface

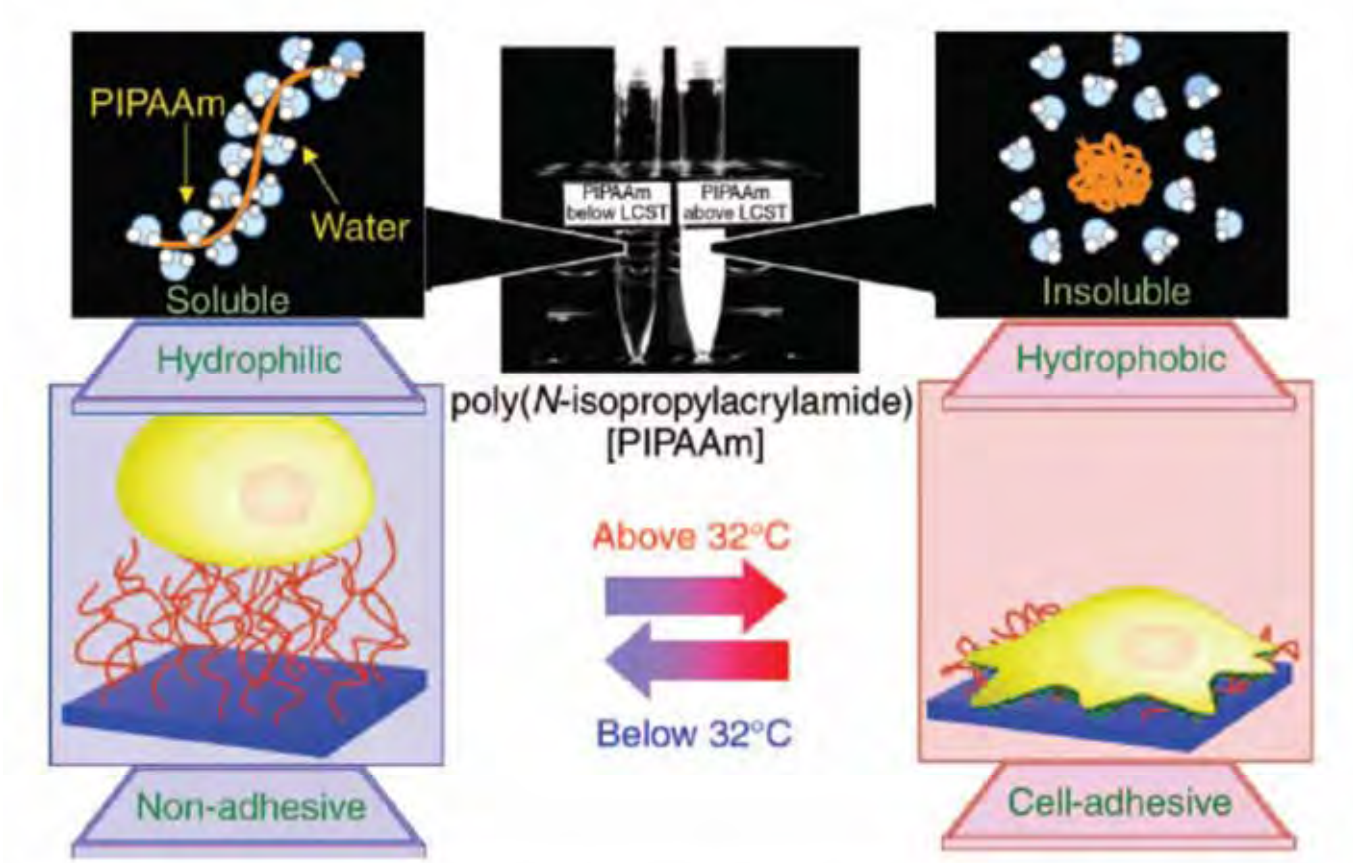

Figure 1. Temperature-responsive culture dishes. The temperature-responsive polymer poly(N-isopropylacrylamide) (PIPAAm) exhibits a transition from hydrophobic to hydrophilic across its lower-critical solution temperature (LCST) of 32°C. After electron-beam polymerization and grafting to normal tissue-culture polystyrene (TCPS) dishes, temperature-responsive culture surfaces can be produced. The non-invasive harvest of various cell types as intact sheets, along with deposited extracellular matrix, can be achieved by reducing the culture temperature.

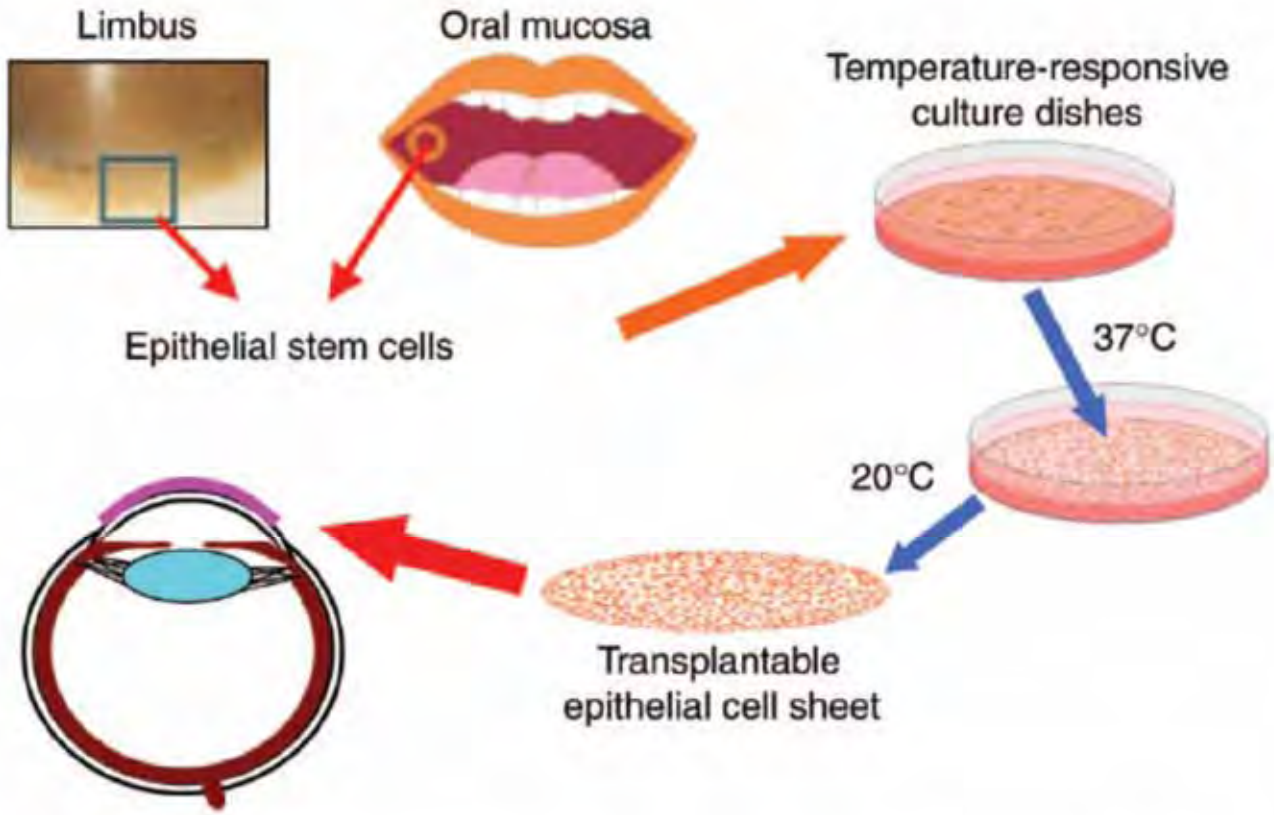

Figure 2. Corneal surface reconstruction. Small biopsies from the limbus (the border between the cornea and neighboring conjunctiva) or from oral mucosa provide for the isolation of epithelial stem cells. Cell sheets fabricated on temperature-responsive culture dishes can be harvested and transplanted directly to the ocular surface without the need for carrier substrates or sutures.

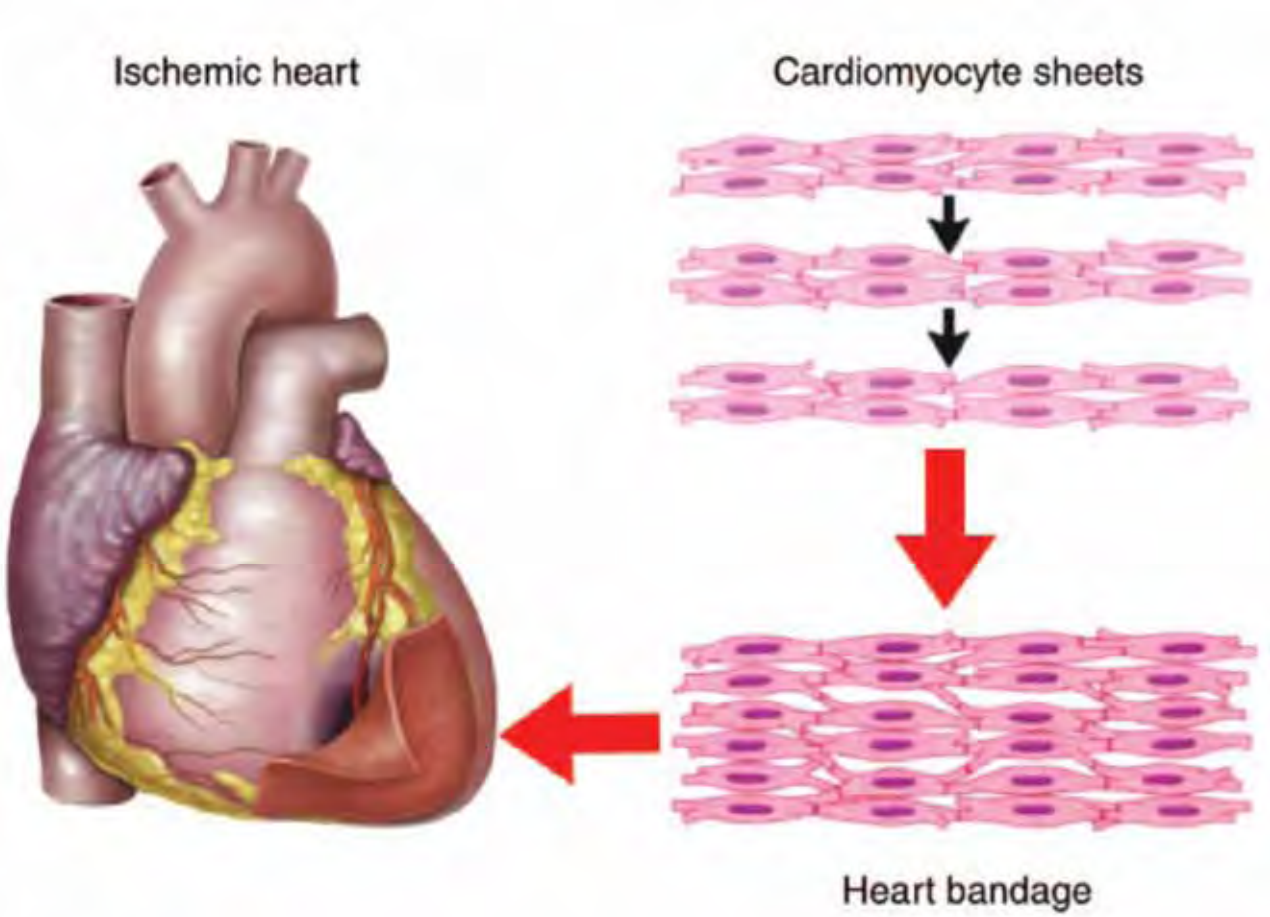

Figure 3. Myocardial cell-sheet engineering. Cardiomyocyte sheets harvested from temperature-responsive culture surfaces can be layered to form three-dimensional tissues that beat synchronously and simultaneously. We believe that layered cardiomyocyte sheets can act as a "heart bandage" for the recovery of ischemic cardiac tissue.

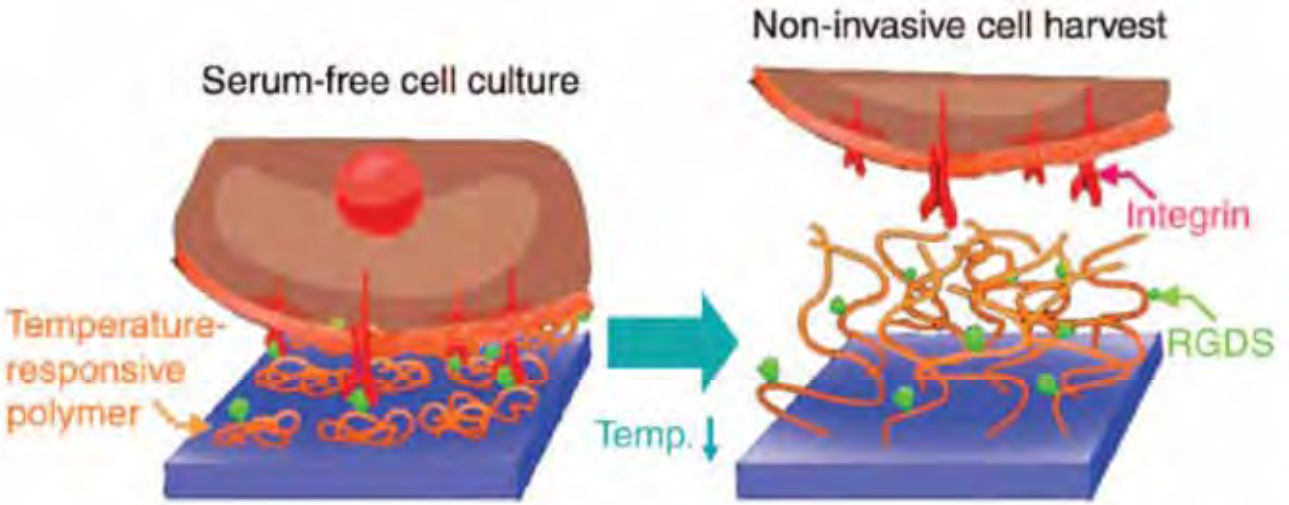

Figure 4. Immobilization of Arg-Gly-Asp-Ser (RGDS) peptides to temperature-responsive surfaces. Cells can be cultured in serum-free conditions by immobilizing the synthetic cell-adhesive RGDS peptide to temperature-responsive culture dishes. By decreasing the culture temperature, cells can still be non-invasively harvested, while the RGDS peptides remain attached to the temperature-responsive polymer surface.